Regulation of the key mitotic checkpoint protein Dma1 through post-translational modifications

By

Christine Marie Jones

Dissertation

Submitted to the Faculty of the

Graduate School of Vanderbilt University

in partial fulfillment of the requirements

for the degree of

DOCTOR OF PHILOSOPHY

in

Cell and Developmental Biology

February 28, 2018

Nashville, Tennessee

Approved:

Kathleen L. Gould, Ph.D.

William Tansey, Ph.D.

Todd Graham, Ph.D.

David Cortez, Ph.D.

To my husband and my family

for their boundless love and support

TABLE OF CONTENTS

Page

LIST OF FIGURES

LIST OF ABBREVIATIONS

APC	anaphase promoting complex
BPP	background per pixel
CDK	Cyclin dependent kinase
CR	cytokinetic ring
DDR	DNA damage response
Dma1	defective in mitotic arrest
DSB	double strand break
DUBs	deubiquitinating enzymes
F-ACTIN	filamentous-actin
FHA	Forkhead-associated
GAP	GTPase-activating protein
GFP	green fluorescent protein
HECT	Homologous to the E6-AP Carboxyl Terminus
MBP	maltose binding protein
MEN	mitotic exit network
MS	mass spectrometry
MTOC	microtubule-organizing center
mNG	mNeonGreen
NDR	nuclear Dbf-2-related
PAK	p21-activated kinase
PTMs	post-translational modifications
PVDF	poly-vinylidene difluoride

RING	Really Interesting New Gene
ROB	region of background
ROI	region of interest
PCR	polymerase chain reaction
SAC	spindle assembly checkpoint
SIN	septation initiation network
SPB	spindle pole body
SPOC	spindle positioning checkpoint
USP	ubiquitin specific protease
TRITC	tetramethylrhodamine
wt	wild-type
YE	yeast extract

Chapter 1

Introduction

1.1 The eukaryotic cell cycle

The cell is the fundamental unit of life. As proposed by Schleiden and Schwann in 1838, the cell theory states that all living organisms are composed of one or more cells, and new cells arise only from the division of a preexisting cell. This theory has evolved to the commonly held idea that every living organism shares a single common ancestral cell. Thus, cell division is essential to sustain life. It is required both for unicellular organisms to propagate, in which each division yields a new organism, and for multicellular organisms to develop from a single cell into a sustained, complex array of tissues and organs.

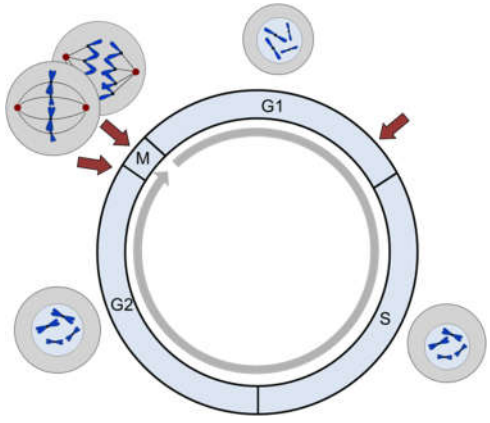

Figure 1-1
The cell division cycle and associated checkpoints
Each properly coordinated cell division consists of an ordered cycle of G1, S, G2, and M phases. Cell growth occurs during G1 and G2 phases, the genome is duplicated in S phase, and chromosome segregation

(mitosis) and cell separation (cytokinesis) occur in M phase. The precision of the cell cycle is ensured through cell cycle checkpoints. These signal transduction mechanisms suspend cell cycle progression in response to errors, enabling error correction and ensuring accurate cell division. The key cell cycle checkpoints include: G1, G2/M, and spindle assembly checkpoints, indicated with arrows.

Each properly coordinated cell division yields two daughter cells with identical complements of genomic material. This requires the duplication and segregation of both the genetic and cytoplasmic cellular components, which is accomplished through an ordered cell cycle of G1, S, G2, and M phases (Fig. 1-1). During G1 and G2, the gap phases, cells grow through a continuous process that includes the synthesis of new ribosomes, membranes, mitochondria, endoplasmic reticulum, and most cellular proteins. In S-phase, the synthesis phase, cells replicate the genome. Combined, the G1, S, and G2 phases comprise interphase and fulfill the requirement for duplication of genetic and cytoplasmic material, preparing the cell for segregation in M-phase. During M-phase cells perform mitosis, a coordinated process of chromosome segregation, and cytokinesis, which follows nuclear division and results in the physical separation of the two daughter cells.

1.2 Ensuring accuracy of cell division with cell cycle checkpoints

It is critical that cells accurately complete cell division as defects can lead to cell death or aneuploidy, and have been linked to developmental disorders and cancer. Thus, the phases of the cell cycle must occur sequentially such that each phase is fully completed before the next begins and that no phase repeats out of order (Nurse, 2000). To facilitate this, cells have several mechanisms to ensure that the cell cycle advances unidirectionally. For example, the high CDK activity characteristic of early mitosis is

eliminated at the metaphase-to-anaphase transition as its activator, cyclin B, is targeted by the anaphase promoting complex (APC) for degradation through the ubiquitin proteasome system. This not only enables cells to exit mitosis, it also couples mitotic exit with activation of cytokinesis and prevents mitotic re-entry until the completion of the following G2 phase (Glotzer, Murray, & Kirschner, 1991; Wickliffe, Williamson, Jin, & Rape, 2009).

In addition to maintaining the appropriate order of events, the cell cycle must also properly respond to any errors that occur in the numerous cell division processes. This response is coordinated through several cell cycle checkpoints including the G1, G2/M, and spindle assembly checkpoints (Fig. 1-1). Checkpoints are signal transduction pathways that detect errors in cell cycle processes, transmit biochemical signals to delay progression, and enable error correction to ensure accurate cell division (Harashima, Dissmeyer, & Schnittger, 2013; D. G. Johnson & Walker, 1999). For example, the spindle assembly checkpoint (SAC) monitors the formation of a bipolar spindle wherein each of the sister chromatids, of every chromosome, form kinetochore-based stable attachments with microtubules emanating from opposite poles of the mitotic spindle. In the absence of even one of these amphitelic attachments, as in the case of a syntelic attachment when both sister chromatids form attachments to microtubules emanating from the same pole, the checkpoint transmits a signal to inhibit the Anaphase-Promoting Complex (APC) and delay anaphase onset and mitotic exit (Musacchio, 2011, 2015).

Checkpoint signaling typically impacts the localization, activity, or stability of target proteins in a rapid and temporary manner, and is therefore executed through post-translational modifications (PTMs). As the name implies, PTMs are modifications made

to proteins during or after translation by the ribosome. There are numerous ways that proteins can be modified including the covalent addition of functional groups or small proteins, such as phosphorylation and ubiquitination, through enzymatic reactions, exemplified by kinases and the ubiquitination cascade, respectively. These modifications are removable through the action of various modification-specific enzymes, including phosphatases and deubiquitinating enzymes (DUBs) that hydrolyze phosphorylation and ubiquitination, respectively. The reversible nature of PTMs enables many of their downstream impacts to occur transiently, allowing them to provide the spatial and temporal regulation necessary in checkpoint signaling (Bohnert & Gould, 2011; Zhao, Brickner, Majid, & Mosammaparast, 2014).

Cell cycle checkpoints are essential to ensuring the accuracy of cell division and as such are an important area of research. Several decades of study into cell cycle checkpoints have successfully identified many key players (Hartwell, Culotti, Pringle, & Reid, 1974; Hartwell & Weinert, 1989; D. G. Johnson & Walker, 1999; Nurse, Thuriaux, & Nasmyth, 1976), yet elucidating the molecular mechanisms of checkpoint function requires still further investigation. The model organism *Schizosaccharomyces pombe* has a cell cycle similar to higher eukaryotes and is an excellent system for such studies.

1.3 *Schizosaccharomyces pombe* as a model organism

S. pombe, originally used in the brewing of African millet beer, was established as a model organism in the 1940s and 1950s through the pioneering work of Urs Leupold and Murdoch Mitchison (Horowitz & Leupold, 1951; Mitchison, 1957). *S. pombe*

expanded in popularity as a model organism over time as many of Leupold and Mitchison's former trainees established their own labs and several additional investigators adopted its use. Today there is a thriving international *S. pombe* research community that convenes at the International Fission Yeast Meeting, a biennial organism specific research conference (Fantes & Hoffman, 2016).

This rod shaped unicellular yeast is genetically haploid, grows primarily from its tips, undergoes a closed mitosis, and has a cell wall that must septate when cells divide. *S. pombe* is an excellent model organism for investigation of the molecular mechanisms advancing and regulating the cell cycle as many of its key cell division genes are evolutionarily conserved and its cell length is coupled with cell cycle stage. Furthermore, it is easy and inexpensive to culture, genetically tractable with a fully sequenced genome, amenable to biochemical analyses, and well suited for live cell imaging. In addition, there are several readily available *S. pombe* resources including a comprehensive collection of deletion and temperature sensitive mutants as well as a database of protein localization information. Thus, *S. pombe* accommodates a wide range of experimental techniques including genetics, microscopy, biochemistry, and proteomics (Goyal, Takaine, Simanis, & Nakano, 2011). Studies using *S. pombe* have clarified our current understanding of the cell cycle, most notably the discovery and characterization of the key conserved regulator CDK (cyclin dependent kinase) by Sir Paul Nurse (Nurse et al., 1976) for which he shared the 2001 Nobel Prize in Physiology or Medicine with Leland Hartwell and Tim Hunt.

1.4 Cytokinesis

Cytokinesis is the final stage of the cell cycle and results in the physical separation of a single cell into two daughter cells. This process must be temporally regulated to occur only after nuclear division and spatially regulated to occur at the bisection of the mitotic spindle in order to ensure accurate cell division and prevent cell death or aneuploidy. Cytokinesis is a complex process that includes selection of the division site, recruitment of cytokinetic proteins, assembly and constriction of the cytokinetic ring (CR), and abscission of the membrane. Successful completion of these events necessitates the orchestration of a diverse collection of proteins including those that provide spatial cues, perform structural rearrangements, and generate force. Furthermore, as cytokinesis must be temporally coordinated, signaling enzymes provide timing cues to coordinate these proteins (Fededa & Gerlich, 2012; Green, Paluch, & Oegema, 2012; Skoneczna, Kaniak, & Skoneczny, 2015).

S. pombe is an ideal model organism for examination of this complicated process as, like many mammalian cells, it divides symmetrically through the assembly and constriction of an actomyosin-based CR (Gu & Oliferenko, 2015; Pollard, 2010; Pollard & Wu, 2010). In *S. pombe* the division site is determined by the position of the nucleus, which in wild-type cells is maintained in the middle of the cell through a microtubule array (Daga & Chang, 2005; Tolic-Norrelykke, Sacconi, Stringari, Raabe, & Pavone, 2005; Tran, Marsh, Doye, Inoue, & Chang, 2001). This positioning is marked by the anillin family protein Mid1 (Rincon & Paoletti, 2012). Mid1 shuttles between the nucleus and medial cortical (Paoletti & Chang, 2000; Rincon & Paoletti, 2012) during interphase and is exported from the nucleus as cells enter mitosis, increasing the amount

of Mid1 in cortical nodes (Paoletti & Chang, 2000; Sohrmann, Fankhauser, Brodbeck, & Simanis, 1996). Division site placement is further reinforced by Pom1 which prevents Mid1 localization to the cell tips (Bahler & Pringle, 1998; Padte, Martin, Howard, & Chang, 2006).

As mitosis progresses, the components of the contractile apparatus are recruited and assembled into a CR. This recruitment occurs through two parallel Mid1 dependent modules (Rincon & Paoletti, 2016). In the first module, Mid1 recruits the IQGAP Rng2 concomitantly with the myosin II light chain Cdc4 to the medial cortical nodes (Eng, Naqvi, Wong, & Balasubramanian, 1998; Laporte, Coffman, Lee, & Wu, 2011). The recruitment of Rng2 and Cdc4 reinforces Mid1 recruitment and promotes the downstream recruitment of the myosin II heavy chain Myo2 (Kitayama, Sugimoto, & Yamamoto, 1997; Laporte et al., 2011). In the second module, Mid1 recruits the F-BAR protein Cdc15 (Fankhauser et al., 1995). Together these modules cooperate to recruit the formin Cdc12, which nucleates medial F-actin (Carnahan & Gould, 2003; F. Chang, Drubin, & Nurse, 1997; Willet et al., 2015b). Upon the formation of the F-actin network, the medial cortical nodes coalesce into a tight CR. This compaction process requires F-actin and the motor activity of myosin II as well as the F-actin crosslinkers Ain1 and Fim1 and the myosin V Myo51 (Coffman, Nile, Lee, Liu, & Wu, 2009; Laplante et al., 2015; Laporte, Ojkic, Vavylonis, & Wu, 2012; Wu, Bahler, & Pringle, 2001).

After assembly, the CR undergoes a maturation period which prepares it for the next stage of cytokinesis. CR maturation requires the addition of several components that are necessary for both CR constriction and the coordination of constriction with septum formation (I. J. Lee, Coffman, & Wu, 2012). Also, during maturation and prior to

constriction, Mid1 leaves the CR (Sohrmann et al., 1996). Proteins accumulating at the assembled CR include unconventional myosin II Myp2, equatorial microtubule-organizing center (MTOC) controller Mto1, F-BAR proteins Imp2 and Rga7, and proteins that enable anchoring of the CR to the membrane and proper septum formation such as Fic1 and Pxl1 (Cortes et al., 2015; Demeter & Sazer, 1998; Laplante et al., 2015; Martin-Garcia, Coll, & Perez, 2014; Samejima, Miller, Rincon, & Sawin, 2010; Wu, Kuhn, Kovar, & Pollard, 2003).

CR constriction follows maturation and occurs concurrently with septum synthesis (Pollard & Wu, 2010). Though constriction is the least well understood part of cytokinesis, cellular studies and mathematical modeling indicate that constriction occurs through the force generated by randomly distributed membrane-anchored myosin II clusters (Stachowiak et al., 2014). As the CR constricts, septum synthesis counters the high turgor pressure of fission yeast and ensures membrane furrowing (Roncero & Sanchez, 2010). The septum, a specialized cell wall, is a three-layered structure composed of an inner, primary septum that is flanked by two secondary septa (Cabib, Roh, Schmidt, Crotti, & Varma, 2001; Cortes et al., 2007). Once the CR is fully constricted and the septum is formed, abscission resolves the daughter cell membranes and the primary septum is dissolved resulting in daughter cell separation (Dekker et al., 2004; Martin-Cuadrado, Duenas, Sipiczki, Vazquez de Aldana, & del Rey, 2003; Rincon & Paoletti, 2016).

1.5 The septation initiation network (SIN)

In *S. pombe,* initiation of CR constriction is linked to mitotic exit by the septation initiation network (SIN) which activates cytokinesis only when CDK activity drops in anaphase (L. Chang, Morrell, Feoktistova, & Gould, 2001; Guertin, Chang, Irshad, Gould, & McCollum, 2000). In short, the SIN is a GTPase driven kinase cascade composed of Cdc7, Sid1 with its binding partner Cdc14, and Sid2 with its coactivator Mob1 (Fig. 1-2) (Simanis, 2015b). The proteins of the SIN are anchored through a bipartite scaffold, composed of Sid4 and Cdc11, to both the old SPB, inherited from the mother cell, and the new SPB, synthesized in interphase (L. Chang & Gould, 2000; Krapp, Schmidt, Cano, & Simanis, 2001; Morrell et al., 2004; Tomlin, Morrell, & Gould, 2002). Though both SPBs act as SIN signaling hubs, they do so in an asymmetric manner (A. E. Johnson, McCollum, & Gould, 2012a).

SIN activation is controlled through the GTPase Spg1, which initiates the signaling cascade when in a GTP-bound state. Though Spg1 constitutively localizes to the scaffold protein Cdc11, it is maintained in a GDP-bound inactive state by a bipartite GTPase-activating protein (GAP) consisting of the scaffolding subunit Byr4 and the catalytic subunit Cdc16 until the cell is prepared to initiate cytokinesis (Furge et al., 1999; Furge, Wong, Armstrong, Balasubramanian, & Albright, 1998; Krapp, Collin, Cano Del Rosario, & Simanis, 2008; Morrell et al., 2004; Song, Mach, Chen, Reynolds, & Albright, 1996). Activation of Spg1 occurs through removal of the inhibitory GAP which is stimulated by the mitotic kinases Cdk1 and Plo1. Cdk1 phosphorylates Byr4 in early mitosis creating an environment permissive for cytokinesis. Then, upon localization to the scaffolding protein Sid4, Plo1 phosphorylates Byr4 stimulating

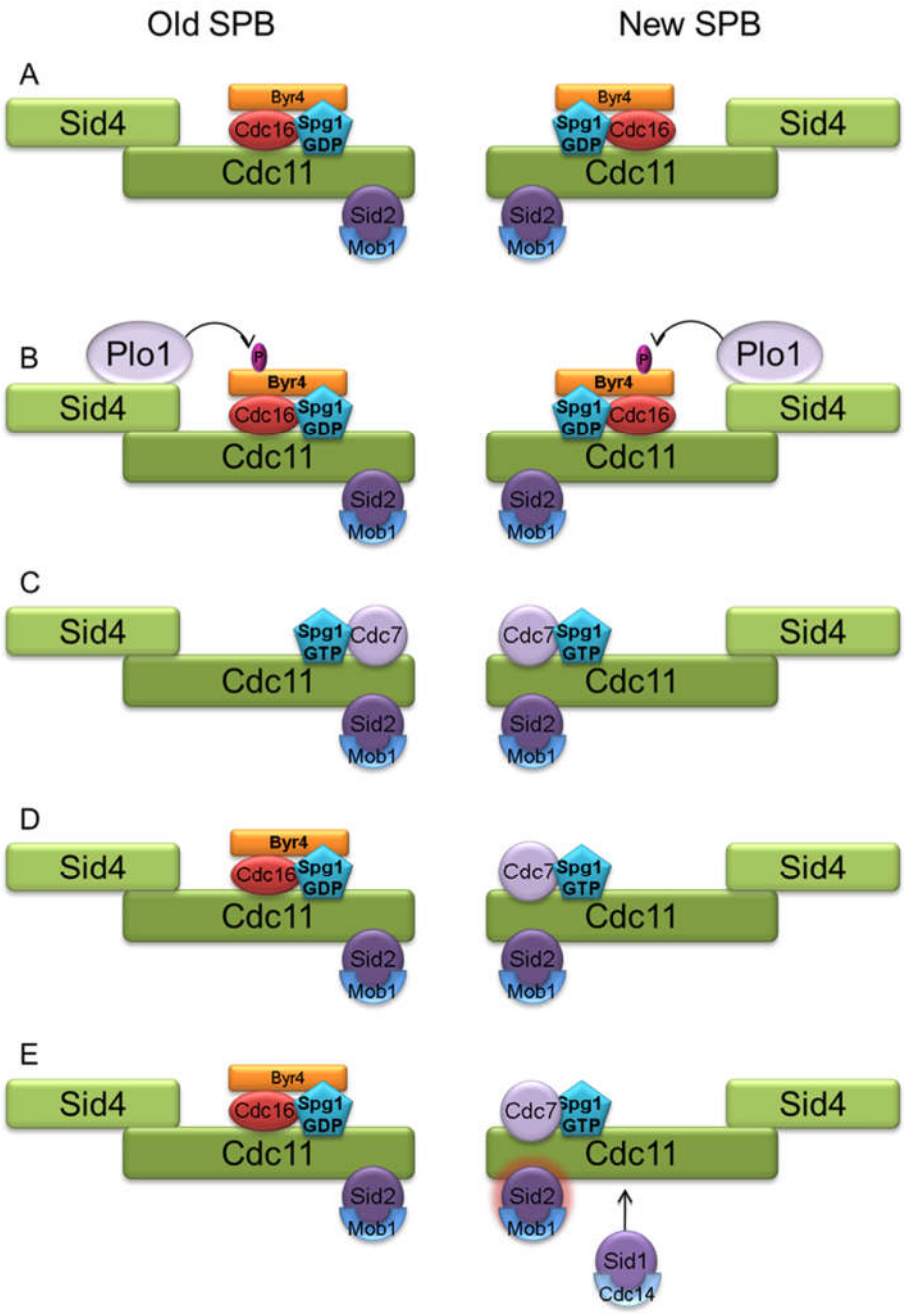

Figure 1-2
The SIN signaling pathway
In *S. pombe*, initiation of cytokinetic ring (CR) constriction is activated by the septation initiation network (SIN). A) In interphase, the GTPase Spg1, which controls SIN activation, is maintained in a GDP-bound state by the bipartite GTPase-activating protein (GAP) consisting of Byr4 and Cdc16. B) Plo1 phosphorylates Byr4, stimulating the dissociation of Byr4-Cdc16 from Spg1, allowing Spg1 to switch to the GTP-bound state. C) Cdc7 localizes to the GTP-bound Spg1 at both SPBs. D) Byr4-Cdc16 returns to Cdc11, preferentially binding the hypophosphorylated form at the old SPB. This contributes to the asymmetric localization of Cdc7 at the new SPB. E) Cdc7 localization at the new pole contributes to localization of active Sid1 and Sid2, resulting in asymmetric signaling.

dissociation of Byr4-Cdc16 from Spg1. This relieves Spg1 inhibition, allowing it to switch to the GTP-bound active state (Rachfall, Johnson, Mehta, Chen, & Gould, 2014).

As Byr4-Cdc16 dissociate from Spg1 in early mitosis, Cdc7, a member of the STE-20 family of kinases, localizes to the GTP-bound active Spg1 at both SPBs where it binds GTP-bound Spg1 and Sid2-phosphorylated Cdc11. As the mitotic spindle elongates, Byr4-Cdc16 preferentially binds hypophosphorylated Cdc11 at the old SPB, contributing to the loss of Cdc7 from the old SPB and its accumulation at the new SPB. As Cdc7 accumulates at the new SPB so does active Sid1 and Sid2, generating a positive feedback loop that results in asymmetric signaling (Fankhauser & Simanis, 1994; Krapp et al., 2008; Sohrmann, Schmidt, Hagan, & Simanis, 1998). The target of Cdc7 is not known but research in the analogous budding yeast mitotic exit network (MEN) suggests Sid2 (Mah et al., 2005).

The PAK (p21-activated kinase)-related protein kinase Sid1 and its binding partner Cdc14 localize to Spg1 at the new SPB in a Cdc7 dependent manner beginning in anaphase onset and peaking in late anaphase (Fankhauser & Simanis, 1993; Guertin et al., 2000; Guertin & McCollum, 2001). The Sid1 target(s) remains unidentified, though potential substrates include the NDR (nuclear Dbf-2-related) family protein kinase Sid2 and its co-activator Mob1. Downstream of Sid1-Cdc14, the Sid2-Mob1 complex, which localizes constitutively to both SPBs, activates at the new SPB in a Sid1 and Cdc7 dependent manner. Sid2 kinase activity requires Mob1 association which in turn requires phosphorylation of Sid2 (Fig. 1-2). The kinase that phosphorylates Sid2 is not known, but is likely Cdc7 and/ or Sid1 (Hou, Guertin, & McCollum, 2004; Hou, Salek, & McCollum, 2000; Sohrmann et al., 1998; Sparks, Morphew, & McCollum, 1999). Sid2-

Mob1 also localize to the division site and, as the terminal kinase of the SIN signaling cascade, Sid2 activity at the division site likely drives CR assembly and constriction. Though there are several identified targets of Sid2 at the CR (Gupta et al., 2013), only three have been characterized including Clp1, Cdc12, and Cdr2. While cells exhibit cytokinetic defects in the absence of Sid2 mediated phosphorylation of Clp1, Cdc12 and Cdr2, none of the phosphorylations are essential and thus other Sid2 CR targets are likely responsible for CR assembly and constriction (Bohnert et al., 2013; C. T. Chen et al., 2008).

The SIN is a conserved protein network homologous to the *Saccharomyces cerevisiae* MEN and the mammalian Hippo pathway. Similar to the SIN, the MEN regulates cytokinesis and mitotic exit, while the Hippo pathway regulates cell growth and proliferation. These three pathways exhibit several common core components including, a scaffold, an inhibitory GAP, an activating Polo kinase, a Ste20 protein kinase, and an NDR-family kinase. However, compared with these pathways, the SIN contains an additional kinase module consisting of the PAK-related protein kinase Sid1 and its binding partner Cdc14. Determining whether signaling through these pathways parallels one another at a molecular level requires further investigation (A. E. Johnson, McCollum, et al., 2012a; Simanis, 2015b).

1.6 The mitotic checkpoint protein Dma1

Proper coordination of anaphase onset, mitotic exit, and cytokinesis are essential to ensure accurate segregation of chromosomes. In the event of a mitotic spindle error,

several mechanisms act simultaneously to sufficiently delay each process. Anaphase onset and mitotic exit are delayed by the kinetochore-dependent spindle assembly checkpoint (SAC), which targets the APC to prevent securin and cyclin B destruction (discussed above) (Musacchio, 2011). Conversely, cytokinesis is delayed by a kinetochore-independent pathway (Alexandru, Zachariae, Schleiffer, & Nasmyth, 1999; Beltraminelli, Murone, & Simanis, 1999; Gardner & Burke, 2000). In *S. cerevisiae* this genetically independent pathway is Bub2/Cdc16-dependent and localized to the SPBs (Fesquet et al., 1999; Fraschini, Formenti, Lucchini, & Piatti, 1999; R. Li, 1999). Similarly, in *S. pombe* inhibition of cytokinesis occurs through a SPB-based checkpoint pathway that targets the SIN (Guertin, Venkatram, Gould, & McCollum, 2002; A. E. Johnson, McCollum, et al., 2012a).

In order to identify additional components of the spindle checkpoint in fission yeast, Simanis and Murone performed a genetic screen for multi-copy suppressors of the *cdc16-116* temperature sensitive mutant, which lacks Spg1 inhibition and results in multi-septated cells when shifted to the restrictive temperature. Through this study they discovered Dma1 (defective in mitotic arrest), a non-essential FHA and RING domain containing protein required for cell cycle arrest in the event of impaired mitotic spindle assembly. Specifically, when exposed to mitotic spindle stress, wild-type cells inhibited cytokinesis enabling proper cell cycle coordination, and Dma1-deficient cells continued through cytokinesis resulting in aneuploidy and cell death (Murone & Simanis, 1996). Examination of mitotic checkpoint defects in the spindle checkpoint mutant *dma1Δ* and the SAC mutant *mad2Δ* showed that both mutants bypassed the checkpoint with similar kinetics and the double *dma1Δ mad2Δ* mutant exhibited an additive checkpoint defect

phenotype (A. E. Johnson, Chen, & Gould, 2013a). Thus, consistent with experiments in budding yeast, Dma1-dependent inhibition of cytokinesis is genetically independent of the SAC.

Additional research utilizing microscopy, biochemistry, and proteomics defined the molecular mechanism of Dma1 activity in the spindle checkpoint. In the event of impaired mitotic spindle assembly, the *S. pombe* CK1 homologs Hhp1 and Hhp2 phosphorylate the SIN scaffold protein, Sid4. Dma1 binds phosphorylated Sid4 through its FHA domain and then ubiquitinates Sid4 through its RING domain, antagonizing Plo1 localization. This prevents Plo1 phosphorylation of its downstream target Byr4 and the subsequent activation of the SIN kinase cascade delaying cytokinesis (Fig. 1-3) (A. E. Johnson et al., 2013a; A. E. Johnson & Gould, 2011b).

Further characterization showed Dma1 is a homodimer and that dimerization requires residues in both its RING domain and C-terminal tail. Moreover, dimerization of Dma1 is required for its proper localization, Sid4 ubiquitination *in vivo*, and Dma1 auto-ubiquitination *in vitro* (A. E. Johnson, Collier, Ohi, & Gould, 2012a). In addition, Dma1 is regulated, in part, through interaction with Dnt1, a poorly characterized inhibitor of the SIN. In the absence of Dnt1 Dma1 localization to SPBs and E3 ligase activity are slightly increased (Y. Wang et al., 2012b). However, as accurate temporal coordination of cytokinesis with mitotic exit requires both the delay of cytokinesis in the event of mitotic spindle stress and checkpoint resolution upon error correction, it is likely that Dma1 is regulated through additional means.

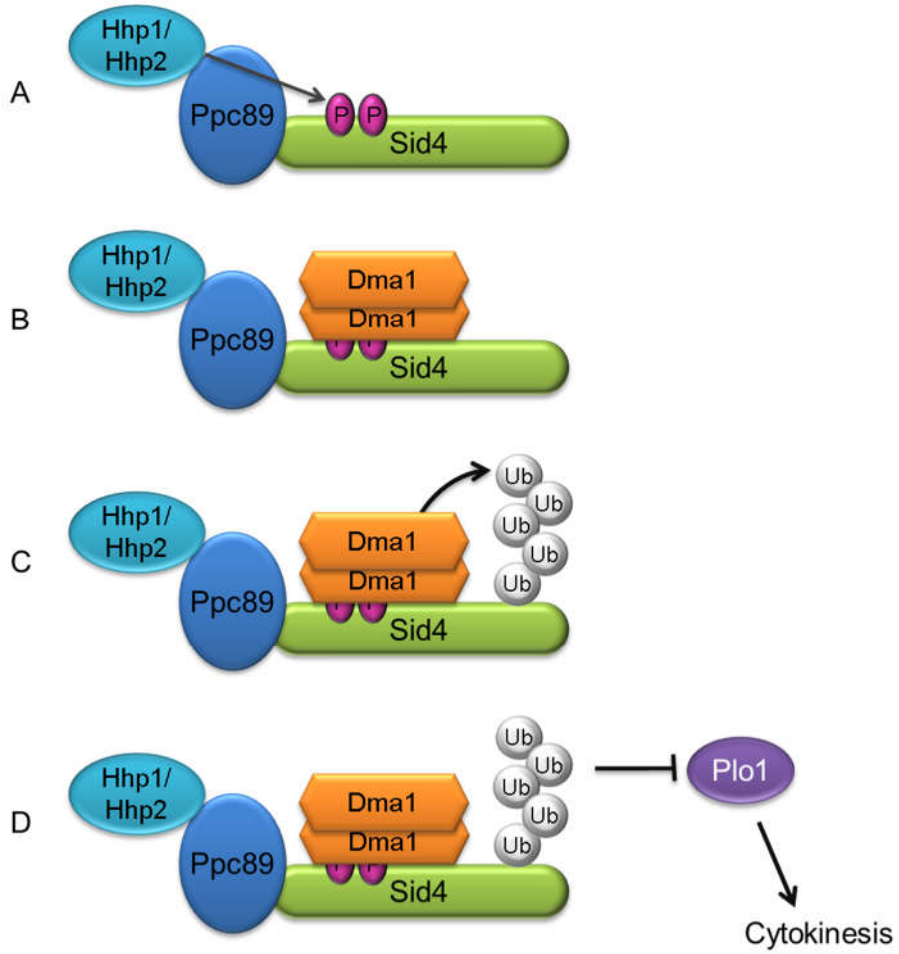

Figure 1-3
The molecular mechanism of Dma1 in the spindle checkpoint
Dma1 inhibits the SIN in response to mitotic spindle stress. A) Hhp1 and Hhp2 phosphorylate the SIN scaffold protein Sid4 at T275 and S278. B) Dma1, an obligate dimer, binds phosphorylated Sid4 through its FHA domain. C) Dma1 ubiquitinates Sid4 with its RING domain. D) Ubiquitination of Sid4 prevents Plo1 localization and subsequent activation of the SIN kinase cascade delaying cytokinesis.

1.7 The FHA-RING class of proteins

Dma1 is the only *S. pombe* member of the FHA-RING class of proteins, a small class of proteins that function in cell cycle checkpoints. While many proteins contain either an FHA or a RING domain, only five characterized proteins contain both an FHA domain, which directs binding to phosphorylated threonines, and a RING domain, which

confers E3 ubiquitin ligase activity. These proteins include the *S. pombe* homolog Dma1 (discussed above), the two functionally redundant *Saccharomyces cerevisiae* homologues Dma1 and Dma2, and the two mammalian paralogs CHFR and RNF8 (Brooks, Heimsath, Loring, & Brenner, 2008).

The *S. cerevisiae* proteins Dma1 and Dma2 function in the MEN (discussed above) to control septin dynamics and the spindle positioning checkpoint (SPOC) by promoting the efficient recruitment of Elm1 to the bud neck (Cassani et al., 2013; Fraschini, Bilotta, Lucchini, & Piatti, 2004; Merlini et al., 2012). In addition, the budding yeast Dma proteins are required for proper formin distribution and subsequent assembly of a robust actin cable network as well as accurate detachment of the vacuole from Myo2 (Juanes & Piatti, 2016; Yau et al., 2014).

The mammalian homolog CHFR is expressed ubiquitously in normal human tissues and functions in the antephase checkpoint to ensure accurate cell division when cells are exposed to cold temperatures, osmotic shock, or microtubule poisons (Kang, Chen, Wong, & Fang, 2002; Scolnick & Halazonetis, 2000). This checkpoint enables cells in early mitosis, that have not yet undergone nucleolar breakdown, to transiently return to antephase, the period in early prophase prior to chromosome condensation (Mikhailov & Rieder, 2002; Rieder & Cole, 2000; Rieder & Cole, 1998). The CHFR mechanism of action has not been well characterized but data indicate that it targets the Plo1 homologue Plk1, activates p38, and excludes Cyclin B from the nucleus (Burgess et al., 2008; Matsusaka & Pines, 2004; Mikhailov, Shinohara, & Rieder, 2005; Summers, Bothos, & Halazonetis, 2005). Additionally, studies show CHFR is post translationally

modified by both phosphorylation and ubiquitination (Kim et al., 2011; Sanbhnani & Yeong, 2012).

RNF8 supports accurate cell division through functions in both interphase and mitosis. During interphase RNF8 localizes to DNA double-strand breaks (DSBs), where it binds to ATM phosphorylated MDC1 and facilitates K63-linked ubiquitination of histones. This ubiquitination is necessary for the subsequent recruitment of RNF168 and downstream repair factors (Huen & Chen, 2010; Luijsterburg & van Attikum, 2012; Mattiroli et al., 2012; Nakada, Yonamine, & Matsuo, 2012). During mitosis RNF8 stabilizes Tpp1 to promote telomere maintenance and end protection (Rai et al., 2011). Additionally, during mitosis RNF8 is phosphorylated, inhibiting its recruitment to DSB sites which in turn protects against telomere fusions (Orthwein et al., 2014; Peuscher & Jacobs, 2011).

The importance of FHA-RING proteins to the maintenance of genome integrity is highlighted by studies using knockout mice. CHFR $^{-/-}$ mice form tumors when exposed to low doses of carcinogens (Yu et al., 2005), while RNF8 $^{-/-}$ mice are predisposed to cancer (L. Li et al., 2010). Furthermore, CHFR is epigenetically silenced in a variety of human tumors including lung, colorectal, and nasopharyngeal cancers (Chaturvedi et al., 2002; Cheung et al., 2005; Corn et al., 2003; Erson & Petty, 2004; Mariatos et al., 2003). Thus, though these proteins are not essential for cell viability, their roles in checkpoints are necessary to protect cells from stressors and ensure accurate and faithful cell division. Determining the mechanism of Dma1 regulation in the spindle checkpoint may provide insights into the general mechanisms of FHA-RING protein regulation as the processes governing the *S. pombe* cell cycle are largely conserved.

The importance of FHA-RING proteins to the maintenance of genome integrity is highlighted by studies using knockout mice. CHFR $^{-/-}$ mice form tumors when exposed to low doses of carcinogens and show increased incidence of spontaneous tumor formation (Yu et al., 2005), while RNF8 $^{-/-}$ mice are predisposed to cancer (L. Li et al., 2010). Furthermore, CHFR is epigenetically silenced in a variety of human tumors including lung, colorectal, and nasopharyngeal cancers (Chaturvedi et al., 2002; Cheung et al., 2005; Corn et al., 2003; Erson & Petty, 2004; Mariatos et al., 2003). Thus, though these proteins are not essential for cell viability, their roles in checkpoints are necessary to protect cells from stressors and ensure accurate and faithful cell division. Determining the mechanism of Dma1 regulation in the spindle checkpoint may provide insights into the general mechanisms of FHA-RING protein regulation as the processes governing the *S. pombe* cell cycle are largely conserved.

1.8 Phospho-dependent binding through FHA domains

Protein phosphorylation occurs when an amino acid, typically a threonine, serine, or tyrosine residue, is modified with the covalent addition of a phosphate group (PO_4^{-3}) in an esterification reaction mediated by a protein kinase. This modification can in turn be removed through hydrolysis mediated by a protein phosphatase. Phosphorylation has a substantial impact on the charge and structure of the modified amino acid and as such can create protein binding sites, disrupt protein-protein interactions, or introduce allosteric effects. Furthermore, protein phosphorylation is integral to cellular signal transduction, which requires both the modifying enzymes as well as protein interaction domains to

recognize the modified substrates (Bohnert & Gould, 2011; Holt, 2012; Hunter, 2007). Forkhead-associated (FHA) facilitate such phosphorylation-dependent protein interactions exhibiting strict specificity for phosphothreonine (pT)-containing motifs (Durocher et al., 2000). FHA domains have been identified in thousands of proteins and have exhibited operational roles in a wide range of processes including cell growth, cell cycle regulation, differentiation, programmed cell death, and DNA repair (Mahajan et al., 2008).

The tertiary structure of all FHA domains is a large twisted β-sandwich of six-stranded and five-stranded β-sheets (Durocher & Jackson, 2002). Despite the structural conformity displayed across FHA domains, this approximately 100 amino acid fold exhibits low sequence homology and contains only five conserved residues. The conserved residues, which are all found in the binding surface of the β-sandwich, work in combination with non-conserved residues to stabilize the domain structure and bind the phospho-peptide (Almawi, Matthews, & Guarne, 2016; Liang & Van Doren, 2008).

FHA domains bind the phospho-peptide through interactions with both the pT residue and additional substrate residues. Binding to the pT occurs through interactions with the phosphate group as well as the threonine methyl group, which likely accounts for the strict pT requirement as it is the only phosphorylated residue containing a methyl group in the side chain (Durocher et al., 2000). The FHA domain binding site is comprised of loops connecting the eleven β-stands of the FHA domain which can vary substantially by length and/or the presence of an α-helix. The interactions and associated movements between these loops define the shape of the binding site and dictate the

preferred recognition sequences, and therefore the specific substrates, of each FHA domain. Because the binding site-peptide interactions involve complicated conformations of moderately rigid loops, the FHA domain family displays a wide range of substrate variability while maintaining phosphopeptide recognition specificity (Huang & Chang, 2014; Mahajan et al., 2008). Accordingly, FHA domains do not recognize a universal consensus sequence; however, there are a few broad categories of substrate selection. The first is based on the pT+3 rule wherein the amino acid in the third position C-terminal to the pT governs binding specificity for either negatively charged or branched hydrophobic residues. The other two categories of substrate selection include recognition of residues both N-terminal and C-terminal to the pT, and recognition of an extended binding surface. The diverse ligand binding specificity these domains exhibit provides structural and functional versatility to FHA domain containing proteins (Liang & Van Doren, 2008; Mahajan et al., 2008).

FHA domain binding is not only phosphorylation-dependent, indicating the presence of an upstream kinase, it is also characterized by low micromolar dissociation constants, indicating fast off-rates (Huen et al., 2007). Together these properties are ideal for checkpoint signaling, which requires a rapid and reversible response to a biochemical signal. In fact, the checkpoint function of all characterized FHA-RING proteins requires an intact FHA domain (Brooks et al., 2008). For example, in the absence of a functional FHA domain, Dma1 does not exhibit proper localization or Sid4 ubiquitination *in vivo*, and thus lacks checkpoint activity (Guertin et al., 2002; A. E. Johnson & Gould, 2011b).

The FHA domain-binding interaction, which requires phosphorylation of the binding partner, can also be regulated by phosphorylation of the FHA domain containing

protein. Phosphorylation of the FHA domain near the phospho-peptide binding site can prevent binding, presumably by disrupting the ionic interactions necessary for pT binding. This is seen in Plk1 phosphorylation of the Chk2 FHA domain, which abolishes its binding to phospho-peptide ligands (van Vugt et al., 2010). Alternatively, phosphorylation of the FHA domain containing protein, outside the FHA domain itself, can create an intramolecular phospho-ligand that binds the FHA domain and results in auto-inhibition. This is seen in PknB and PknG phosphorylation of the Rv1827 N-terminus, which generates an intramolecular interaction between the Rv1827 FHA domain and phosphorylated threonines in its own N-terminus, preventing interaction between Rv1827 and its target enzymes (Nott et al., 2009). These phosphorylation events provide additional mechanisms of regulating FHA domain binding interactions which may prove relevant to their roles in checkpoint activation and resolution.

1.9 Ubiquitination through RING E3 ligases

RING domain E3 ligases function in the ubiquitination enzyme cascade to covalently modify proteins with the small regulatory protein ubiquitin. This cascade consists of an E1 activating enzyme, an E2 conjugating enzyme, and an E3 ligating enzyme; as a whole, the cascade attaches the carboxyl terminus of ubiquitin to the amino group of a lysine residue in the target protein via an isopeptide bond. E3 ubiquitin ligases facilitate the transfer of ubiquitin from an E2 to a target protein and are characterized by the presence of either a HECT domain or a RING domain. HECT domain ligases accept

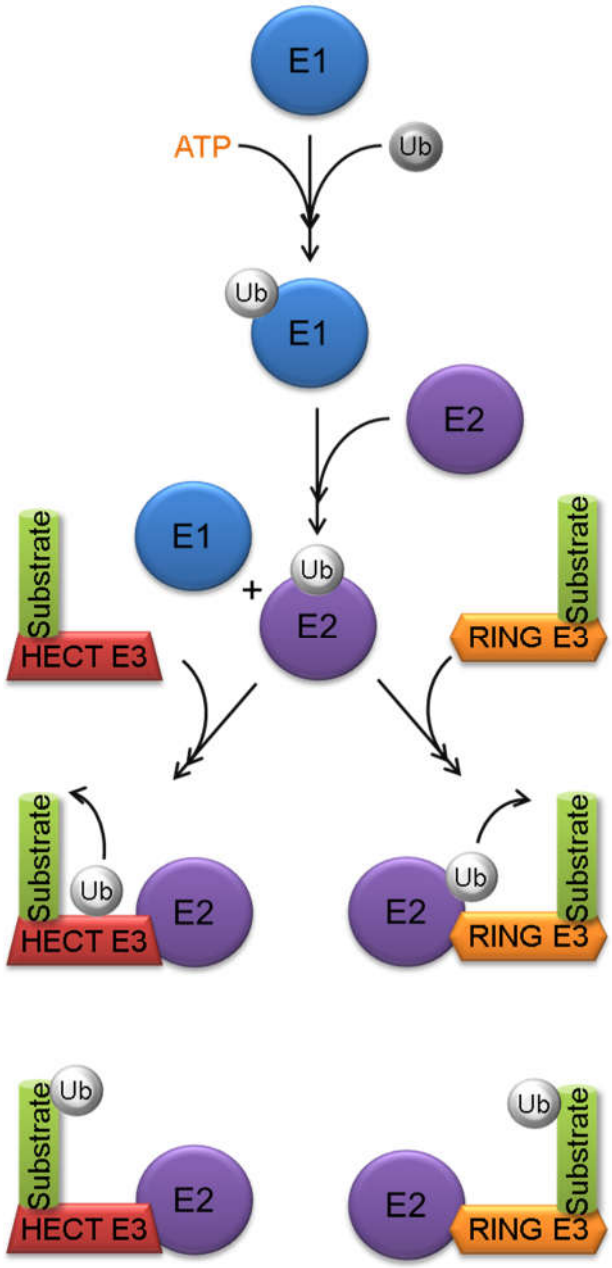

Figure 1-4
The ubiquitination enzyme cascade with HECT vs RING E3 ligases
Ubiquitin is activated by an E1 (ubiquitin-activating enzyme). Activated ubiquitin is transferred to an E2 (ubiquitin-conjugating enzyme). The E2~ubiquitin interacts with an E3 (ubiquitin-ligating enzyme) to transfer Ub from the E2 to a lysine residue of a substrate. HECT E3s bind the E2 and accept the ubiquitin, forming a covalent E3~ubiquitin intermediate. HECT E3s then transfer the ubiquitin to the substrate (left pathway). RING E3s bind the E2 and promote the formation of a closed active conformation. The activated E2 then transfers the ubiquitin to the substrate (right pathway).

ubiquitin, forming a covalent E3~ubiquitin intermediate, prior to substrate ubiquitination. In contrast, RING domain ligases facilitate the direct transfer of ubiquitin from the E2 to the substrate without ever accepting the ubiquitin (Deshaies & Joazeiro, 2009). RING domain E3 ligases function in this transfer to both provide substrate selectivity and promote E2 activation through direct binding interactions with both the substrate and the E2. The substrate binds the E3 outside the RING domain, typically through a protein interaction domain, while the E2 binds a shallow cleft on the surface of the RING domain. Upon binding the E2, an intermolecular E3:E2 hydrogen bond forms and causes allosteric effects within the E2. Consequently, the E2~ubiquitin complex adopts a closed active conformation that promotes ubiquitin transfer to the bound substrate (Fig. 1-4) (Pruneda et al., 2012).

Substrate ubiquitination occurs in a variety of forms including mono-ubiquitination through the attachment of a single ubiquitin to a single lysine residue, multi-ubiquitination through the attachment of a single ubiquitin to multiple lysine residues, or poly-ubiquitination though the attachment of a ubiquitin chain to one or more lysine residues. Poly-ubiquitin chains contain multiple ubiquitin moieties connected to each other through one of seven internal lysines (K6, K11, K27, K29, K33, K48, and K63) or the N-terminus, and can be comprised of homogeneous or heterogeneous linkages in either linear or forked arrays. The various forms of ubiquitination impact the modified protein in different ways. For example, K48 linked poly-ubiquitin chains typically mark proteins for degradation through the proteasome system, while K63 linked poly-ubiquitin chains effect checkpoint signaling and protein activation (Heride, Urbe, & Clague, 2014).

Because the numerous ubiquitin modifications have substantial and differing effects on the target protein, E3 ligases experience several forms of regulation that ensure accurate substrate selection and appropriate ubiquitination. Post translational modifications are used to control several aspects of the ubiquitination cascade including substrate binding, E2:E3 interaction, and enzyme activation. In addition, RING domain ligases can be regulated through binding partners and competing pseudo substrates (Hunter, 2007).

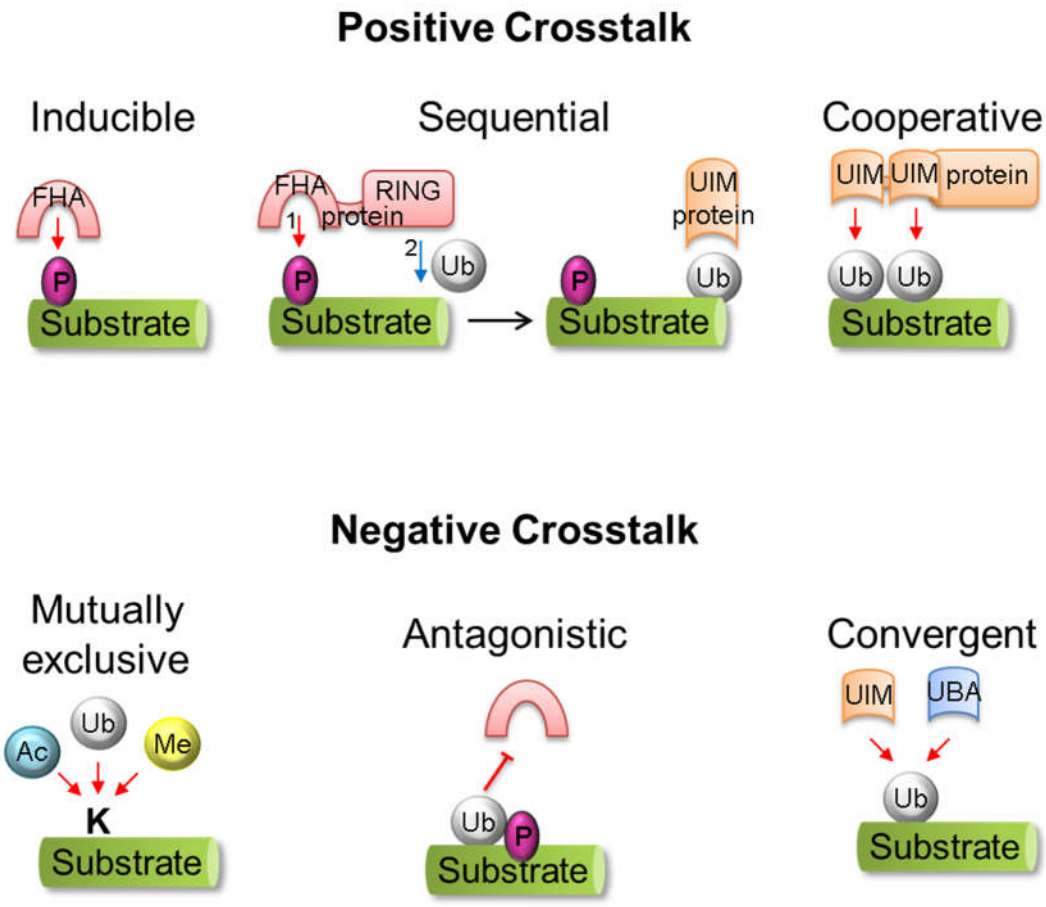

Figure 1-5
Post-translational modification (PTM) crosstalk
PTMs can act in concert through positive or negative crosstalk. (Top) Positive crosstalk includes inducible interactions (left), sequential PTM-dependent interactions (center), and cooperative interactions (right). (Bottom) Negative crosstalk includes mutually exclusive interactions (left), antagonistic interactions (center), and convergent interactions (right). Examples shown are based on hypothetical interacting partners.

1.10 Post-translational modification (PTM) crosstalk

In addition to protein modification with a single PTM, such as phosphorylation or ubiquitination, multiple PTMs can act in concert through positive or negative crosstalk. Positive crosstalk occurs when a PTM facilitates additional modification(s), and includes singular and sequential PTM-dependent interactions, and cooperative interactions. Conversely, negative crosstalk occurs when a PTM or PTM-dependent interaction prevents subsequent modification or PTM-dependent interaction and can be either mutually exclusive, antagonistic, or convergent (Fig. 1-5) (Seet, Dikic, Zhou, & Pawson, 2006).

Cross talk between phosphorylation and ubiquitination is central to the spatial and temporal regulation of FHA-RING proteins. Examples of both PTM-dependent positive and negative crosstalk are clearly demonstrated in the spindle checkpoint. PTM-dependent positive crosstalk is seen in the phosphorylation-dependent recruitment of Dma1 that leads to ubiquitination of Sid4. This is followed by PTM-dependent negative crosstalk as ubiquitination of Sid4 prevents Plo1 localization and subsequent phosphorylation if it's downstream target Byr4 (A. E. Johnson et al., 2013a; A. E. Johnson & Gould, 2011b).

However, as the delay in cell cycle progression induced by the spindle checkpoint is transient, the Dma1-dependent checkpoint signal must be withdrawn to allow checkpoint resolution. The mechanisms by which Dma1 is removed from SPBs and ubiquitination of Sid4 is reversed are not known, yet these processes are also likely facilitated through phosphorylation and ubiquitination crosstalk.

1.11 Summary

In this work I addressed the major outstanding question regarding Dma1 regulation: how is Dma1 regulated to not only quickly and efficiently activate the checkpoint in response to stress, but also allow cytokinesis to proceed in the absence of stress or upon resolution of an activating stress? In Chapter 2, I characterized Dma1 SPB localization dynamics and explored the mechanisms regulating removal of Dma1 from the SPB, showing that Dma1 localization dynamics are impaired in the absence of Dma1 auto-ubiquitination. Thus, indicating that Dma1 auto-ubiquitination enables the release of Dma1 from the SPBs, at which point it is no longer positioned to activate the checkpoint. In Chapter 3, I examined regulation of Dma1 activity through phosphorylation, showing phosphorylation of specific residues prevents Dma1 auto-ubiquitination without impairing Dma1 substrate ubiquitination. Combined with the findings outlined in Chapter 2, this may provide a mechanism by which the checkpoint can be efficiently maintained, as Dma1 continues to ubiquitinate Sid4 without auto-ubiquitination releasing it from the SPB. Together, these findings clarify the mechanisms by which the spindle checkpoint response is both efficiently activated and also removed upon resolution of mitotic stress.

Chapter 2

Regulation of Dma1 localization

2.1 Introduction

Accurate cell division, yielding two genetically identical daughter cells, requires coordination between mitosis and cytokinesis. In the fission yeast *Schizosaccharomyces pombe,* the septation initiation network (SIN), a protein kinase cascade, coordinates these two events by initiating cytokinesis after chromosome segregation (for review see (A. E. Johnson, McCollum, & Gould, 2012b; Krapp & Simanis, 2008; Simanis, 2015a)). When there is a mitotic error, a checkpoint mechanism inhibits SIN signaling to prevent cytokinesis from occurring before chromosomes have safely segregated (Guertin et al., 2002; A. E. Johnson & Gould, 2011a; Marks, Fankhauser, & Simanis, 1992; Murone & Simanis, 1996). This checkpoint operates in parallel to the spindle assembly checkpoint (A. E. Johnson, Chen, & Gould, 2013b; Murone & Simanis, 1996; Musacchio, 2015).

SIN inhibition during a mitotic error depends on the dimeric E3 ubiquitin ligase Dma1, a member of the FHA and RING finger family (Brooks et al., 2008). Dma1 was identified as a high copy suppressor of a hyperactive SIN mutant and it is required to prevent septation during a prometaphase arrest elicited by the ß-tubulin mutant *nda3-km311* (Hiraoka, Toda, & Yanagida, 1984; Murone & Simanis, 1996). Overproduction of Dma1 completely blocks SIN activity and results in cell death (Guertin et al., 2002),

indicating its levels and activity must be properly regulated. Dma1 co-localizes with SIN components both at the cell division site and at the mitotic spindle pole body (SPB) (Guertin et al., 2002), however it is Dma1's SPB localization and its ubiquitination of the SIN scaffold protein, Sid4 (L. Chang & Gould, 2000; Morrell et al., 2004), that is required for SIN inhibition during a mitotic checkpoint (A. E. Johnson & Gould, 2011a). Sid4 ubiquitination antagonizes the SPB localization of the Polo-like kinase Plo1 (Guertin et al., 2002; A. E. Johnson & Gould, 2011a), the major SIN activator (Mulvihill, Petersen, Ohkura, Glover, & Hagan, 1999; Ohkura, Hagan, & Glover, 1995; Tanaka et al., 2001) so that SIN signaling is attenuated and cytokinesis is delayed.

Upon resolution of the mitotic spindle error, the Dma1-dependent checkpoint signal must be extinguished in order to resume SIN activation and cell division. Here we report that Dma1 exhibits striking fluctuations in its localization to SPBs and the cell division site during the cell cycle. We found that both SIN activity and Dma1 auto-ubiquitination modulate its SPB localization dynamics and therefore its ability to inhibit the SIN. Further, by permanently tethering Dma1 to SPBs and preventing these fluctuations, the SIN fails to become active and cells fail cytokinesis. Therefore, Dma1's dynamic SPB localization is a critical feature of *S. pombe* cytokinesis.

2.2 Results

Dma1's E3 ligase activity impacts its abundance and localization

Consistent with previous literature (Guertin et al., 2002; A. E. Johnson & Gould, 2011a), we observed that Dma1 tagged at its endogenous locus with mNeonGreen

(mNG) (Shaner et al., 2013; Willet et al., 2015a) (Fig. 2-1A) concentrates at SPBs during mitosis, where it is required for SIN inhibition (Guertin et al., 2002). We also observed localization at cell tips during interphase and at the division site during mitosis and cytokinesis. Given that wildtype Dma1 did not appear to localize to SPBs during the majority of interphase (Fig. 2-1A), we sought to identify the mechanism(s) that influences Dma1 SPB targeting.

Because Dma1 localization changes over the course of the cell cycle, we undertook time-lapse imaging experiments to clarify the timing of Dma1 localization to the SPB and cell division site. Dma1-mNG became enriched at SPBs prior to SPB separation (Fig. 2-1B and Fig. 2-S1A). Unexpectedly, at the onset of mitosis, Dma1-mNG appeared in node-like structures, a pattern previously undetected for Dma1 (Guertin et al., 2002), before forming a ring at the division site (Fig. 2-1B). Then, Dma1-mNG appeared to transiently leave SPBs during anaphase B, returning to them before telophase and then leaving again after cell division; similarly, Dma1-mNG was observed to leave and then return to the division site although with delayed kinetics (mins 18-26) compared to what was observed at SPBs (mins 14-16) (Fig. 2-1B and C, Fig. 2-S1A and B). In 24 out of 28 (86%) mitotic SPBs, Dma1-mNG signal transiently dimmed or became undetectable whereas the SPB markers Sid4-mCherry or Sad1-mCherry did not. Dma1 SPB dimming occurred within 2 minutes of anaphase B onset in 90% of cells showing this phenomenon, and it returned to SPBs in all cases before the end of anaphase B, marked by maximal SPB separation, and then left again at cell division. In a few cases, the Dma1 signal was observed to "flicker" on and off a SPB during anaphase B and to shift in intensity between the two SPBs.

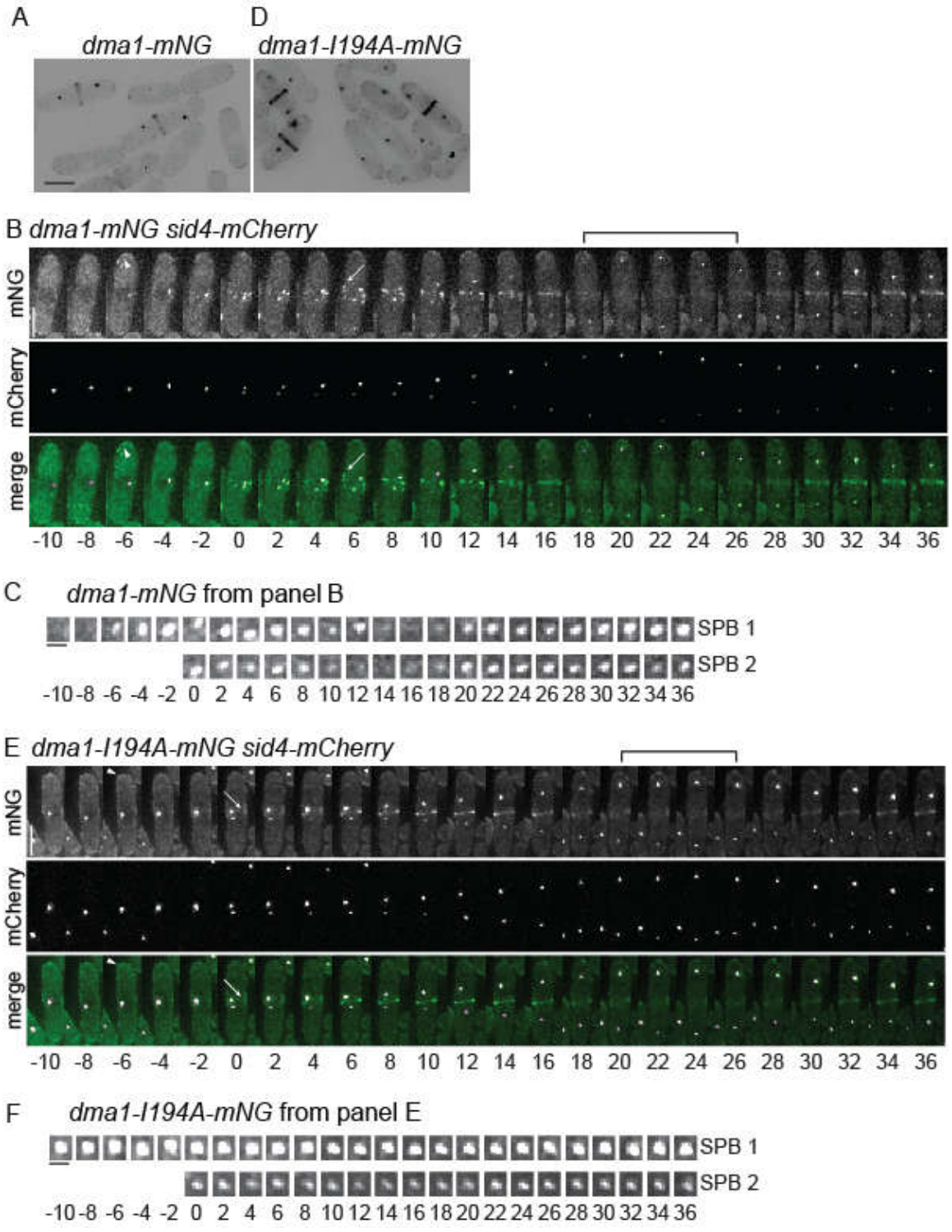

Figure 2-1
Dynamics of Dma1 localization through the cell cycle.
(A and D) Live cell images of *dma1-mNG* (A) and *dma1-I194A-mNG* (D). Scale bar, 5 μm. (B and E) Images from representative movies of *dma1-mNG sid4-mCherry* (B) and *dma1-I194A-mNG sid4-mCherry* (E). Arrows indicate Dma1 localization in cytokinetic node-like structures. Arrowheads indicate Dma1

localization to cell tips. Brackets indicate times of reduced Dma1 detection at the division site. Time in minutes denoted below images; 0 indicates initial frame of SPB separation. Scale bars, 5 µm. (C and F) Enlarged SPB region(s) from movies in B and E. Scale bars, 1 µm.

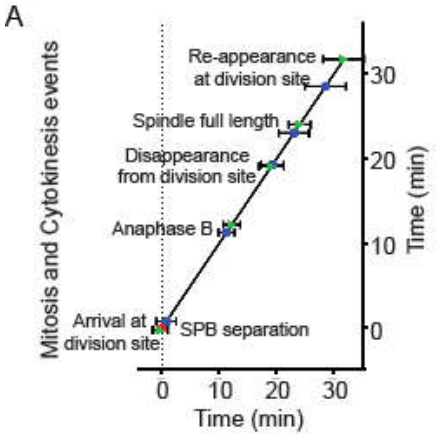

	Dma1-mNG (minutes)	Dma1-194A-mNG (minutes)
Onset of anaphase B	11.3 ± 1.4	12.1 ± 1.5
Maximal SPB separation	23.0 ± 2.6	24.0 ± 1.9
Arrival to the division site	0.75 ± 1.7	-0.31 ± 1.3
Loss from the division site	19.3 ± 2.0	19.1 ± 2.2
Re-accumulation at the division site	28.5 ± 3.6	31.7 ± 3.6

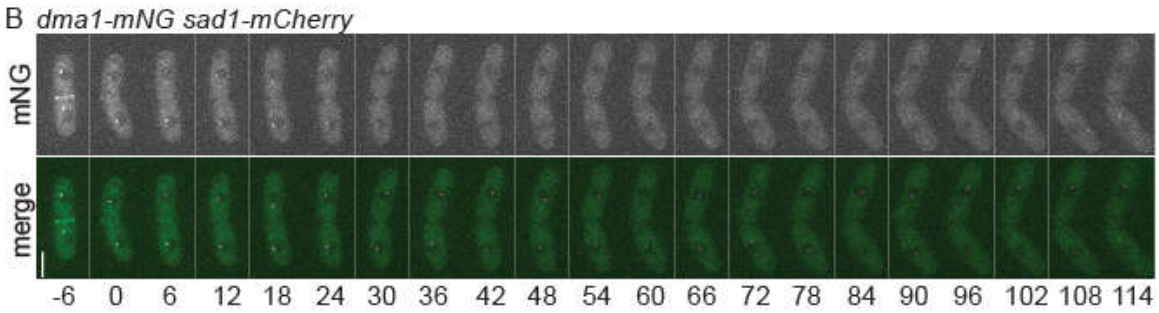

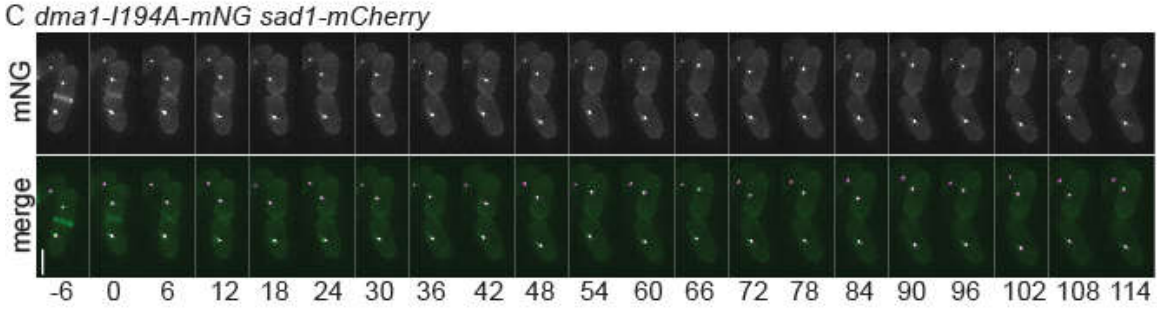

Figure 2-1 sup
Timing of Dma1 localization relative to mitotic events.
(A) (Left, graph) Time line showing the detection of Dma1-mNG (blue circles) and Dma1-I194A-mNG (green triangles) at the division site. Time 0 was defined as SPB separation (red star), and the mean time of detection of each event ± SD is plotted. (Right, table) Average times (minutes) for each strain (top of column) for the onset of anaphase B, maximum SPB separation (end of anaphase B), arrival to the division site, loss from the division site and re-accumulation at the division site. Timing of Dma1-mNG events were determined from 8 cells and Dma1-I194A-mNG events were determined from 13 cells. (B-C) Images from representative movies of dividing *dma1-mNG sad1-mCherry* (B) and *dma1-I194A-mNG sad1-mCherry* (C) cells. Time in minutes denoted below images, 0 indicates initial frame that physical separation of daughter cells began. Scale bars, 5 µm.

Interestingly, in contrast to wildtype Dma1, we found that the Dma1-I194A mutant, which lacks ubiquitin ligase activity due to a mutation in the RING-finger domain (A. E. Johnson & Gould, 2011a), was detectable at SPBs throughout the cell cycle when it was tagged with mNG (Fig. 2-1D) or GFP (unpublished observations, C.M.J. and J-S.C.) at its C-terminus, or either fluorophore at its N-terminus (unpublished observations, J-S.C.). Dma1-I194A-mNG signal persisted at SPBs throughout the cell cycle, only detectably dimming at 14% of mitotic SPBs, although its dynamic localization at the cell division site appeared like wildtype (Fig. 2-1E and Fig. 2-S1C). Also, in 20 of 20 cells Dma1-I194A-mNG localized more intensely at one of the two SPBs for most of mitosis (Fig. 2-1E and F). Thus, Dma1 localization is more dynamic than previously appreciated, and Dma1 catalytic activity affects its dynamics at SPBs.

Sid4 ubiquitination does not impact Dma1 accumulation at SPBs

To determine why Dma1-I194A was less dynamic at SPBs during mitosis than Dma1, we examined whether the ubiquitination status of either of Dma1's two known substrates, Sid4 and Dma1 itself (A. E. Johnson & Gould, 2011a), modulated its localization. To investigate if the absence of Sid4 ubiquitination promoted Dma1 localization to SPBs, we first needed to develop a mutant strain in which Sid4 ubiquitination was abrogated. The canonical approach is to replace target lysines with arginines; however, previous attempts to construct such a Sid4 variant were unsuccessful (A. E. Johnson et al., 2013b; A. E. Johnson & Gould, 2011a). We therefore turned to a

method described previously to eliminate ubiquitination of a protein of interest—fusion to a deubiquitinating enzyme (DUB) catalytic domain (Stringer & Piper, 2011).

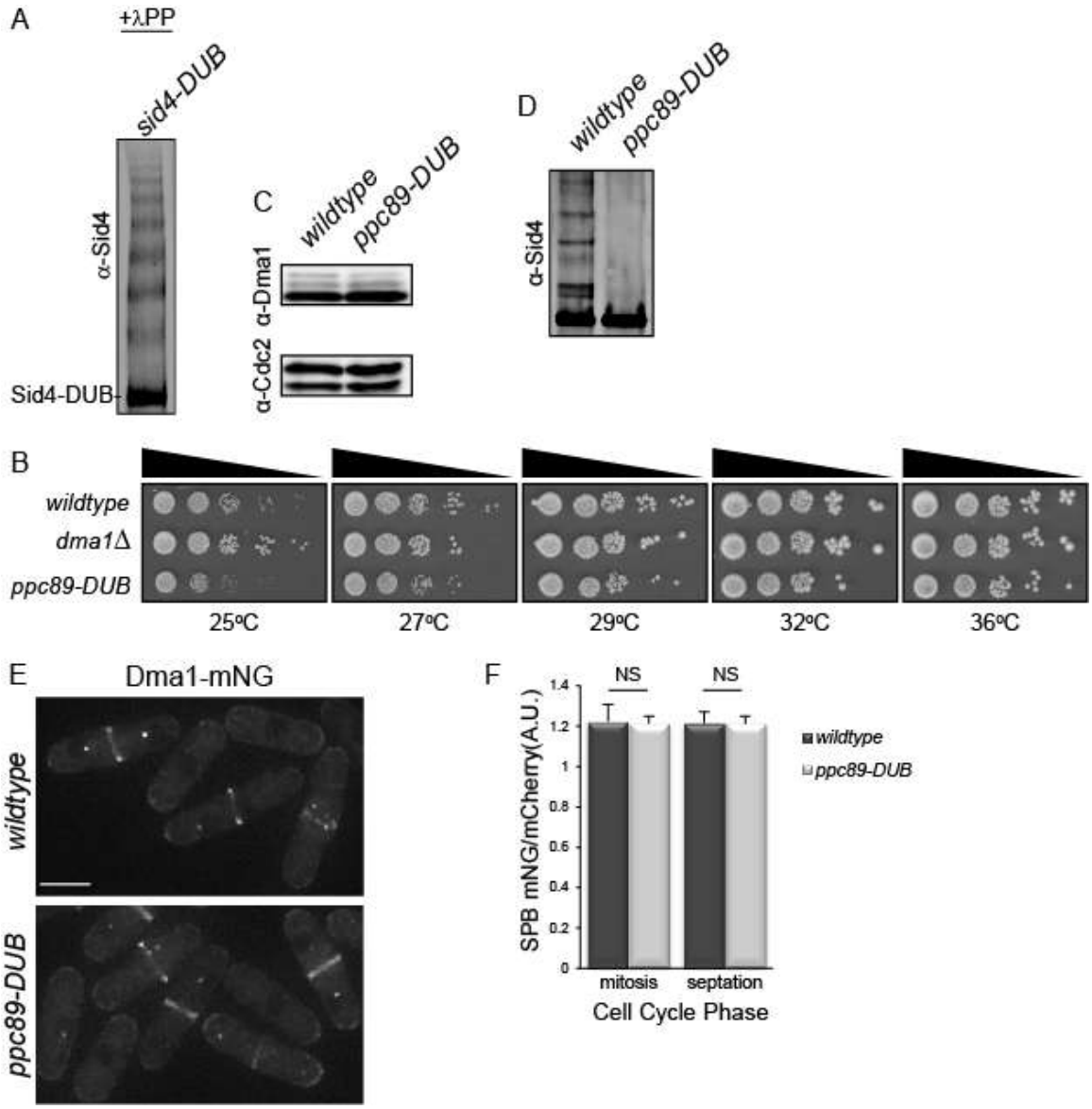

Figure 2-2 sup
A ppc89-DUB fusion eliminates Sid4 ubiquitination.
(A) A Sid4-DUB fusion was immunoprecipitated from the indicated strain, treated with phosphatase, and visualized by immunoblotting. (B) The indicated strains were grown at 29°C, and then the same number of cells were spotted in 10-fold serial dilutions and incubated at the indicated temperatures on YE plates. (C-D) Relative protein levels of Dma1-FLAG (C) and Sid4 (D) in the indicated strains as determined by immunoblotting of immunoprecipitates from the same amount of protein lysates as determined by immunoblotting for Cdc2 in C. (E) Live cell images of Dma1-mNG in *wildtype* and *ppc89-DUB* cells. Scale bar, 5 μm. (F) Quantification of Dma1-mNG at SPBs in the indicated strains, relative to Sad1-mCherry. $n \geq 40$ cells for each; error bars represent standard error of the mean, NS = not significant.

To identify the appropriate DUB for fusion to Sid4, we screened eighteen of the twenty *S. pombe* DUBs for their ability to rescue Dma1 overexpression-induced cytokinesis failure and cell death (Guertin et al., 2002; Murone & Simanis, 1996). Four of the eighteen DUBs (Ubp1, Ubp2, Ubp7, and Ubp14) suppressed Dma1-induced cell death, presumably by reversing Sid4 ubiquitination. Of these, only Ubp7 has diffuse cytoplasmic localization and functions independently of other subunits *in vivo* (Kouranti et al., 2010), making it well-suited for our purpose. The ubiquitin specific protease (USP) domain of Ubp7 was fused to the C-terminus of Sid4 (Sid4-DUB) and produced under control of the native $sid4^{+}$ promoter as the sole version of Sid4 in the cell. The fusion did not affect cell viability, but the Sid4-DUB fusion was still ubiquitinated (Fig. 2-S2A), indicating that the DUB was not able to access Sid4 ubiquitination sites.

We next tested whether adding the Ubp7 USP domain to the C-terminus of the Sid4 binding partner Ppc89 (Rosenberg et al., 2006) eliminated Sid4 ubiquitination. The Ppc89-Ubp7 USP fusion (hereafter called Ppc89-DUB) abolished Sid4 ubiquitination comparable to deletion of *dma1* (Fig. 2-2A). The *ppc89-DUB* strain grew similarly to wildtype at a variety of temperatures (Fig. 2-2B), and the levels of Dma1 and Sid4 were unchanged relative to their levels in wildtype cells (Fig. 2-S2C and D). As would be expected when Sid4 cannot accumulate ubiquitin modifications, the *ppc89-DUB* strain resisted Dma1 overexpression-induced cell death (Fig. 2-2B).

To determine if lack of Sid4 ubiquitination affected Dma1-mNG localization, we measured and compared Dma1-mNG SPB intensity relative to Sad1-mCherry in *wildtype* and *ppc89-DUB* strains and found no difference (Fig. 2-S2E and F). Moreover, the dynamic localization of Dma1-mNG to the SPB and division site was unchanged in the

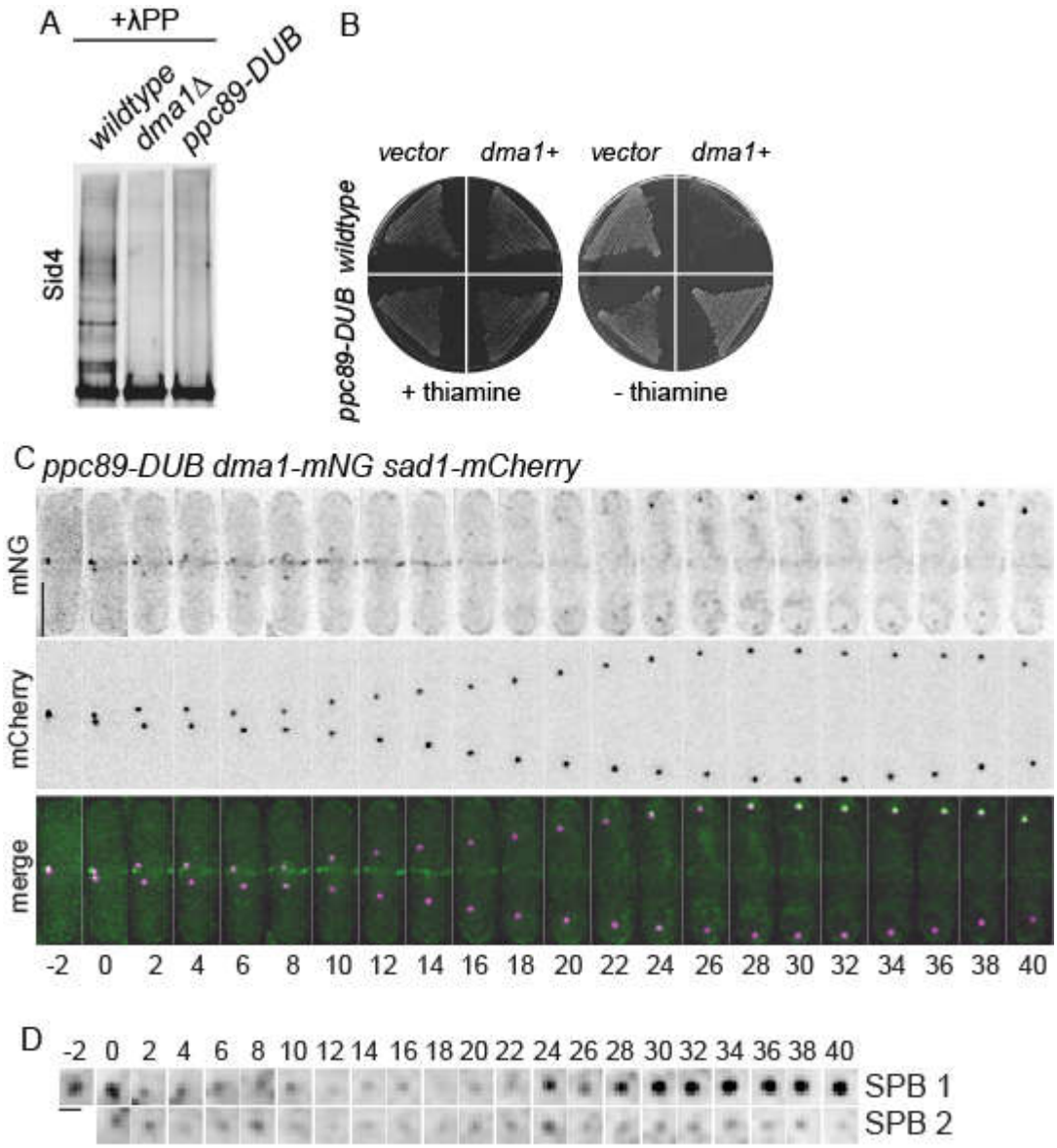

Figure 2-2
A Ppc89-DUB fusion eliminates Sid4 ubiquitination.
(A) Sid4 was immunoprecipitated from equal amounts of protein lysates from the indicated strains, treated with phosphatase, and visualized by immunoblotting. (B) *wildtype* and *ppc89-DUB* strains were transformed with either vector alone (pREP42) or vector containing *dma1*$^{+}$ (pREP42*dma1*$^{+}$). Transformants were incubated on medium containing thiamine (left) or lacking thiamine (right) at 29°C. (C) Images at 2-min intervals from a representative movie of *ppc89-DUB dma1-mNG sad1-mCherry*. Time 0 indicates initial frame of SPB separation. Scale bar, 5 μm. (D) Enlarged SPB region(s) from movie in C. Scale bar, 1 μm.

ppc89-DUB strain, although mitotic progression took longer in this strain; of 22 SPBs examined in 11 cells, Dma1-mNG was transiently undetectable on 17 and diminished on 5 others during anaphase (Fig. 2-2C and D). These data demonstrate that an absence of Sid4 ubiquitination does not account for the differences observed in catalytically inactive Dma1 dynamic localization at SPBs relative to wildtype Dma1.

Dma1 exhibits promiscuous auto-ubiquitination *in vivo* and *in vitro*

In addition to displaying distinct dynamics, by comparing Dma1-mNG and Dma1-I194A-mNG intensities normalized to the SPB marker Sad1-mCherry (I. Hagan & Yanagida, 1995), we found that Dma1-I194A-mNG was more abundant (ca. 4 fold) at SPBs in both mitotic and septated cells compared to wildtype Dma1 (Fig. 2-3A). Although we did not quantitate Dma1-I194A abundance at the division site or cell tips, it was visibly more intense than wildtype Dma1 at these sites as well (Fig. 2-1D).

To determine if the different intensities measured at SPBs reflected increased abundance of Dma1-I194A relative to wildtype Dma1, we examined protein levels by whole cell fluorescence intensity and immunoblotting (Fig. 2-3B and C). By both methods, the mutant protein was 2.6-fold higher in abundance, indicating that inactivating the catalytic activity of Dma1 causes an increase in total Dma1 protein. However, the overall difference in protein abundance was not as high as the difference in SPB intensity (2.6-fold increase vs. 3.2-fold increase) and so cannot fully account for the increased protein and lack of dynamics of Dma1-I194A observed at SPBs. Dma1 auto-

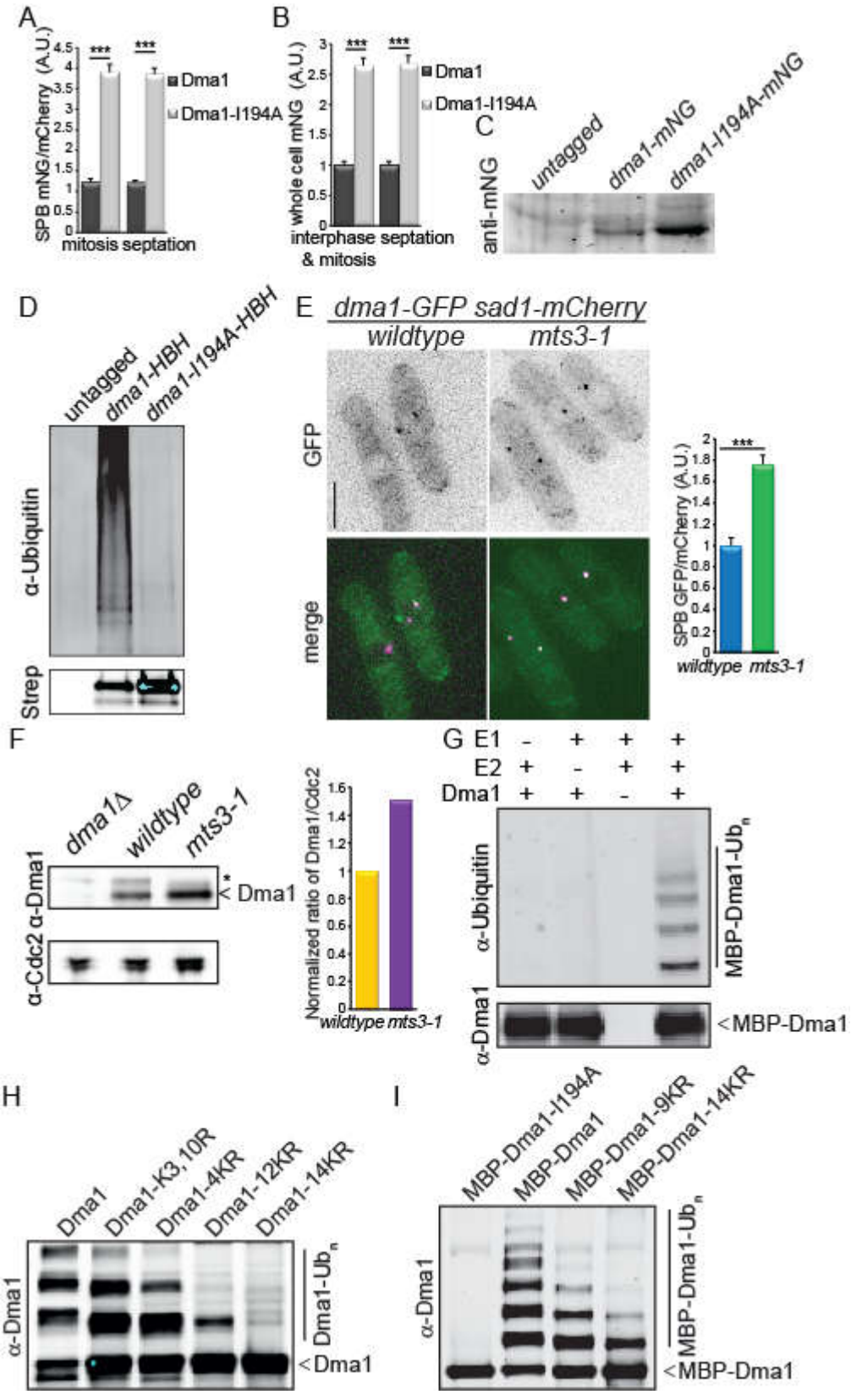
A
SPB mNG/mCherry (A.U.)
Dma1
Dma1-I194A
mitosis septation
B
whole cell mNG (A.U.)
interphase septation & mitosis
C
untagged
dma1-mNG
dma1-I194A-mNG
anti-mNG
D
untagged
dma1-HBH
dma1-I194A-HBH
α-Ubiquitin
Strep
E
dma1-GFP sad1-mCherry
wildtype
mts3-1
GFP
merge
SPB GFP/mCherry (A.U.)
F
dma1Δ
wildtype
mts3-1
α-Dma1
α-Cdc2
Dma1
Normalized ratio of Dma1/Cdc2
G
E1
E2
Dma1
α-Ubiquitin
MBP-Dma1-Ub$_n$
α-Dma1
MBP-Dma1
H
Dma1
Dma1-K3,10R
Dma1-4KR
Dma1-12KR
Dma1-14KR
α-Dma1
Dma1-Ub$_n$
Dma1
I
MBP-Dma1-I194A
MBP-Dma1
MBP-Dma1-9KR
MBP-Dma1-14KR
α-Dma1
MBP-Dma1-Ub$_n$
MBP-Dma1

Figure 2-3
Dma1 auto-ubiquitination influences its abundance and localization dynamics.
(A) Quantification of Dma1-mNG and Dma1-I194A-mNG intensities at SPBs, relative to Sad1-mCherry in mitotic or septated cells. $n \geq 42$ cells for each measurement; error bars represent standard error determined by two-tailed Student's t-test, ***$p = 4.9x10^{-43}$ (mitosis) and $1.3x10^{-11}$ (septation). A.U. = arbitrary units. (B) Quantification of Dma1-mNG and Dma1-I194A-mNG whole cell fluorescence intensities in non-septated interphase and mitotic cells, or septated cells. $n \geq 20$ cells for each measurement; error bars represent standard error determined by two-tailed Student's t-test, ***$p = 1.3x10^{-7}$ (interphase and mitosis) and $4.9x10^{-9}$ (septation). A.U. = arbitrary units. (C) Abundance of Dma1-I194A-mNG relative to wildtype Dma1-mNG was determined by immunoblotting. One representative blot of 3 independent repetitions is shown. (D) Dma1-HBH, Dma1-I194A-HBH, or non-specifically purified proteins were isolated from *mts3-1* cells that had been shifted to 36°C for 3 hr. Dma1 ubiquitination was detected by immunoblotting with an anti-ubiquitin antibody (top panel) and unmodified Dma1 was detected with fluorescently-labelled streptavidin (bottom panel). (E) Live cell images (left) of Dma1-GFP and Sad1-mCherry in *wildtype* and *mts3-1* cells shifted to 36˚C for 3 hr. Scale bar, 5 μm. Quantification (right) of Dma1-GFP at mitotic SPBs relative to Sad1-mCherry. A.U. = arbitrary units. $n \geq 16$ SPBs for each strain; error bars represent SEM, ***$p = 7x10^{-8}$. (F) Relative protein levels of Dma1 (top) in the indicated strains as determined by immunoblotting immunoprecitates relative to Cdc2 in the lysates (bottom) (left panel) followed by quantification with Odyssey (right panel). * = non-specific band. (G) Recombinant MBP-Dma1 was incubated with an E1-activating enzyme and/or the E2-conjugating enzyme, UbcH5a/UBE2D1, and methylated ubiquitin. Ubiquitin-modified Dma1 was detected by immunoblotting with an anti-ubiquitin antibody (top panel) and unmodified Dma1 was detected with anti-Dma1 serum (bottom panel). (H) Recombinant MBP-Dma1 proteins were incubated with an E1-activating enzyme, the E2-conjugating enzyme UbcH5a/UBE2D1 and methylated ubiquitin. Dma1 was cleaved from MBP and auto-ubiquitination was detected by immunoblotting with anti-Dma1 serum. (I) Recombinant MBP-Dma1 proteins were incubated with an E1-activating enzyme, the E2-conjugating enzyme UbcH5a/UBE2D1, and methylated ubiquitin. MBP-Dma1 ubiquitination was detected by immunoblotting with anti-Dma1 serum.

ubiquitinates *in vitro* (A. E. Johnson, Collier, Ohi, & Gould, 2012b; Y. Wang et al., 2012a). Therefore, we next asked whether a lack of auto-ubiquitination in catalytically inactive Dma1-I194A could explain its increased SPB localization abundance and decreased SPB localization dynamics.

First, we established that Dma1 auto-ubiquitinates *in vivo*. Dma1 and Dma1-I194A, both tagged with his_6-biotin-his_6 (HBH), were purified under fully denaturing conditions and probed for the presence of ubiquitinated forms by immunoblotting. We detected ubiquitin modification of wildtype Dma1 but not catalytically inactive Dma1-I194A when the proteasome was inhibited with the *mts3-1* temperature-sensitive mutation (Fig. 2-3D) (Gordon, McGurk, Wallace, & Hastie, 1996). Thus, Dma1 auto-ubiquitinates *in vivo* as well as *in vitro*.

We hypothesized that Dma1 auto-ubiquitination could promote its proteasomal degradation and its removal from SPBs. To test this idea, we performed live cell imaging of Dma1-GFP in wildtype and *mts3-1* arrested cells. Comparison of Dma1-GFP intensities relative to Sad1-mCherry showed that Dma1 was more abundant at SPBs in *mts3-1* arrested mitotic cells than in wildtype mitotic cells (Fig. 2-3E). Immunoblot analysis also indicated an increase in total protein levels of Dma1 in *mts3-1* relative to wildtype (Fig. 2-3F). These data support the idea that Dma1 auto-ubiquitination promotes its own degradation and removal from SPBs during anaphase.

To investigate directly if ubiquitin modifications affected Dma1's ability to localize to SPBs, we sought to identify and mutate the auto-ubiquitinated residues. We first examined the sites of Dma1 auto-ubiquitination *in vitro* using recombinant Dma1 that exhibits E1 and E2-dependent auto-ubiquitination (Fig. 2-3G) (A. E. Johnson, Collier, et al., 2012b; Y. Wang et al., 2012a). Dma1 contains fourteen lysines that could potentially be targeted for ubiquitination. A series of mutants containing increasing numbers of lysine to arginine mutations was generated. These recombinant Dma1 variants were assayed for auto-ubiquitination using methyl ubiquitin to prevent chain elongation. Though the number of ubiquitin moieties added to Dma1 decreased with decreasing availability of lysines, only lysine-less Dma1 (Dma1-14KR) was completely unmodified (Fig. 2-3H). Dma1 also ubiquitinated its MBP tag if the tag was not removed prior to the ubiquitination reaction (Fig. 2-3I), indicating that Dma1 promiscuously ubiquitinates lysines in its proximity.

To determine which Dma1 lysines are ubiquitinated *in vivo*, we performed LC-MS/MS analyses on Dma1 purified from cells at different cell cycle stages. Nine

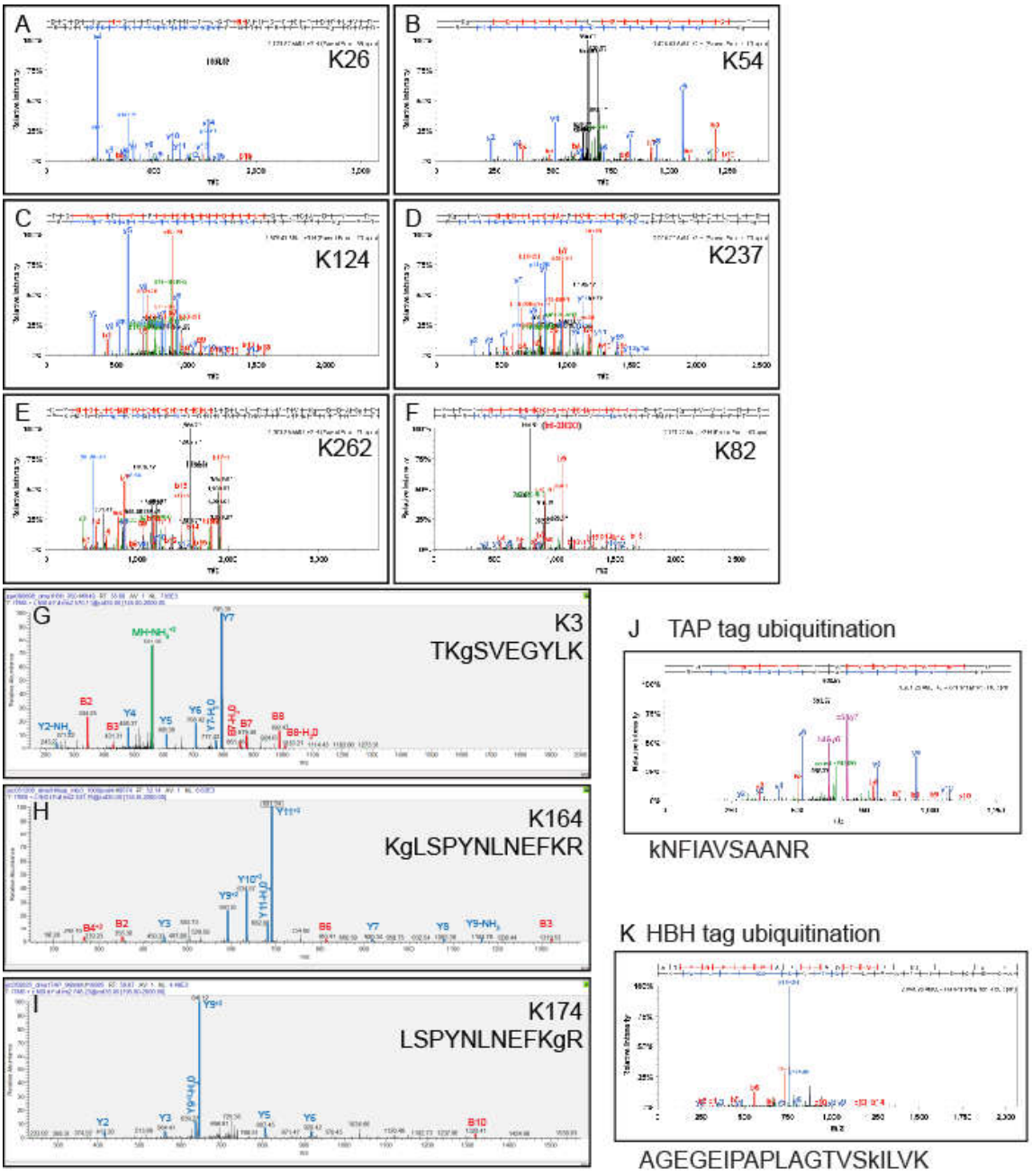

Figure 2-3 sup
Mass spectra indicative of Dma1 ubiquitination.
(A-I) Representative MS^2 spectra of Dma1 ubiquitination at K26 (A), K54 (B), K124 (C), K237 (D), K262 (E), K82 (F), K3 (G), K164 (H), and K174 (I) and K49 of the TAP tag (J) and K35 of the HBH tag (K). Spectra shown in A-F and J-K were generated and annotated in Scaffold and G-I were identified by Myrimatch, displayed in Xcalibur (v 2.2, Thermo Scientific) and manually annotated. Fragment ions are indicated in each spectrum (y-ions in blue, b-ions red and neutral loss ions in green).

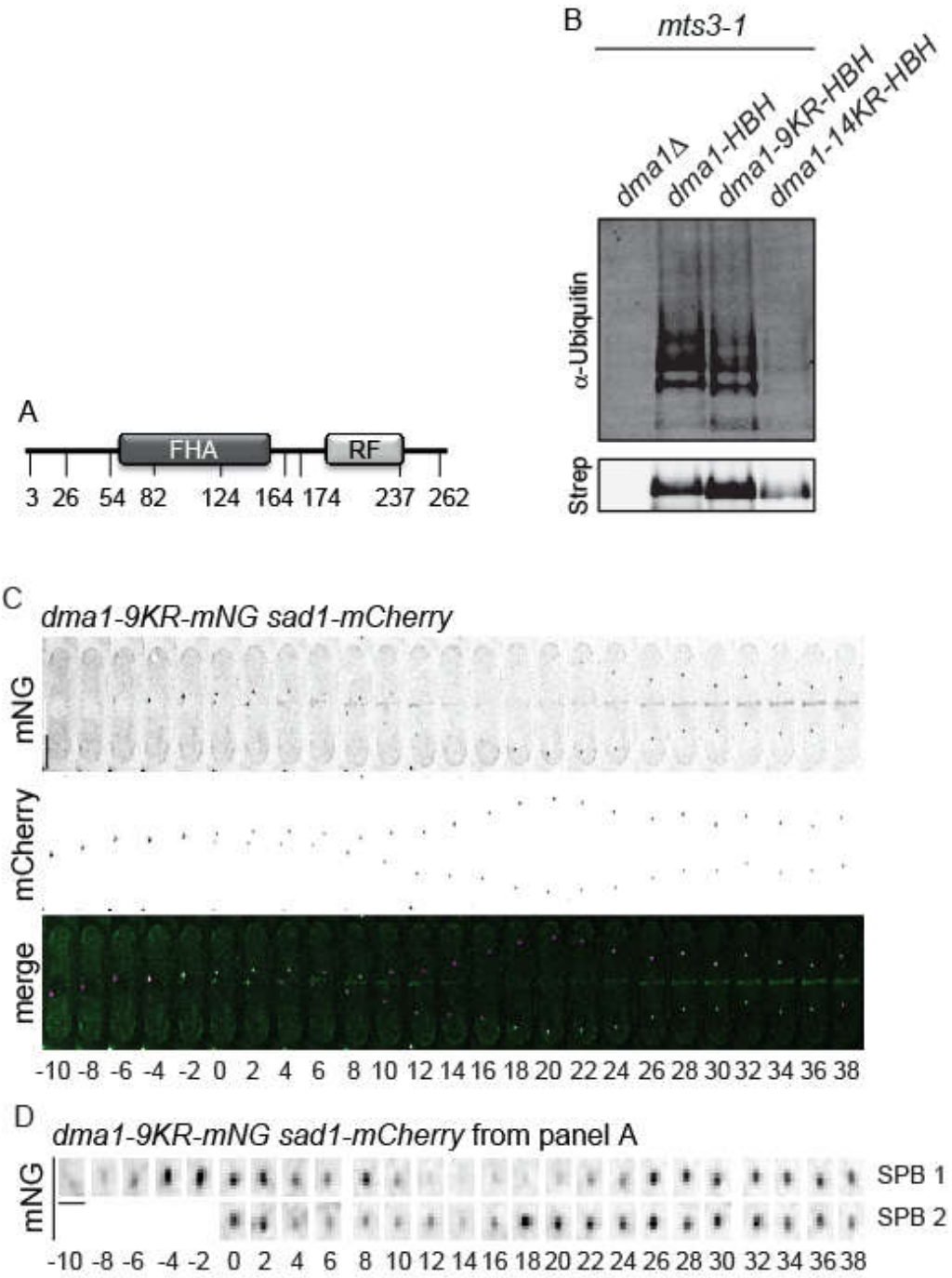

Figure 2-4 sup
Dma1-9KR-mNG mutant exhibits wildtype localization dynamics.
(A) Schematic of Dma1 with ubiquitination sites identified by LC-MS/MS indicated. (B) Dma1-HBH, Dma1-9KR-HBH, Dma1-14KR-HBH, or non-specifically purified proteins were isolated from *mts3-1* cells shifted to 36˚C for 3 h. Dma1 ubiquitination was detected by immunoblotting with an anti-ubiquitin antibody (top panel) and unmodified Dma1 was detected with fluorescently-labelled streptavidin (bottom panel). (C) Images from representative movie of *dma1-9KR-mNG sad1-mCherry*. Time in minutes denoted below images; 0 indicates initial frame of SPB separation. Scale bar, 5 μm. (D) Enlarged SPB region(s) from movie in C. Scale bars, 1 μm.

ubiquitinated lysines of the fourteen possible were identified (Fig. 2-S3A-I and Fig. 2-S4A). We therefore constructed mutant strains in which the nine identified modified lysines or all fourteen lysines in the protein were substituted with arginine (9KR and 14KR, respectively). Surprisingly, both Dma1 mutants tagged endogenously with the HBH tag were ubiquitinated (Fig. 2-S4B). The abundance of Dma1-14KR was significantly reduced, likely because so many mutations led to a disruption of its structure (Fig. 2-S4B). However, that both were still ubiquitinated, combined with the ability of Dma1 and Dma1-14KR to ubiquitinate an MBP tag *in vitro* (Fig. 2-3I), suggested that tags on the protein could be ubiquitinated in lieu of, or in addition to, Dma1 lysines. Indeed, LC-MS/MS analyses of Dma1-TAP and Dma1-HBH purified from cells identified ubiquitinated lysine residues in both tags (Fig. 2-S3J and K), confirming that Dma1 ubiquitinates its tags both *in vitro* and *in vivo*. Therefore, we predict that although the Dma1-9KR-mNG and Dma1-14KR mutants exhibited wildtype localization dynamics (Fig. 2-S4C and D and unpublished observations, C.M.J), this is because Dma1 is still able to ubiquitinate the mNG tag, and this event signals Dma1 degradation.

We next reasoned that wildtype Dma1 would be able to auto-ubiquitinate an inactive form of itself in close proximity and therefore restore wildtype dynamics to the catalytically inactive mutant. To test this, we constructed three diploid strains containing one mNG-tagged allele: *dma1-mNG/dma1*$^{+}$; *dma1-I194A-mNG/dma1*$^{+}$; *dma1-I194A-mNG/dma1-I194A*. When both alleles were wildtype or both inactive, the localization dynamics of the tagged protein mirrored the haploid situation, with Dma1-mNG dimming or disappearing from 100% of 20 SPBs during anaphase (Fig. 2-4A and D) and Dma1-I194A-mNG showing no change at 84% of 44 SPBs (Fig. 2-4B and E). In contrast, when

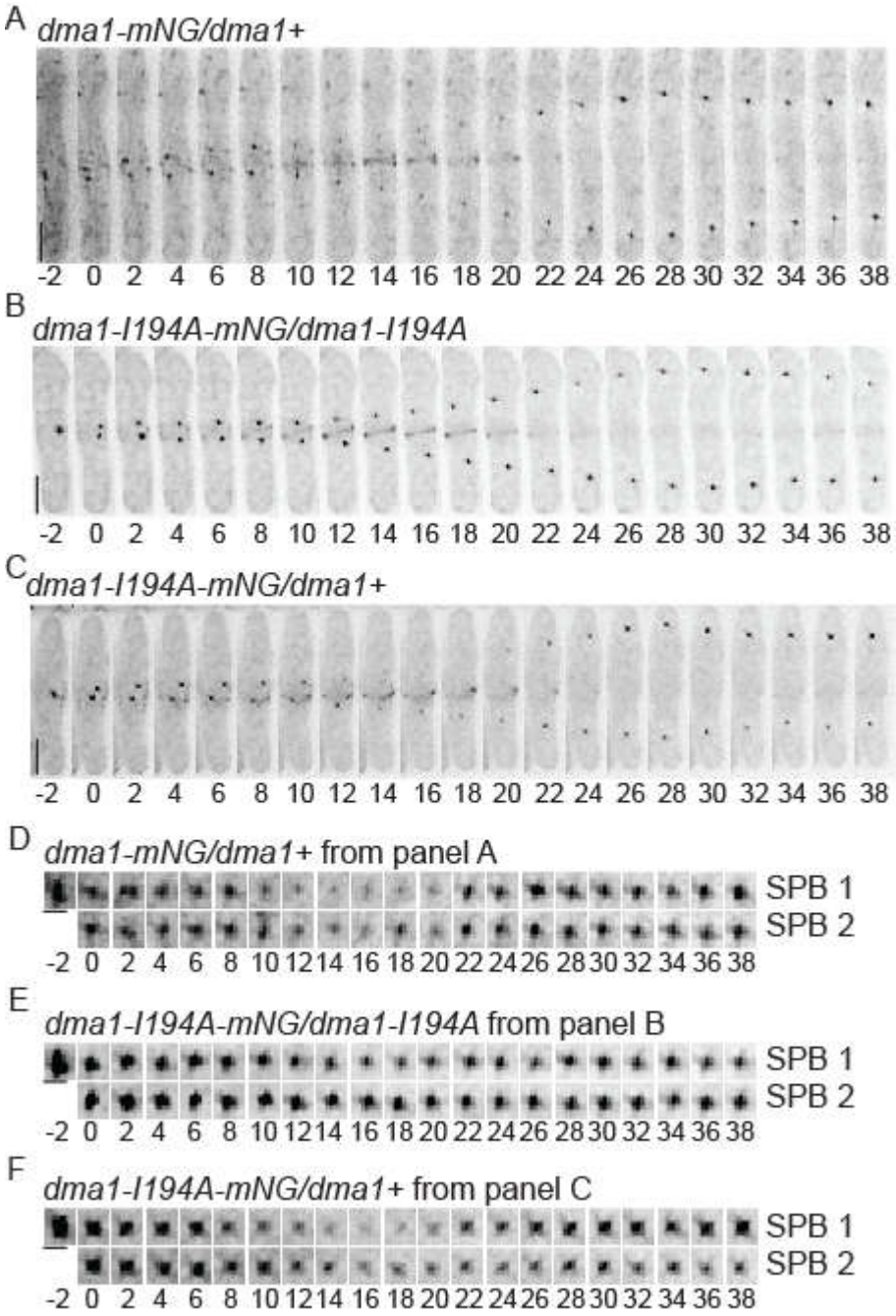

Figure 2-4
Dma1 catalytic activity drives its localization dynamics.
(A-C) Images from representative movies of *dma1-mNG/dma1+* (A), *dma1-I194A-mNG/dma1-I194A* (B), and *dma1-I194A-mNG/dma1+* (C). Time in minutes denoted below images. Time 0 indicates initial frame of SPB separation. (D-F) Enlarged SPB region(s) from movies in A-C. Scale bars, 1 µm.

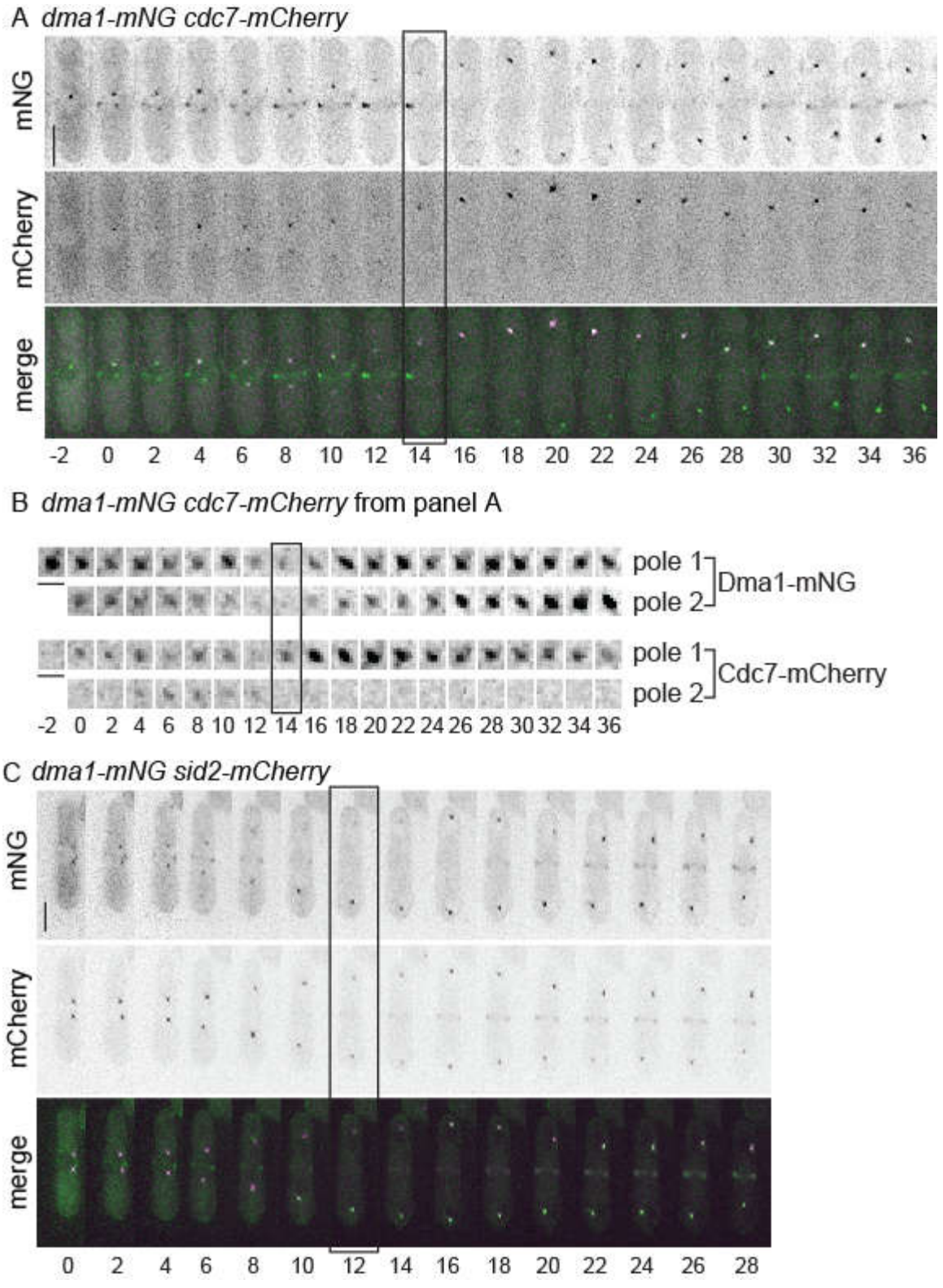
A dma1-mNG cdc7-mCherry
mNG
mCherry
merge
-2 0 2 4 6 8 10 12 14 16 18 20 22 24 26 28 30 32 34 36
B dma1-mNG cdc7-mCherry from panel A
pole 1
pole 2
Dma1-mNG
pole 1
pole 2
Cdc7-mCherry
-2 0 2 4 6 8 10 12 14 16 18 20 22 24 26 28 30 32 34 36
C dma1-mNG sid2-mCherry
mNG
mCherry
merge
0 2 4 6 8 10 12 14 16 18 20 22 24 26 28

Figure 2-5
SPB dynamics of Dma1 relative to SIN components.
Images from representative movies of *dma1-mNG cdc7-mCherry* (A) and *dma1-mNG sid2-mCherry* (C). Time in minutes denoted below images. In A, time 0 indicates initial frame of SPB separation while in C, time 0 indicates the beginning of imaging. Scale bars, 5 μm. (B) Enlarged SPB region(s) from movie in A. Scale bars, 1 μm. In A and B, boxes indicate initial frame of asymmetric Cdc7 SPB localization. In C, the box indicates the first frame Sid2 localization to the division site was detected.

Dma1-I194A-mNG was combined with wildtype Dma1, the tagged inactive protein now exhibited dynamics similar to wildtype, with the Dma1-I194A-mNG signal dimming or disappearing at 93% of 28 SPBs during anaphase (Fig. 2-4C and F). This result indicates that the untagged wildtype Dma1 ubiquitinates the inactive Dma1-I194A-mNG, a reaction that could occur in *cis* or *trans* because Dma1 is a dimer (A. E. Johnson, Collier, et al., 2012b). These results are consistent with a model in which auto-ubiquitination triggers the transient loss of Dma1 from SPBs during anaphase.

Relationship between Dma1 SPB dynamics and the SIN

The dynamic localization of Dma1 during mitosis is reminiscent of that displayed by several SIN components (A. E. Johnson, McCollum, et al., 2012b; Simanis, 2015a). Asymmetric SPB localization of Cdc7 to one SPB and localization of Sid2 to the division site are considered markers of maximal SIN activation and Cdk1 inhibition (A. E. Johnson, McCollum, et al., 2012b; Simanis, 2015a). Therefore, we imaged Dma1-mNG in combination with those two SIN components (Fig. 2-5) to place the timing of dynamic Dma1 localization in the context of SIN activation. Dma1-mNG SPB dimming occurred 1-2 minutes in 14 cells and 3-5 minutes in 3 cells prior to the development of detectable asymmetry in Cdc7-mCherry signal in the 17 cells examined (Fig. 2-5A and B), and the

transient reduction in Dma1 division site localization preceded Sid2 division site localization in all 8 cells examined (Fig. 2-5C).

To test whether SIN activity modulated some aspect of Dma1's localization pattern, Dma1-mNG was imaged in the SIN mutant *cdc7-24* as cells passed through mitosis. Dma1-mNG intensity dimmed or disappeared at 21 of 22 SPBs in 11 cells but it never re-intensified at SPBs as in wildtype cells (Fig. 2-6A and B), indicating that SIN activity is important for Dma1 re-accumulation at SPBs in late anaphase. Dma1 did re-intensify at the division site in all 11 cells examined. We next imaged Dma1-mNG in the hyperactive SIN mutant *cdc16-116*. In these cells that have constitutive SIN activity (Fankhauser, Marks, Reymond, & Simanis, 1993), Dma1-mNG was detected on 97% (116/119) of SPBs (Fig. 2-6C). Since the SIN is not maximally active until later in anaphase in wildtype cells, these results suggest that the SIN promotes Dma1 SPB re-accumulation at the end of anaphase, possibly as part of a negative feedback loop.

Constitutive Dma1 localization to SPBs prevents cytokinesis

We next wanted to determine the importance of Dma1 transiently cycling off of SPBs during anaphase by permanently tethering it to SPBs. To do this, we tagged Sid4 at its endogenous locus with GFP-binding protein (GBP), which has a high affinity for GFP (Rothbauer et al., 2008; Rothbauer et al., 2006). When a *sid4-GBP-mCherry* or *sid4-GBP* strain was crossed to *dma1-GFP*, the majority of double mutants (27/28 and 7/19, respectively) were dead. Similarly, synthetic lethality was previously observed when the tags were reversed and *dma1-GBP-mCherry* was expressed in a *sid4-GFP* strain

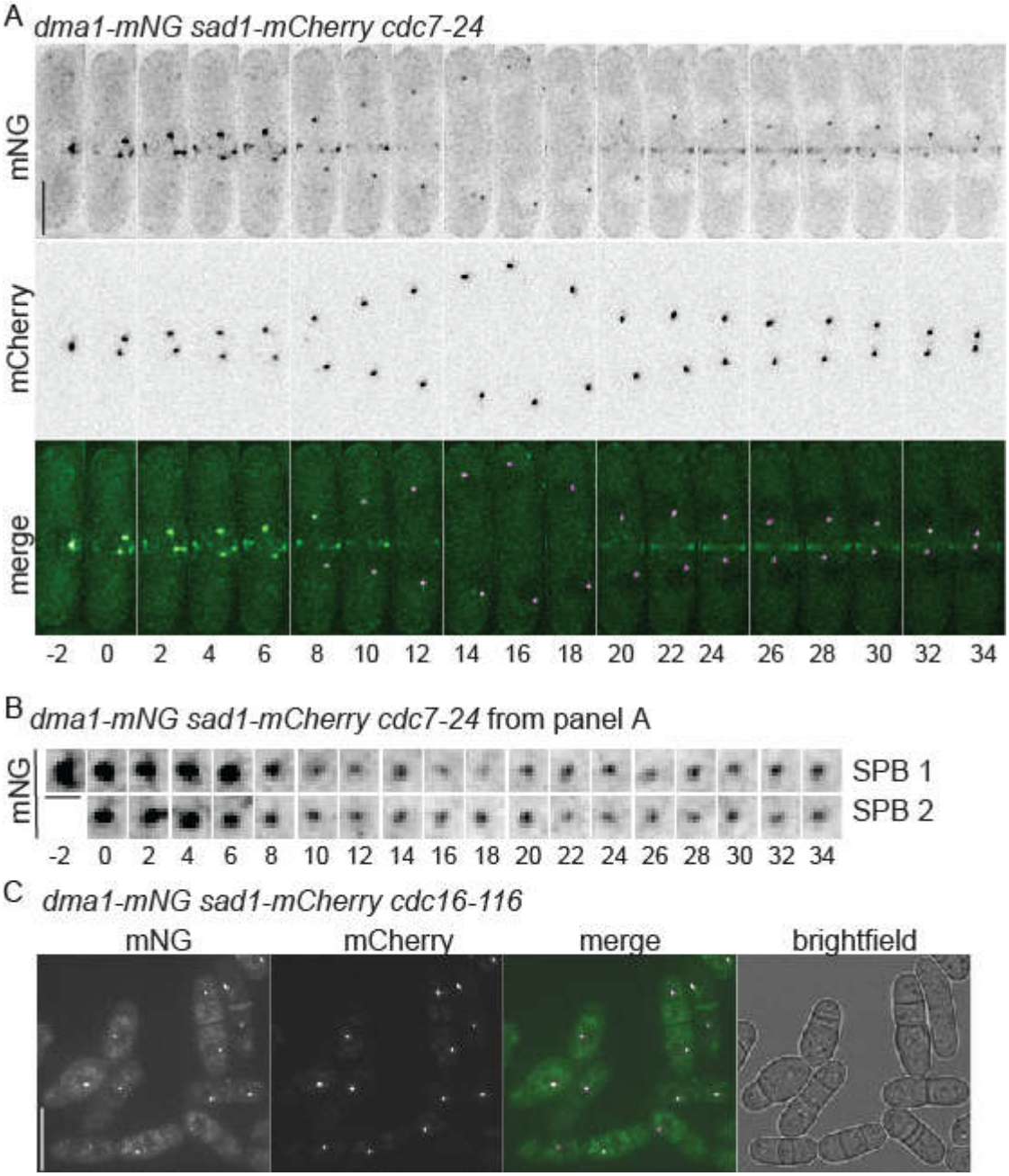

Figure 2-6
Influence of SIN function on Dma1 localization dynamics.
(A) Images from a representative movie of *dma1-mNG sad1-mCherry cdc7-24* following shift to 36˚C for 2 h. Time in minutes denoted below images; time 0 indicates initial frame of SPB separation. Scale bar, 5 µm. (B) Enlarged SPB region(s) from movie in A. Scale bars, 1 µm. (C) Representative live cell image of *dma1-mNG sad1-mCherry cdc16-116* shifted to 36˚C for 3 h. Scale bar, 10 µm.

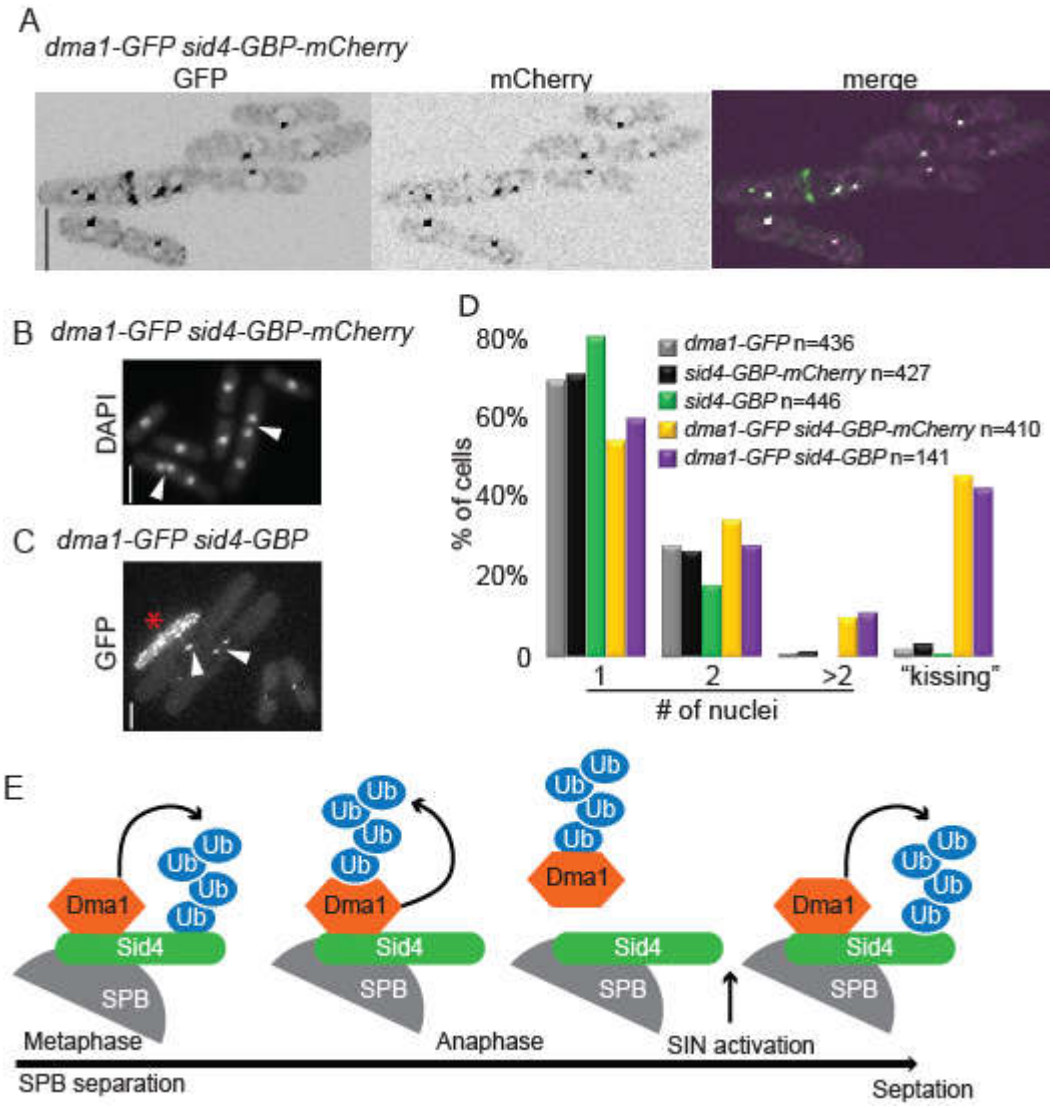

Figure 2-7
Dma1 must leave the SPBs for cytokinesis.
(A) Representative live cell images of *dma1-GFP sid4-GBP-mCherry*. (B) Representative DAPI stained images of *dma1-GFP sid4-GBP-mCherry*. (C) Representative image of *dma1-GFP sid4-GBP* cells illustrating "kissing nuclei" phenotype indicated with arrows in B and C. (D) Quantification of cells from B and C with 1, 2, and >2 nuclei and separately "kissing nuclei". (E) Cartoon showing the dynamic localization of Dma1 throughout mitosis and cytokinesis. In metaphase when the mitotic checkpoint is activated, Dma1 binds and ubiquitinates Sid4. Then, in early anaphase, Dma1 auto-ubiquitinates and leaves the SPB. Only after the SIN is maximally activated, Dma1 re-accumulates at the SPB, and potentially ubiquitinates Sid4 again to help inhibit the SIN in a negative feedback loop.

(Y. H. Chen et al., 2017), though in this study, co-localization at SPBs and whether the cells died because of a failure in the SIN and cytokinesis was not determined. Fortunately, we were able to recover four double-tagged strains for analysis, although they grew poorly: 22% of *dma1-GFP sid4-GBP-mCherry* and 11% of *dma1-GFP sid4-GBP* cells were dead or lysing. In the live *dma1-GFP sid4-GBP-mCherry* cells, Dma1-GFP localized to the division site normally and co-localized with Sid4-GBP-mCherry at SPBs at all stages of the cell cycle (Fig. 2-7A), suggesting that Dma1-GFP had been tethered permanently to SPBs. In both double mutant strains, there was a higher percentage of bi- and multi-nucleated cells than in wildtype (Fig. 2-7B-D). Furthermore, 46% of bi-nucleated cells had "kissing" nuclei (Fig. 2-7B-D) indicative of SIN failure (I. M. Hagan & Hyams, 1988). We reasoned if the SIN was inhibited in these strains via Dma1-mediated Sid4 ubiquitination, introducing the *ppc89-DUB* fusion allele that prevents Sid4 ubiquitination (Fig. 2-2A) might rescue growth of *dma1-GFP sid4-GBP-mCherry* cells. As predicted, *dma1-GFP sid4-GBP-mCherry ppc89-DUB* triple mutant strains were all viable (Fig. 2-S5A). These data indicate that constitutive association of Dma1 with Sid4 drives Sid4 ubiquitination, compromises SIN activity, and results in cytokinesis failure.

2.3 Discussion

SPB localization of the ubiquitin ligase Dma1 is required for its function in a mitotic checkpoint that stalls cytokinesis through SIN inhibition when a mitotic spindle cannot form (Guertin et al., 2002; Murone & Simanis, 1996). In this report, we show that

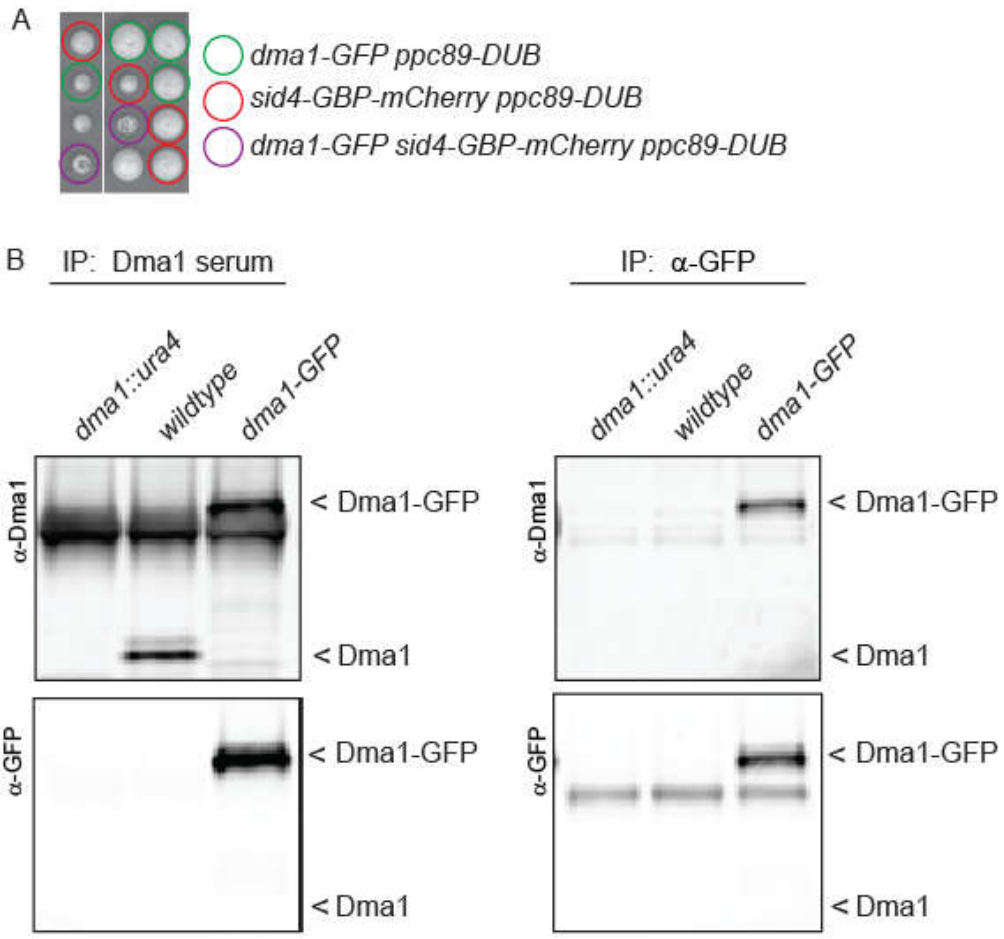

Figure 2-5 sup
Characterization of anti-Dma1 serum.
(A) Tetrads from the indicated cross with genotypes determined by whole cell PCR provided for each colony. (B) Dma1 or Dma1-GFP was immunoprecipitated from the indicated strains with anti-Dma1 serum (left panels) or anti-GFP antibody (right panels). Dma1 and Dma1-GFP were detected by immunoblotting with an anti-Dma1 serum (top panels) or anti-GFP antibody (bottom panels). Dma1 and Dma1-GFP are marked with arrowheads.

Dma1 exhibits previously unrecognized dynamic localization to SPBs and the cell division site during anaphase. We found that both the SIN and auto-ubiquitination modulate Dma1 SPB localization dynamics, and therefore its function in the checkpoint. Further, our data show that if Dma1 is prevented from leaving Sid4 on the SPBs, cells fail division, indicating that Dma1's transient loss from SPBs is a critical step in cytokinesis and cell survival.

Dma1 division site localization

Though Dma1 was previously shown to localize to the division site (Guertin et al., 2002), our time-lapse imaging experiments with the brighter mNG fluorophore (Shaner et al., 2013) revealed more detail. Dma1-mNG initially appears in node-like structures, reminiscent of cytokinetic precursor nodes (Rincon & Paoletti, 2012), before coalescing into a ring. In addition, Dma1 leaves the division site after anaphase B onset and before ring constriction and then re-appears at the division site before cell division. The role of Dma1 at the division site is not yet understood because no binding partners or substrates at the medial cortex have been identified. Because neither Dma1 activity nor the SIN impacts its cell division site localization dynamics, a different mechanism of targeting to this site must be in place. Importantly, tethering Dma1 to Sid4 at the SPB using the GBP-GFP system did not preclude Dma1 localization to the division site, validating that it is Dma1's SPB localization that is important in modulating SIN function. We also detected Dma1 localization to cell tips in this study, but again, its mechanism of targeting and function there are not known.

SIN regulation of Dma1 dynamics

Although the transient dip in Dma1 SPB localization in early anaphase depends on its catalytic activity and is independent of SIN function, SIN activity is required for Dma1's re-accumulation at SPBs later in anaphase. We speculate that promoting the re-localization of Dma1 to SPBs may be a component of negative feedback in which the SIN directs its own silencing (Garcia-Cortes & McCollum, 2009). Since Dma1 is a

phosphoprotein (Koch, Krug, Pengelley, Macek, & Hauf, 2011), it will be interesting to determine the role of phosphorylation in Dma1 regulation and whether this is controlled directly or indirectly by SIN kinases.

Dma1 auto-ubiquitination controls its dynamic localization at SPBs, which is required to relieve checkpoint inhibition

Our data show that Dma1 is capable of extensive auto-ubiquitination *in vitro* and *in vivo.* Its promiscuous auto-ubiquitination, which extended to any tag that we tested that includes lysines, complicated our investigation of its role as we were unable to visualize the dynamic localization of a lysine-less catalytically-active Dma1 protein with confidence in a haploid cell. However, we were able to use heterozygous diploids to show that the active form of the protein was sufficient to remove the inactive form from SPBs during early anaphase. Our localization data provided an unusual glimpse into the timing of ubiquitin ligase action in intact cells because we were able to visualize Dma1 disappearance and then re-appearance at SPBs, dynamics that strictly depend on its catalytic activity. Our data support the idea that auto-ubiquitination at the onset of anaphase triggers transient Dma1 removal from SPBs to allow full SIN activation (Fig 7E). By preventing Dma1 from leaving the SPB using the GBP trap, the SIN was inhibited. These results are consistent with the role of Dma1 as a SPB-localized SIN antagonist in early mitosis whose function must be relieved at the onset of anaphase (Guertin et al., 2002; A. E. Johnson et al., 2013b; A. E. Johnson & Gould, 2011a).

Degradation of Dma1

Because the catalytically inactive form of Dma1 is more abundant than wildtype, its levels are clearly regulated by its own activity state. While we do not yet know all the factors modulating Dma1 catalytic activity, our data is consistent with auto-ubiquitination triggering Dma1 destruction. This could happen directly at SPBs, analogously to proteasome-mediated degradation of many regulatory proteins at centrosomes (Vora & Phillips, 2016), or off the centrosome if ubiquitination prevents Dma1 association with its SPB tethers, similar to what has been observed for another SIN inhibitor, Byr4 (Krapp et al., 2008). Since loss of Dma1 from SPBs is transient during anaphase, auto-ubiquitination might also be transient and reflect a switch in substrate preference; SPB-localized Dma1 may shift from preferring its checkpoint substrate, Sid4, to auto-ubiquitination (Fig 7E) in much the same way that the anaphase-promoting complex, another E3 ubiquitin ligase, can shut itself off by switching from preferred substrates to auto-ubiquitination of its activator, Cdc20 (Gilberto & Peter, 2017). Further studies will clarify the possibility that this is a conserved mechanism of action for E3 ligases.

Chapter 3

Regulation of Dma1 auto-ubiquitination activity through phosphorylation

3.1 Introduction

Each accurate cell division cycle yielding two daughter cells with identical complements of genomic material requires coordination between mitosis and cytokinesis. In the fission yeast *Schizosaccharomyces pombe* the septation initiation network (SIN), a protein kinase cascade, is largely responsible for coordinating these two events and initiating cytokinesis at the correct time with respect to chromosome segregation (for review see (A. E. Johnson, McCollum, et al., 2012a; Krapp & Simanis, 2008; Simanis, 2015b)). In the event of a mitotic error, the E3 ligase Dma1 inhibits SIN signaling to prevent cytokinesis from occurring before chromosomes have segregated. The casein kinase I (CKI) enzymes, Hhp1 and Hhp2 phosphorylate Sid4 at two residues, which recruits Dma1 to bind Sid4 through its FHA domain and thus enables Dma1 to ubiquitinate Sid4 through its RING domain. This ubiquitination antagonizes the localization of the Polo-like kinase Plo1, and prevents the subsequent activation of the SIN kinase cascade (Guertin et al., 2002; A. E. Johnson et al., 2013a; A. E. Johnson & Gould, 2011b).

Dma1 is a member of the FHA-RING class of proteins, a small class of proteins that function in cell cycle checkpoints. While many proteins contain either an FHA

domain or a RING domain, only five characterized proteins contain both. These proteins include the *S. pombe* homolog Dma1, the two functionally redundant *Saccharomyces cerevisiae* homologues Dma1 and Dma2, and the two mammalian paralogs CHFR and RNF8 (Brooks et al., 2008). CHFR is a tumor suppressor protein, which functions in the early mitotic antephase checkpoint; however, its molecular mechanism is poorly characterized (Matsusaka & Pines, 2004; Scolnick & Halazonetis, 2000). Conversely, RNF8 has a well understood role in the DNA damage response (DDR) checkpoint (Huen et al., 2007; Kolas et al., 2007; B. Wang & Elledge, 2007). During interphase RNF8 localizes to DNA double-strand breaks (DSBs), where it binds to phosphorylated MDC1 and facilitates K63-linked ubiquitination of histones. This ubiquitination is necessary for the subsequent recruitment of RNF168 and downstream repair factors (Huen & Chen, 2010; Luijsterburg & van Attikum, 2012; Mattiroli et al., 2012; Nakada et al., 2012). Additionally, during mitosis CDK1 phosphorylates RNF8, inhibiting its recruitment to DSB sites and activation of the DDR checkpoint, and in turn protects against telomere fusions (Orthwein et al., 2014; Peuscher & Jacobs, 2011).

As we have shown (see Chapter 2), Dma1 exhibits remarkable SPB and the cell division site localization dynamics during the cell cycle that are modulated by both SIN activity and Dma1 auto-ubiquitination, yet the molecular mechanisms of these modulations are not clear. As Dma1 is functionally related to the human checkpoint protein RNF8, it is likely that these proteins have similar mechanisms of regulation, potentially including inhibition via phosphorylation. In this chapter, we examined regulation of Dma1 activity by phosphorylation. We identified Dma1 as a phospho-protein that is phosphorylated *in vivo* throughout the cell cycle. This phosphorylation

occurs on seven sites across the protein, and these sites can be targeted *in vitro* by at least three master kinases: Cdk1, Plo1 and CKII. Sets of Dma1 phospho-ablating and phospho-mimetic mutations were made according to the targeting kinases identified *in vitro*, and ubiquitination activity was examined in each mutant. All of the Dma1 phosphomutants were catalytically active toward the checkpoint protein Sid4. However, Dma1 auto-ubiquitination was impaired specifically in the Cdk1-Plo1 phospho-mimetic. This regulation of Dma1 through phosphorylation provides a mechanism by which Dma1 auto-ubiquitination can be inhibited without compromising checkpoint activity.

3.2 Results

Dma1 is phosphorylated throughout the cell cycle

Dma1 mediated ubiquitination of Sid4 is cell cycle dependent (A. E. Johnson & Gould, 2011b), leading us to explore the molecular mechanisms that regulate Dma1 activity. Because phosphorylation provides a rapid and reversible means of regulating protein function (Bohnert & Gould, 2011; Holt, 2012; Hunter, 2007), we examined whether Dma1 is phosphorylated *in vivo*. Using immunoblot analysis of Dma1 immunoprecipitates, treated with or without λ phosphatase, we observed Dma1 phosphorylation in asynchronous cells (Fig. 3-1A). Further examination of Dma1 in various cell cycle arrests showed that Dma1 phosphorylation occurs throughout the cell cycle (Fig. 3-1B).

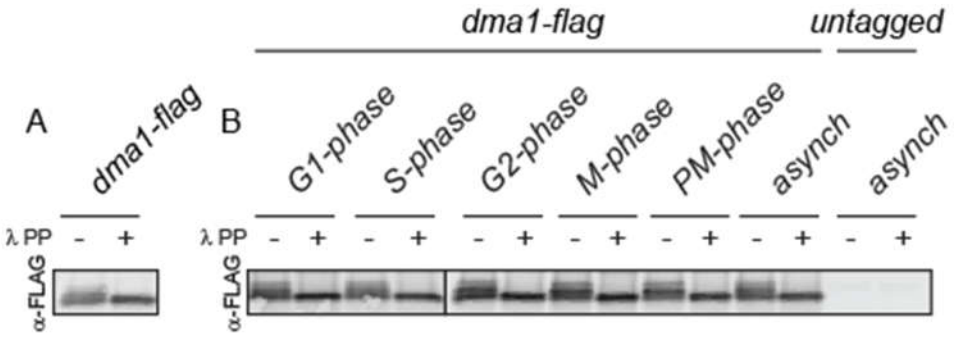

Figure 3-1
Dma1 is phosphorylated through the cell cycle.
(A-B) Immunoblot analysis of Dma1-Flag immunoprecipitates, treated (+) or not (-) with lambda phosphatase, from asynchronous cells (A) or cells arrested at a variety of cell cycle stages (G1 phase, *cdc10-V50*; S phase, HU; G2 phase, *cdc25-22*; metaphase, *mts3-1*; and prometaphase, *nda3-KM311*) (B).

Dma1 is phosphorylated on 7 sites

To determine the sites of Dma1 phosphorylation, we performed LC-MS/MS analysis on Dma1 purified from *S. pombe* cells. Seven sites were identified, including 1 threonine and 6 serines (Fig. 3-2A). To investigate if this cohort was the full complement of Dma1 phosphorylation sites, we began by analyzing its mobility by SDS-PAGE with and without λ phosphatase treatment (Fig. 3-2B). While wild-type Dma1 migrated as several bands, Dma1-7A migrated as a single band that co-migrated with λ phosphatase treated Dma1, a result consistent with the possible removal of all phosphorylation in the Dma1-7A mutant. To verify this finding, we tested whether Dma1-7A could be labeled *in vivo* by ^{32}P orthophosphate radiolabeling (Fig. 3-2C). Though Dma1 was clearly detectable by radiolabeling, Dma1-7A was not, again indicating that the seven identified sites are likely to be the complete cohort of Dma1 phosphorylation sites *in vivo*.

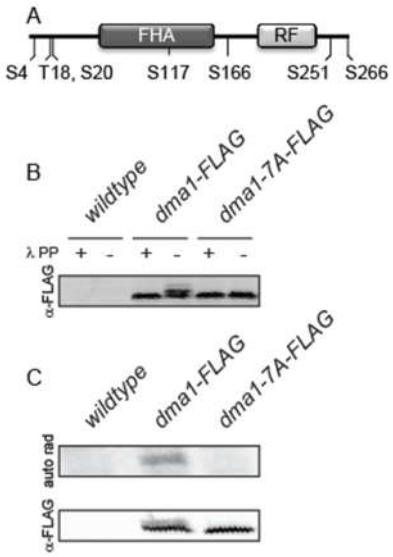

Figure 3-2
Identification of Dma1 phosphorylation sites.
(A) Schematic of Dma1 with phosphorylation sites identified by LC-MS/MS indicated. FHA = Forkhead-associated domain, RF = Ring Finger domain. (B) Immunoblot analysis of Dma1-FLAG immunoprecipitates from the indicated strains, treated (+) or not (-) with lambda phosphatase. (C) Autoradiography and immunoblot analysis of Dma1-FLAG immunoprecipitates from the indicated strains, that were labeled *in vivo* with ^{32}P-orthophosphate.

Dma1 is phosphorylated *in vitro* by several maser kinases

Examination of the linear sequences surrounding the seven phosphorylated residues showed that five of the seven identified sites fit known kinase consensus sequences; S117 and S166 fit the Cdk1 consensus (Moreno & Nurse, 1990; Songyang et al., 1994), S251 fits the Plo1 consensus (Nakajima, Toyoshima-Morimoto, Taniguchi, & Nishida, 2003), and T18 and S20 fit the CK2 consensus (Meggio, Marin, & Pinna, 1994; Songyang et al., 1996). To determine if Cdk1, Plo1, and CK2 were indeed capable of phosphorylating Dma1, *in vitro* kinase assays were performed with recombinant Dma1 and commercially or insect cell-produced kinases (Fig. 3-3A-C). Consistent with the consensus sites, the kinase assays validated that Dma1 can be phosphorylated by Cdk1,

Plo1 and CK2, and confirmed the predicted phosphorylation sites for each kinase. Cdk1 phosphorylation of MBP-Dma1-S166A was diminished compared to MBP-Dma1 and MBP-Dma1-S117A S166A was not phosphorylated at all (Fig. 3-3A). Similarly, while Plo1 phosphorylated MBP-Dma1, it did not phosphorylate MBP-Dma1-S251A (Fig. 3-3B). Lastly, CK2 was unable to phosphorylate MBP-Dma1-T18A S20A S266A though it robustly phosphorylated MBP-Dma1 and was still able to phosphorylate MBP-Dma1-T18A S20A at a diminished level (Fig. 3-3C); indicating that CK2 phosphorylation can occur not only at the predicted T18 and S20 sites but also at the previously unassigned S266 site. Unfortunately the S4 phosphorylation site does not fit a known kinase consensus sequence, and it is not phosphorylated by Cdk1, Plo1 or CK2 indicating that a fourth, yet to be identified, kinase can target Dma1.

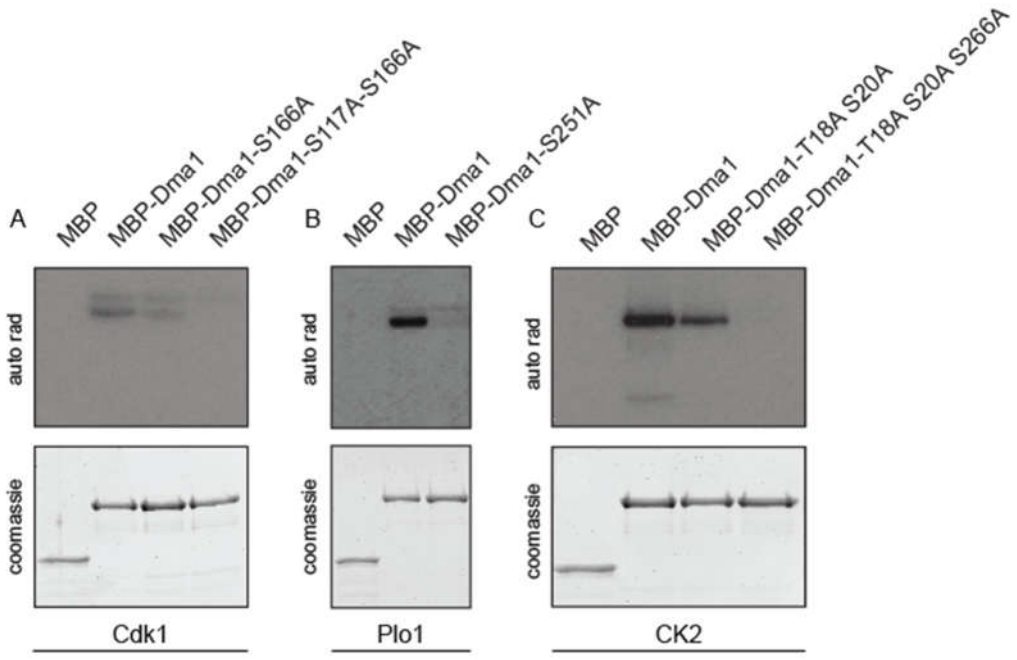

Figure 3-3
Identification of the kinases that phosphorylate Dma1 *in vitro*.
(A-C) Recombinant MBP-purified proteins were incubated *in vitro* with Cdk1 complex (Cdc2-Cdc13) (A), Plo1 (B), or CK2 (C), resolved by SDS–PAGE, and visualized by Coomassie staining (upper panels). Labeled proteins were detected by autoradiography (lower panels).

The Cdk1-Plo1 mimetic, Dma1-S117D S166D S251D, is catalytically active but lacks Dma1 auto-ubiquitination activity

To investigate the potential role of phosphorylation in Dma1 regulation we examined Dma1's two known activities, Sid4 ubiquitination and Dma1 auto-ubiquitination, using *dma1* phospho-ablating and *dma1* phospho-mimetic mutations integrated at the endogenous *dma1* locus. To examine if *dma1* phospho-mutants could ubiquitinate Sid4, we performed immunoblot analysis on Sid4 immunoprecipitated from cells and treated with λ phosphatase to remove Sid4 phosphorylation and clarify ubiquitination bands. Sid4 was ubiquitinated in both the phospho-ablating and phospho-mimetic strains, but not in *dma1Δ* (Fig. 3-4A-B), demonstrating that the Dma1 phosphomutants are all catalytically active and capable of ubiquitinating Sid4.

We next examined the ability of the Dma1 phosphomutants to auto-ubiquitinate. Wild-type and mutant Dma1 proteins, tagged with GFP at the endogenous locus, were immunoprecipitated from cells and incubated with E1 activating enzyme, E2 conjugating enzyme, ATP, and methylated ubiquitin in an *in vitro* ubiquitination assay. The Dma1 phospho-ablation mutants and the CK2 mimetic, Dma1-T18E S20D S266D, exhibited wild-type auto-ubiquitination (Fig. 3-5A-B). However, the Cdk1-Plo1 mimetic, Dma1-S117D S166D S251D, and the complete mimetic, Dma1-7E/D, lacked auto-ubiquitination as did the catalytically inactive Dma1-I194A mutant (Fig. 3-5B). To further analyze the effect of phosphorylation of Dma1 at the Cdk1 and Plo1 sites we performed additional *in vitro* auto-ubiquitination assays using recombinantly purified MBP-Dma1 proteins (Fig. 3-5C). The Plo1 mimetic, Dma1-S251D, showed a slight

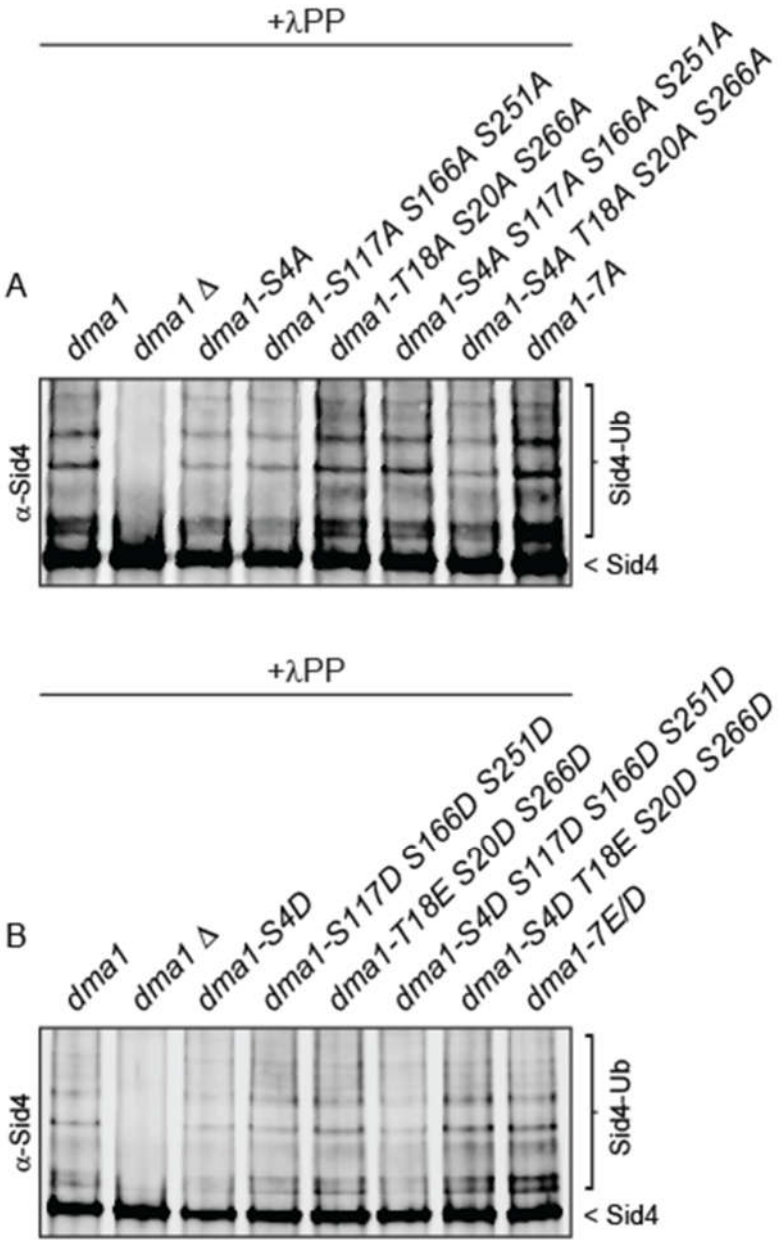

Figure 3-4
Dma1 phosphomutants ubiquitinate Sid4.
(A-B) Immunoblot analysis of Sid4 immunoprecipitates from the indicated strains, treated with λ phosphatase to remove smearing due to Sid4 phosphorylation.

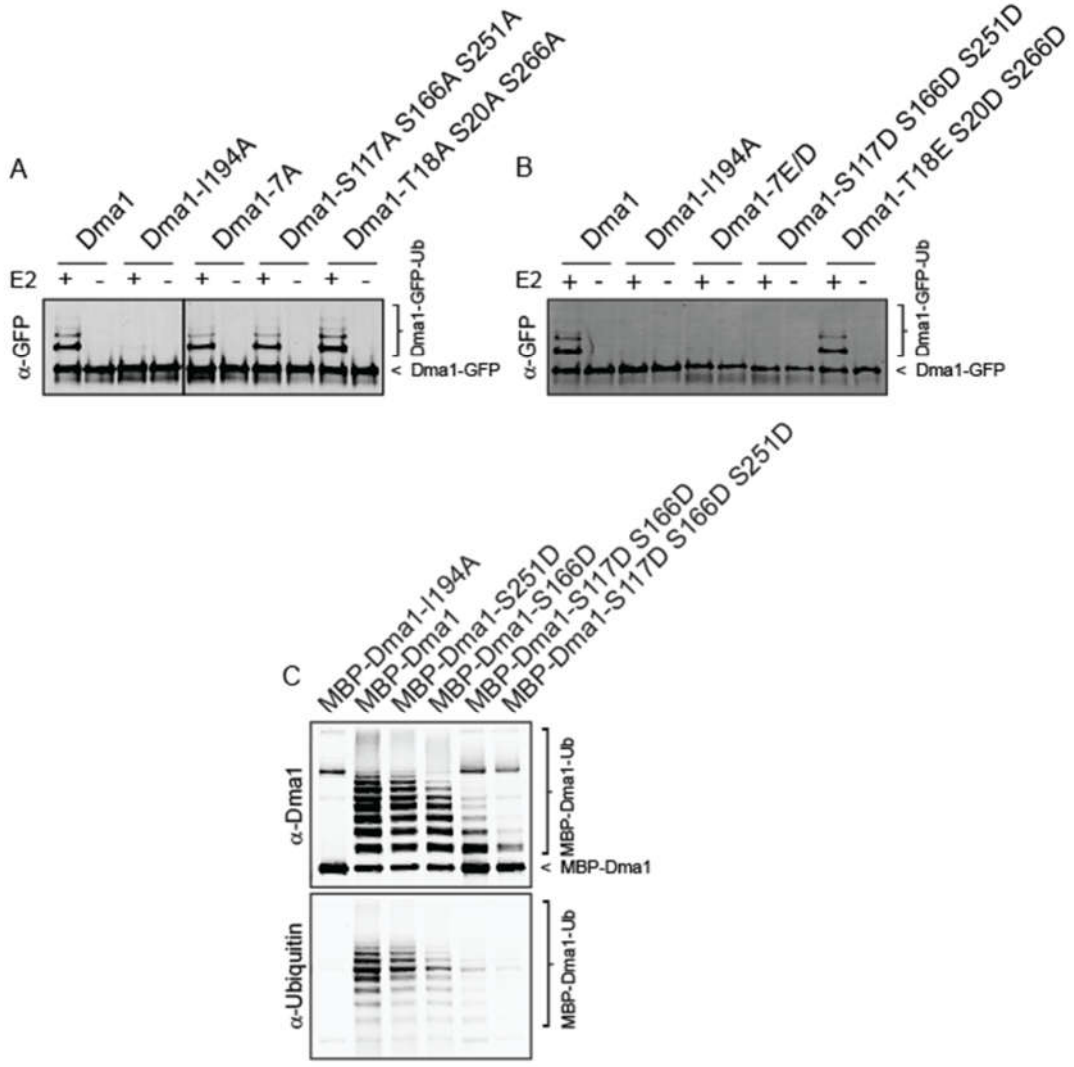

Figure 3-5
The Cdk1/Plo1 phospho-mimetic Dma1-S117D S166D S251D exhibits diminished auto-ubiquitination activity i*n vitro*.
(A-B) Immunoblot analysis of the indicated Dma1-GFP immunoprecipitates that were incubated with E1 activating enzyme, ATP, methylated ubiquitin, and with (+) or without (-) E2 conjugating enzyme. (C) Immunoblot analysis of the indicated recombinantly purified MBP-Dma1 proteins that were incubated with E1 activating enzyme, E2 conjugating enzyme, ATP, and methylated ubiquitin.

decrease in auto-ubiquitination activity relative to wild-type. Similarly, the partial Cdk1 mimetic, Dma1-S166D, showed a decrease in auto-ubiquitination activity that was further reduced in the full Cdk1 mimetic, Dma1-S117D S166D. Lastly, the Cdk1-Plo1 mimetic exhibited minimal auto-ubiquitination activity, consistent with the previous assay.

Provided that the phospho-mimetic residues accurately mimic the phosphorylated state, these results indicate that though phosphorylation of Dma1 at the Cdk1 and Plo1 sites does not affect Dma1's catalytic activity towards its checkpoint substrate Sid4, it does inhibit Dma1 auto-ubiquitination.

3.3 Discussion

Dma1 phosphorylation as a mechanism of regulation

Dma1 checkpoint signaling must be properly regulated to ensure that it is quickly activated in the event of a mitotic spindle error and is also reversed when the error is resolved. Here we have presented evidence indicating that Dma1 phosphorylation likely provides multiple points of regulation. We determined that Dma1 is phosphorylated *in vivo* throughout the cell cycle and that this phosphorylation occurs on seven sites. Examination of the kinases responsible for Dma1 phosphorylation showed that Cdk1, Plo1, and CK2 are all able to phosphorylate Dma1 *in vitro*. The combination of differing phosphorylation consensus sequences and the identification of three master kinases capable of targeting Dma1, indicates that Dma1 is most likely phosphorylated by multiple kinases *in vivo*. The kinases identified *in vitro* play differing roles in the cell cycle and phosphorylate Dma1 at distinct sites (Ahmed, Gerber, & Cochet, 2002; Barr, Sillje, & Nigg, 2004; Malumbres, 2011; Morgan, 1997; Reinhardt & Yaffe, 2013), suggesting that Dma1 may be regulated through phosphorylation in multiple ways from a variety of signaling inputs.

Phosphorylation of Dma1 at the Cdk1-Plo1 sites as a mechanism of regulating auto-ubiquitination

In Chapter 2 we showed that Dma1 auto-ubiquitination plays a role in regulating Dma1 localization dynamics and here we have shown that phosphorylation impacts Dma1 auto-ubiquitination. The Cdk1/Plo1 phospho-mimetic, Dma1-S117D S166D S251D, exhibits impaired auto-ubiquitination activity, while continuing to demonstrate catalytic activity towards the checkpoint protein Sid4. Therefore, phosphorylation of Dma1 at these sites provides a mechanism of inhibiting Dma1 auto-ubiquitination and likely dampening Dma1 localization dynamics, while enabling continued Dma1 checkpoint signaling through ubiquitination of the SIN scaffold Sid4.

How does phosphorylation of Dma1 at the Cdk1/Plo1 sites prevent auto-ubiquitination without disrupting catalytic activity?

Dma1 is known to function as an obligate dimer (A. E. Johnson, Collier, et al., 2012a). While dimerization is required for both Sid4 ubiquitination and auto-ubiquitination, the mechanism of Dma1 auto-ubiquitination has yet to be investigated. Auto-ubiquitination may potentially occur via an intra-dimer reaction where a single dimer auto-ubiquitinates itself, or through an inter-dimer reaction where one Dma1 dimer ubiquitinates a second dimer. As the Cdk1/Plo1 phospho-mimetic, which exhibits impaired auto-ubiquitination, continues to exhibit catalytic activity towards Sid4 whereas disruption of the dimer cannot (A. E. Johnson, Collier, et al., 2012a), it is unlikely that the phospho-mimetic disrupts the Dma1 dimer. Rather, I hypothesize that Dma1 auto-

ubiquitination occurs between dimers and that the phospho-mimetic inhibits the interaction of one Dma1 dimer with a second. However, further investigation is required to address this hypothesis.

Conservation of phosphorylation as a mechanism of regulation in FHA-RING proteins

As previously mentioned, Dma1 is functionally related to the human tumor suppressor proteins RNF and CHFR (Brooks et al., 2008). Here we have shown that Dma1 auto-ubiquitination activity is inhibited by the mitotic kinases Cdk1 and Plo1, similar to the inhibition of RNF8 through phosphorylation by CDK1 during mitosis (Orthwein et al., 2014). While a clear molecular mechanism has yet to be identified for CHFR, the inhibition through phosphorylation seen with both RNF8 and Dma1 will likely extend to CHFR. Thus, our results may provide insight into the mechanisms that regulate CHFR and activation of the antephase checkpoint (Matsusaka & Pines, 2004; Scolnick & Halazonetis, 2000).

Chapter 4

Conclusions and future directions

4.1 Chapter summaries

In response to mitotic spindle stress, the mitotic checkpoint protein Dma1 delays cytokinesis by inhibiting the septation initiation network (SIN). Dma1 is recruited to the SIN scaffold protein, Sid4, through phosphorylation by Hhp1 and Hhp2 (A. E. Johnson et al., 2013a). There Dma1 ubiquitinates Sid4, antagonizing the localization of the Polo-like kinase Plo1 and preventing phosphorylation of its downstream target Byr4 (A. E. Johnson & Gould, 2011b). Upon resolution of the mitotic spindle error, the Dma1 checkpoint signal must be reversed to allow the cell division cycle to continue. However, it is not known how the Dma1 ubiquitination of Sid4 is inhibited. Furthermore, whether Dma1 itself is regulated by the checkpoint remains unclear. In this work, I have investigated the regulation of Dma1 through post-translational modifications including auto-ubiquitination and phosphorylation.

In Chapter 2, I presented work investigating the regulation of Dma1 localization. I found Dma1 to exhibit previously unreported localization dynamics that were dependent on both its catalytic activity and activity of the SIN. We showed that the transient decrease in Dma1 SPB localization in early anaphase depends on its catalytic activity, while Dma1's re-accumulation at SPBs later in anaphase requires SIN activity.

Furthermore, I was able to demonstrate the presence of promiscuous Dma1 auto-ubiquitination *in vivo*. This work also addressed the complications of investigating auto-ubiquitination of an E3 ligase including promiscuous ubiquitination of internal lysines, differential ubiquitination of epitope tags, and the modification's compounding effects such as protein stability and localization. Thus, this investigation may provide insights into the regulation and examination of other E3 ligases including Dma1's human homologs CHFR and RNF8, which also function as cell cycle checkpoint proteins.

In Chapter 3, I presented work clarifying the regulation of Dma1 activity by phosphorylation. I determined that Dma1 is phosphorylated *in vivo* throughout the cell cycle and that this phosphorylation occurs on seven sites. Furthermore, I demonstrated that Cdk1, Plo1 and CK2 can phosphorylate Dma1 *in vitro*. I showed that phospho-mimetics of the Cdk1/Plo1 subset of these sites inhibited Dma1 auto-ubiquitination while maintaining checkpoint activity. The mechanism underlying this separation of auto-ubiquitination and checkpoint activity requires further investigation. However, I hypothesize that the Dma1 phospho-mimetics inhibit the interaction of one Dma1 dimer with a second, effectively disrupting auto-ubiquitination between dimers.

4.2 Discussion

Dma1 is regulated through several mechanisms to maintain proper checkpoint signaling

In this work, I have shown that Dma1 is regulated by dynamic localization, auto-ubiquitination, and phosphorylation. These modes of regulation work in conjunction with those previously identified, including recruitment to the SPB by Hhp1/2

phosphorylation of Sid4 and inhibition by the interacting protein Dnt1 (A. E. Johnson et al., 2013a; Y. Wang et al., 2012b). Together, the various forms of Dma1 regulation function predominantly by impacting its localization and E3 ligase activity.

Dma1 localization is directed through its FHA domain, which binds phosphorylated threonines at the SPBs, division site, and cell tips (Durocher et al., 2000). Regulation of this localization includes recruitment via phosphorylation of Dma1's binding partner, and maintenance of the interaction. At the SPBs this is seen in interaction of Dma1 with Sid4. The CK1 homologs Hhp1 and Hhp2 phosphorylate Sid4 at T275 and S278, which generates a binding site for the FHA domain and results in the recruitment of Dma1 to the SPBs prior to SPB separation (A. E. Johnson et al., 2013a). Once bound to Sid4, Dma1 is then maintained at the SPB until it is released in a Dma1 auto-ubiquitination activity dependent manner. In addition, in early mitosis, the Dma1 interacting protein Dnt1 antagonizes Dma1 localization to the SPBs (Y. Wang et al., 2012b).

By regulating Dma1 localization in a cell cycle and mitotic stress dependent manner such that it is recruited to the SPBs just prior to mitosis, it is properly positioned to efficiently ubiquitinate the substrate Sid4 and inhibit the SIN in in the event of mitotic stress. Furthermore, the release of Dma1 from the SPB, in the absence of stress or upon the resolution of stress, prevents Dma1 from inappropriately inhibiting the SIN.

Dma1 E3 ligase activity is directed through its RING domain, which facilitates the direct transfer of ubiquitin from the E2 to the substrate (A. E. Johnson & Gould, 2011b). This E3 ligase activity includes both substrate ubiquitination, wherein Dma1

facilitates the ubiquitination of Sid4 to inhibit the SIN, and auto-ubiquitination, which promotes the release of Dma1 from the SPB. Though Dma1 exhibits promiscuous catalytic activity that is independent of binding partners, it can be regulated through inhibitory mechanisms including phosphorylation of Dma1 and the interaction of Dma1 with Dnt1. The Cdk1-Plo1 mimetic, Dma1-S117D S166D S251D, is catalytically active toward Sid4 but lacks Dma1 auto-ubiquitination activity. Thus, indicating that phosphorylation of Dma1 by Cdk1 and Plo1 would constrain auto-ubiquitination without inhibiting checkpoint activation. Alternatively, interaction with Dnt1 inhibits both substrate ubiquitination and auto-ubiquitination (Y. Wang et al., 2012b).

As a mitotic checkpoint protein, Dma1 must be well regulated to ensure proper coordination of mitosis and cytokinesis, such that it can quickly activate the spindle checkpoint in response to mitotic spindle stress, yet also allow cytokinesis to proceed once the stress is resolved. Dma1 is catalytically active at the SPBs during mitosis and can therefore activate the checkpoint efficiently in response to stress. In addition, in the absence of stress as seen in an unperturbed division or the resolution of checkpoint activation, the mechanisms of inhibitory regulation serve to prevent excessive checkpoint activation.

Implications to the mammalian paralogs CHFR and RNF8

Dma1 is the *S. pombe* member of the FHA-RING class of proteins, a small class of cell cycle checkpoint proteins including the two mammalian paralogs CHFR and RNF8 (Brooks et al., 2008). The absence of either of these mammalian proteins is

associated with an increase in rate and severity of cancers (Privette & Petty, 2008). In addition, case studies and clinical research continues to mount regarding the significance of repressed CHFR gene transcription through DNA methylation in epithelial cancers. However, while CHFR has been shown to act as a checkpoint protein in response to mitotic stress, the mechanisms regulating CHFR activity remain unclear (Kim et al., 2011; Matsusaka & Pines, 2004; Sanbhnani & Yeong, 2012).

In addition to the role of decreased FHA-RING ligase expression in the occurrence of cancer, cancer tissues expressing RNF8 and CHFR are aggressive and recalcitrant to treatment. CHFR expression is associated with taxane resistance in cancer, while RNF8 expression is correlated with disease progression and poor patient survival. Initial studies examining treatments using small molecule inhibitors have shown targeting CHFR and RNF8 to be a promising method to address treatment resistance and tumor aggressiveness (Brodie et al., 2015; H. J. Lee et al., 2016).

Considering the multitude of cancer implications associated with FHA-RING ligases, it is important to understand the mechanisms regulating their action. *S. pombe* is well conserved, particularly in regards to the advancement and regulation of the cell division cycle (Goyal et al., 2011), and as such the Dma1 mechanisms of regulation I have identified here may extend to CHFR and RNF8. This is further supported by the inhibition of Dma1 auto-ubiquitination through phosphorylation shown here, which is consistent with previously identified RNF8 inhibition through phosphorylation.

4.3 Future directions

Regulation of Dma1 at Cdk1/Plo1 sites of phosphorylation.

Though the work presented in Chapter 3 has provided insight into the regulation of Dma1 activity by phosphorylation, the mechanism underlying the separation of auto-ubiquitination and checkpoint activity requires further investigation. First, it is important to show that the inhibition of auto-ubiquitination demonstrated by phospho-mimetic residues accurately mimic the phosphorylated state, and that the inhibition of auto-ubiquitination occurs *in vivo*. Examination of auto-ubiquitination upon phosphorylation can be achieved by coupling *in vitro* kinase assays to the *in vitro* ubiquitination assay. Whereas, the impact on auto-ubiquitination *in vivo* can be examined by purifying HBH tagged Dma1 and Dma1 phospho-mimetics under fully denaturing conditions.

Next, I would investigate the molecular mechanism enabling this differential regulation of Dma1 activity. As previously indicated, I hypothesize that Dma1 auto-ubiquitination occurs through an inter-dimer reaction and that phosphorylation of the S117, S166, and S251 sites inhibits auto-ubiquitination by disrupting the dimer-dimer interaction. The formation of a dimer of dimers is supported by previously published analytical ultra-centrifugation (AU) experiments, which showed Dma1 to exhibit a minor tetramer peak (A. E. Johnson, Collier, et al., 2012a). I predict that AU experiments, including both wild-type and Cdk1/Plo1 phospho-mimetic Dma1 proteins, will show both proteins to exhibit a dimer peak, but only the wild-type protein to exhibit a tetramer peak. Furthermore, performing *in vitro* ubiquitination assays with reducing concentrations of Dma1 can be used to determine if auto-ubiquitination occurs through intra-dimer or inter-

dimer reactions. If auto-ubiquitination occurs through intra-dimer reactions, it will perform in a concentration independent manner, conversely if it occurs through inter-dimer reactions, it will exhibit concentration dependence.

Finally, I would examine of the impact of Dma1 phosphorylation on its localization dynamics. As discussed in Chapter 2, Dma1 localization dynamics are impaired in the absence of Dma1 auto-ubiquitination. Therefore, I anticipate that the Dma1 S117D S166D S251D mutant, which demonstrates impaired auto-ubiquitination, will exhibit reduced SPB localization dynamics, similar to those seen in the catalytically inactive Dma1-I194A mutant.

Regulation of Dma1 at CK2 sites of phosphorylation.

In addition to the Cdk1/Plo1 sites discussed in Chapter 3, Dma1 phosphorylation was identified at T18, S20, and S266. The T18 and S20 sites fit the CK2 consensus sequence and in vitro kinase assays confirmed that CK2 can phosphorylate all three *in vitro*. Though examination of the phospho-ablation and phospho-mimetic mutations of these sites showed no impact on Dma1 activity, it is important to consider the possibility that they regulate another characteristic of Dma1 such as its localization or that the phospho-mimetic residues do not accurately mimic the phosphorylated state.

Interestingly, phosphorylation of the N-terminal CK2 sites T18 and S20 creates an FHA domain binding consensus sequence (KEQELAAEpTDpSEKDDDK) that is very similar to the site Dma1 binds to on Sid4 during spindle checkpoint activation (LTSSpTCVpSSI) (Liang & Van Doren, 2008; Mahajan et al., 2008). Furthermore, the

FHA domain of Dma1 has been shown to specifically recognize phosphorylated threonines and not phospho-mimetics (A. E. Johnson et al., 2013a). Thus, I would begin investigating the role of these sites by examining binding of the Dma1 FHA domain to this phosphorylated peptide. I anticipate that the FHA domain of Dma1 will bind specifically to the peptide in the phosphorylated state.

In the event that the FHA domain does in fact bind the phosphorylated peptide, I would next examine the mechanism of binding. The interaction could potentially occur within a single Dma1 dimer, preventing the FHA domain from binding other substrates (e.g Sid4), and thereby preventing Dma1 from localizing to any specific cellular structures. Alternatively, the interaction could occur across molecules, serving as a means to concentrate Dma1 localization. The T18 phosphorylation site was readily identified in MS analyses from asynchronous populations, wherein most cells are in interphase and thus exhibit diffuse cytoplasmic Dma1 localization. Therefore, I anticipate that phosphorylation of Dma1 at the T18 and S20 sites creates an FHA domain binding consensus and enables the Dma1 N-terminus to bind to FHA domain of the same molecule and effectively block recruitment of Dma1 through its FHA domain.

Conservation of the Dma1 regulatory mechanisms in the mammalian homolog CHFR.

The research presented here provides substantial insights into the regulation of Dma1 through auto-ubiquitination and phosphorylation, however it remains to be seen if these means of regulation apply to the human homolog CHFR. To determine how well

conserved these mechanisms of regulation are, I would first examine the localization and phosphorylation of CHFR.

To date, CHFR localization has only been studied using exogenous expression over the endogenous protein. To develop a more accurate understanding of CHFR localization, I would tag CHFR in normal and cancerous cell lines with the monomeric fluorescent protein mNeonGreen. Using the CRISPR/Cas system not only could I tag wild-type cell lines tagged at the endogenous locus, I could also examine specific mutations including the catalytically inactive I306A mutant (Kang et al., 2002; Salsman & Dellaire, 2017). I would then use live cell imaging to examine CHFR localization throughout the cell cycle.

Assuming CHFR protein localization reflects that seen with Dma1, including dynamic localization to the centrosomes by the wild-type protein and stabile localization by the catalytically inactive mutant, I would proceed to examine the role of auto-ubiquitination in CHFR localization. Using the techniques outlined in the work above, I would examine if the release of CHFR from the centrosomes is dependent on auto-ubiquitination.

In addition, the impact of phosphorylation on CHFR activity has not been well studied. However, CHFR exhibits consensus sequences for several kinases including Plk1, Cdk1, and CK2 (Dinkel et al., 2016), which I have shown to phosphorylate Dma1. I would like to determine if these kinases phosphorylate CHFR and if so whether the Cdk1 and Plo1 phosphorylated protein exhibits catalytic active toward substrates but lacks auto-ubiquitination activity.

4.4 Conclusions

In this work, I have shown that Dma1 exhibits activity-dependent SPB localization dynamics and presented evidence indicating that these dynamics are impaired in the absence of Dma1 auto-ubiquitination. Furthermore, I have identified sites of Dma1 phosphorylation and demonstrated that phospho-mimetics at the Cdk1-Plo1 sites impair auto-ubiquitination activity without disrupting catalytic activity toward Sid4 or checkpoint function. Thus, Dma1 regulatory mechanisms provide an effective means of differentially regulating Dma1's two E3 ligase activities.

Appendix

A. Materials and Methods

Yeast methods

Yeast strains were grown in yeast extract (YE) or four times concentrated yeast extract (4X YE) with appropriate supplements (Moreno, Klar, & Nurse, 1991). Epitope-tagged strains were constructed by tagging genes of interest endogenously at the 3' end of their open reading frame (ORF) with *mNG:kan^R, mNG:Hyg^R*, *GFP:kan^R*, *mCherry:kan^R*, *mCherry:nat^R*, *HBH:kan^R*, *FLAG$_3$:kan^R*, *HA$_3$:kan^R, HA3-TAP:kan^R, MYC$_{13}$:kan^R, GBP-mCherry:kan^R*, or *ubp7$^+$* (residues 201-875) *DUB:kan^R* using pFA6 cassettes as previously described (Bahler et al., 1998; Wach, Brachat, Pohlmann, & Philippsen, 1994). For *dma1* gene replacements, a haploid *dma1*Δ strain was transformed with the appropriate pIRT2–*dma1* mutant. Stable integrants were selected by resistance to 1.5 mg/ml 5-FOA. Mutants were validated first by colony PCR with primers inside and outside of the 3'-flanking regions, then further through DNA sequencing of the entire ORF.

For blocking *nda3-KM311* strains in prometaphase, cultures were grown at 32˚C and then shifted to 18˚C for 6 hrs. For blocking *cdc10-V50, cdc25-22, cdc11-123,* and *mts3-1* strains, cultures were grown at 25˚C and then shifted to 36˚C for 3.5 hr. For blocking strains with hydroxyurea (HU), cultures were grown at 25˚C and treated first with a final concentration of 12 mM HU for 3 hrs then dosed again with a final concentration of 6 mM HU for an additional 2 hr before harvesting. For blocking prior to imaging *mts3-1, cdc7-24, and cdc16-116* were grown at 25˚C and then shifted to 36˚C for 3.5 h, 2 h, and 3 h, respectively before imaging experiments.

For serial dilution spot assays, cells were cultured in liquid YE at 29°C, four serial 10-fold dilutions were made, 3 μL of each dilution was spotted on YE plates and cells were grown at the indicated temperatures for 3-4 d.

Diploid strains were made by crossing *ade6-M210* cells with *ade6-M216* cells on glutamate plates for 24-48 h followed by restreaking to single colonies on MAU plate and incubating at 32˚C for 3 days. White colonies (diploid cells) were then picked for subsequent analysis.

Molecular biology methods

All plasmids were generated by standard molecular biology techniques. *dma1* mutations were made either in the context of a gene fragment in the pIRT2 vector that included 500 bp upstream and downstream of the open reading frame or in the context of the open reading frame in pMAL2-c vector using a QuikChange site-directed mutagenesis kit (Agilent Technologies). The mutations abbreviations are defined as follows: Dma1-4KR = K3R, K10R, K121R, K124R; Dma1-9KR = K3R, K26R, K54R, K82R, K124R, K164R, K174R, K237R, K262R; Dma1-12KR = Dma1-K3R, K10R, K22R, K26R, K121R, K124R, K162R, K164R, K174R, K217R, K237R, K262R; Dma1-14KR = K3R, K10R, K22R, K26R, K54R, K82R, K121R, K124R, K162R, K164R, K174R, K217R, K237R, K262R; *dma1-7A* = T18A, S20A, S117A, S166A, S251A, and S266A; *dma1-7E/D* = S4D, T18E, S20D, S117D, S166D, S251D, and S266D.

cDNAs encoding Ubp2, Ubp3, Ubp4, Ubp8, Ubp14, Ubp15, Ubp16, Uch1, were amplified by PCR from genomic *S. pombe* DNA using primers with specific restriction sites included. The PCR products were digested with the appropriate restriction enzymes

(Nde1/BamHI for *ubp2* and *ubp3* and NdeI/XmaI for *ubp4*, *ubp8, ubp14, ubp15, ubp16*, and *uch1*), subcloned into pREP1, and verified by sequencing. DNAs encoding Ubp1, Ubp7, Ubp9, Ubp11, Otu1, Otu2, and Sst2, were digested from genomic constructs in plasmids KGY5040 (Sal1/BamH1), KGY5036 (Nde1/Xma1), KGY5020 (Nde1/Xma1), (KGY5038 (Nde1/Xma1), KGY5042 (Xma1), KGY5044 (Nde1/Xma1), and KGY5045 (Nde1/Xma1), subcloned into pREP1 and verified by sequencing. *ubp6* and *uch2* cDNAs in pREP1 vectors were gifts from Dr. Colin Gordon (Stone et al., 2004).

Microscopy methods

Fixed- and live-cell images of *S. pombe* cells were acquired with a Personal DeltaVision microscope system (Applied Precision) that includes an Olympus IX71 microscope, 60× NA 1.42 PlanApo oil immersion objective, standard and live-cell filter wheels, a Photometrics CoolSnap HQ2 camera, and softWoRx imaging software. Live-cell imaging was performed at 25°C, and cells were imaged in YE media. Images in figures were maximum intensity projections of z sections spaced at 0.2-0.5 μm. Images used for quantification were not deconvolved and sum projected.

Intensity measurements were made with ImageJ software (National Institutes of Health, Bethesda, MD: http://rsbweb.nih.gov/ij/). For all intensity measurements, the background was subtracted by creating a region of background (ROB) in the same image as the region of interest (ROI) where there were no cells. The raw intensity of the ROB was divided by its area providing a background per pixel (BPP), which was multiplied by the area of the ROI to provide a background subtraction value. This number was

subtracted from the raw integrated intensity of that ROI: ROB area/ ROB raw intensity = BPP; ROI – (BPP x ROI area) (Waters, 2009).

For analysis relative to a SPB marker, an ROI was made based on the SPB marker, mNG or GFP fluorescence intensity and mCherry marker fluorescence intensity were measured with background correction for each. Final values for each cell are expressed as mNG/mCherry or GFP/mCherry ratios. Measurements for the cells in each group were averaged for statistical analysis.

Protein purification and mass spectrometry

Endogenously tagged versions of Dma1 (Dma1-TAP and Dma1-HBH) were purified as previously described (Elmore, Beckley, Chen, & Gould, 2014; Gould, Ren, Feoktistova, Jennings, & Link, 2004; Tagwerker et al., 2006) and analyzed by 2D-LC-MS/MS as previously described (McDonald WH, 2002; Roberts-Galbraith, Chen, Wang, & Gould, 2009). RAW files were processed using two pipelines: 1) using Myrimatch (v 2.1.132) (Tabb, Fernando, & Chambers, 2007) and IDPicker (v 2.6.271.0) (Ma et al., 2009) as previously described (McLean, Kouranti, & Gould, 2011) and 2) using turboSEQUEST, Scaffold (v 4.4.7) and Scaffold PTM (v 3.0.0) as previously described (J. S. Chen et al., 2013), except for ubiquitin modification searches the variable di-Gly modification (114 Da) was included in the searches.

Protein expression and recombinant purification

dma1 variants were cloned into pMAL-2c for production as maltose-binding protein (MBP) fusions. Proteins were induced in *Escherichia coli* Rosetta2(DE3)pLysS

cells by addition of 0.8 mM IPTG and overnight incubation at 18°C. Bacterial cells were lysed by incubating with 300 ug/ml lysozyme for 20 min followed by sonication. Proteins were affinity purified on amylose resin (NEB E8021) in MBP column buffer (100 mM NaCl, 20 mM Tris-HCl, 1 mM EDTA, 1 mM DTT, and 1% Nonidet P40). Resin was washed with MBP column buffer and either kept on resin or eluted with the addition of 10 mM maltose and, in some cases, the MBP tag was cleaved with Factor Xa protease (New England Biolabs).

In vitro kinase assays

Kinase reactions were performed in protein kinase buffer (10 mM Tris, pH 7.4, 10 mM $MgCl_2$, and 1 mM DTT or NEB supplied buffer) with 5 μM cold ATP, 3 μCi of ^{32}P-ATP, and recombinant CK2 (New England Biolabs), insect cell-produced Cdc2-Cdc13 or insect cell-produced Plo1 at 30°C for 30 min. Reactions were quenched by the addition of SDS sample buffer. Proteins were separated by SDS–PAGE and detected by Coomassie Blue (Sigma) staining or transferred to polyvinylidene fluoride (PVDF) membrane for detection by autoradiography.

In vitro ubiquitination assays

Ubiquitination reagents were combined in 20 ul reactions and included: either 0.25 to 1 ug recombinant MBP-Dma1 (or variant thereof) or immunoprecipitated Dma1-GFP that was washed twice with ubiquitination buffer (50 mM Tris, pH 7.4, 2.5 mM $MgCl_2$, and 0.5 mM DTT), 175 nM E1 (Boston Biochem E-304), 3 uM E2 (Boston Biochem E2-616), 50 ug/ml methylated ubiquitin, 5 mM ATP, and ubiquitination buffer.

Reactions were incubated with agitation at 30˚C for 90 min before adding SDS sample buffer to quench the reaction or cleaving Dma1 from MBP. To cleave Dma1 from MBP, 1.8 ul of 1M $CaCl_2$ and 5 ul Factor Xa protease (NEB P8010) were added to each reaction and incubated at room temperature with agitation for 1 hour. 100 ul benzamidine beads (1:1 slurry) and 100 ul amylose beads (1:1 slurry), previously washed in MBP binding buffer, were added to each reaction and incubated room temperature with agitation for 45 min. Supernatants were transferred to fresh Eppendorf tubes before adding SDS sample buffer. To assess the extent of Dma1's ubiquitin modification, proteins were separated by SDS-PAGE and detected by immunobloting with anti-Dma1, anti-GFP, and/or anti-ubiquitin antibodies.

In vivo ubiquitination assay

Dma1-HBH was purified from 250 ml 4X YE pellets (Tagwerker et al., 2006). Cell pellets were resuspended in 10 mls buffer 1 (8 M urea, 300 mM NaCl, 50 mM $NaPO_4$, 0.5% Nonidet P40 and 4 mM Imidazole, pH 8 with 1.3 mM benzamidine, 1 mM PMSF, 50 uM PR-619 (LifeSensors), 50 uM N-Ethylmaleimide, and 1 Complete Protease Inhibitor Cocktail Tablet, EDTA-free per 50 ml), repelleted, and lysed by bead disruption with 500 uls buffer 1. The lysate was first extracted with a total of 15 ml buffer 1 (two extractions: 10 ml then 5 ml), then cleared, and incubated with 200 ul (1:1 slurry) Ni^{2+}-NTA agarose beads (Qiagen) for 3-4 h at room temperature. After incubation, beads were washed four times: once with 10 ml buffer 1 and three times with 10 ml buffer 3 (8 M urea, 300 mM NaCl, 50 mM $NaPO_4$, 0.5% Nonidet P40 and 20 mM Imidazole, pH 6.3). Beads were then eluted for 15 min in 5 ml buffer 4 (8 M urea, 200 mM NaCl, 50

mM $NaPO_4$, 0.5% Nonidet P40 and 2% SDS, 100 mM Tris and 10 mM EDTA, pH 4.3) two times and the eluates were pooled into a single tube. The pH of the eluate was adjusted to 8 before 80 ul streptavidin ultra-link resin (Pierce) was added and incubated overnight at room temperature. After the overnight incubation, the streptavidin beads were washed three times with buffer 6 (8 M urea, 200 mM NaCl, 2% SDS and 100 mM Tris, pH 8). Purified proteins were detected on a western blot using an anti-ubiquitin antibody (Millipore-MAB1510) at a 1:250 dilution or (LifeSensors-VU-1) at a 1:500 dilution and fluorescently labelled streptavidin (Licor).

S. pombe protein methods

Cell lysis

Cell pellets were washed once in NP-40 buffer (10 mM sodium phosphate pH 7.0, 1% Nonidet P40, 150 mM NaCl, 2 mM EDTA) with inhibitors (1.3 mM benzamidine, 1 mM PMSF, and 1 Complete Protease Inhibitor Cocktail Tablet, EDTA-free per 50 ml) and lysed by bead disruption. For denaturing lysis, 500 ul SDS lysis buffer (10 mM sodium phosphate pH 7.0, 1 % SDS, 1 mM DTT, 1 mM EDTA, 50 mM NaF, 100 uM sodium orthovanadate, 1 mM PMSF, and 4 ug/ml leupeptin) was added and samples were incubated at 95˚C for 2 min, lysate was extracted with 800 ul NP-40 buffer and transferred to a fresh Eppendorf tube. For native lysis, the lysate was extracted with 500 ul NP-40 buffer and again with 800 ul, then transferred to a fresh Eppendorf tube. Extractions were followed by a 20 min clearing spin.

Immunoprecipitation

Proteins were immunoprecipitated from protein lysates using an excess of antibody (listed below) and nutating at 4˚C for 1 hour, followed by addition of Protein A or G Sepharose beads (GE Healthcare), as appropriate, and nutating at 4˚C for 30 min. Samples were washed four times with NP-40 buffer. Antibodies: 2 ul of 0.4 ug/ul anti-GFP (Roche, Nutley, NJ), 2 ul of 1 ug/ul anti-FLAG (Sigma-Aldrich), 3 ul rabbit anti-Sid4 antiserum, or 2 ul rabbit anti-Dma1 serum.

Antisera were raised against recombinant GST-mNG or GST-Dma1 (Cocalico) and their specificity was verified by immunoblotting (Fig. 2-3 and Fig. 2-S5B, respectively). The anti-Dma1 serum was further purified by ammonium sulfate precipitation. The serum was cleared by centrifugation and then precipitated with 0.5 volumes of saturated ammonium sulfate added dropwise and incubated overnight at 4˚C. The precipitate was cleared from the serum by centrifugation then the serum was precipitated with an additional 0.5 volumes of saturated ammonium sulfate added dropwise and incubated overnight at 4˚C. The precipitate was pelleted by centrifugation, resuspended in 0.4 volumes PBS, and dialyzed 3X in PBS.

Lambda phosphatase treatment

Immunoprecipitated protein was washed twice with 25 mM HEPES-NaOH (pH 7.4) and 150 mM NaCl, then treated with lambda phosphatase (New England Biolabs) in 1x NEBuffer for PMP and 1 mM $MnCl_2$ and incubated at 30°C for 30 to 60 min with agitation.

Immunoblotting

Proteins were resolved by PAGE (see below), transferred by electroblotting to a poly-vinylidene difluoride (PVDF) membrane (Immobilon P; Millipore, Bedford, MA), blocked with Odyssey Blocking Buffer (LI-COR Biosciences), and incubated with primary antibody at 2 μg/ml or 1:5000 anti-Cdc2 (anti-PSTAIR, Sigma) or 1:500 anti-ubiquitin (VU-1, Life Sensors) or 1:5000 anti-Dma1 serum or 1:2000 anti-Sid4 serum overnight at 4°C. For detection with the VU-1 anti-ubiquitin antibody, the PVDF membrane was washed with water three times, incubated with 0.5% glutaraldehyde in PBS for 20 min, and washed with PBS three times prior to blocking. Primary antibodies were detected with secondary anti-bodies coupled to IRDye680 or IRDye800 (LI-COR Biosciences, Lincoln, NE) and visualized using an Odyssey Infrared Imaging System (LI-COR Biosciences). Resolving gels: 3-8% Tris-acetate PAGE used for Dma1-FLAG blotting; 4-12% NuPAGE used for Sid4 and Dma1 ubiquitination assay blotting, 12% Tris-glycine PAGE used for Cdc2 blotting, 10% Tris-glycine PAGE used for MBP-Dma1 blotting

In vivo radio-labeling

10 ml of *S. pombe* cells were grown in reduced (20 mM NaH_2PO_4) phosphate minimal media supplemented with the appropriate amino acids to mid-log phase. Cells were labeled with 5 mCi ^{32}P-orthophosphate for 4 hr at 36°C. Denatured cell lysates were prepared and Dma1-FLAG was immunoprecipitated with anti-FLAG. Immunoprecipitates were resolved on a 6-20% gradient SDS polyacrylamide gel, transferred to a PVDF membrane and phosphorylated proteins were detected by

autoradiography for 4 d at -80°C with intensifying screen. The membrane was then immunoblotted for anti-FLAG.

BIBLIOGRAPHY

Ahmed, K., Gerber, D. A., & Cochet, C. (2002). Joining the cell survival squad: an emerging role for protein kinase CK2. *Trends Cell Biol, 12*(5), 226-230.

Alexandru, G., Zachariae, W., Schleiffer, A., & Nasmyth, K. (1999). Sister chromatid separation and chromosome re-duplication are regulated by different mechanisms in response to spindle damage. *EMBO J, 18*(10), 2707-2721. doi: 10.1093/emboj/18.10.2707

Almawi, A. W., Matthews, L. A., & Guarne, A. (2016). FHA domains: Phosphopeptide binding and beyond. *Prog Biophys Mol Biol*. doi: 10.1016/j.pbiomolbio.2016.12.003

Bahler, J., & Pringle, J. R. (1998). Pom1p, a fission yeast protein kinase that provides positional information for both polarized growth and cytokinesis. *Genes Dev, 12*(9), 1356-1370.

Bahler, J., Wu, J. Q., Longtine, M. S., Shah, N. G., McKenzie, A., 3rd, Steever, A. B., . . . Pringle, J. R. (1998). Heterologous modules for efficient and versatile PCR-based gene targeting in Schizosaccharomyces pombe. *Yeast, 14*(10), 943-951. doi: 10.1002/(SICI)1097-0061(199807)14:10<943::AID-YEA292>3.0.CO;2-Y

Barr, F. A., Sillje, H. H., & Nigg, E. A. (2004). Polo-like kinases and the orchestration of cell division. *Nat Rev Mol Cell Biol, 5*(6), 429-440. doi: 10.1038/nrm1401

Beltraminelli, N., Murone, M., & Simanis, V. (1999). The S. pombe zfs1 gene is required to prevent septation if mitotic progression is inhibited. *J Cell Sci, 112 Pt 18*, 3103-3114.

Bohnert, K. A., & Gould, K. L. (2011). On the cutting edge: post-translational modifications in cytokinesis. *Trends Cell Biol, 21*(5), 283-292. doi: 10.1016/j.tcb.2011.01.006

Bohnert, K. A., Grzegorzewska, A. P., Willet, A. H., Vander Kooi, C. W., Kovar, D. R., & Gould, K. L. (2013). SIN-dependent phosphoinhibition of formin multimerization controls fission yeast cytokinesis. *Genes Dev, 27*(19), 2164-2177. doi: 10.1101/gad.224154.113

Brodie, S. A., Li, G., Harvey, D., Khuri, F. R., Vertino, P. M., & Brandes, J. C. (2015). Small molecule inhibition of the CHFR-PARP1 interaction as novel approach to overcome intrinsic taxane resistance in cancer. *Oncotarget, 6*(31), 30773-30786. doi: 10.18632/oncotarget.5040

Brooks, L., 3rd, Heimsath, E. G., Jr., Loring, G. L., & Brenner, C. (2008). FHA-RING ubiquitin ligases in cell division cycle control. *Cell Mol Life Sci, 65*(21), 3458-3466. doi: 10.1007/s00018-008-8220-1

Burgess, A., Labbe, J. C., Vigneron, S., Bonneaud, N., Strub, J. M., Van Dorsselaer, A., . . . Castro, A. (2008). Chfr interacts and colocalizes with TCTP to the mitotic spindle. *Oncogene, 27*(42), 5554-5566. doi: 10.1038/onc.2008.167

Cabib, E., Roh, D. H., Schmidt, M., Crotti, L. B., & Varma, A. (2001). The yeast cell wall and septum as paradigms of cell growth and morphogenesis. *J Biol Chem, 276*(23), 19679-19682. doi: 10.1074/jbc.R000031200

Carnahan, R. H., & Gould, K. L. (2003). The PCH family protein, Cdc15p, recruits two F-actin nucleation pathways to coordinate cytokinetic actin ring formation in

Schizosaccharomyces pombe. *J Cell Biol, 162*(5), 851-862. doi: 10.1083/jcb.200305012

Cassani, C., Raspelli, E., Santo, N., Chiroli, E., Lucchini, G., & Fraschini, R. (2013). Saccharomyces cerevisiae Dma proteins participate in cytokinesis by controlling two different pathways. *Cell Cycle, 12*(17), 2794-2808. doi: 10.4161/cc.25869

Chang, F., Drubin, D., & Nurse, P. (1997). cdc12p, a protein required for cytokinesis in fission yeast, is a component of the cell division ring and interacts with profilin. *J Cell Biol, 137*(1), 169-182.

Chang, L., & Gould, K. L. (2000). Sid4p is required to localize components of the septation initiation pathway to the spindle pole body in fission yeast. *Proc Natl Acad Sci U S A, 97*(10), 5249-5254.

Chang, L., Morrell, J. L., Feoktistova, A., & Gould, K. L. (2001). Study of cyclin proteolysis in anaphase-promoting complex (APC) mutant cells reveals the requirement for APC function in the final steps of the fission yeast septation initiation network. *Mol Cell Biol, 21*(19), 6681-6694.

Chaturvedi, P., Sudakin, V., Bobiak, M. L., Fisher, P. W., Mattern, M. R., Jablonski, S. A., . . . Zhou, B. B. (2002). Chfr regulates a mitotic stress pathway through its RING-finger domain with ubiquitin ligase activity. *Cancer Res, 62*(6), 1797-1801.

Chen, C. T., Feoktistova, A., Chen, J. S., Shim, Y. S., Clifford, D. M., Gould, K. L., & McCollum, D. (2008). The SIN kinase Sid2 regulates cytoplasmic retention of the S. pombe Cdc14-like phosphatase Clp1. *Curr Biol, 18*(20), 1594-1599. doi: 10.1016/j.cub.2008.08.067

Chen, J. S., Broadus, M. R., McLean, J. R., Feoktistova, A., Ren, L., & Gould, K. L. (2013). Comprehensive proteomics analysis reveals new substrates and regulators of the fission yeast clp1/cdc14 phosphatase. *Mol Cell Proteomics, 12*(5), 1074-1086. doi: 10.1074/mcp.M112.025924

Chen, Y. H., Wang, G. Y., Hao, H. C., Chao, C. J., Wang, Y., & Jin, Q. W. (2017). Facile manipulation of protein localization in fission yeast through binding of GFP-binding protein to GFP. *J Cell Sci, 130*(5), 1003-1015. doi: 10.1242/jcs.198457

Cheung, H. W., Ching, Y. P., Nicholls, J. M., Ling, M. T., Wong, Y. C., Hui, N., . . . Wang, X. (2005). Epigenetic inactivation of CHFR in nasopharyngeal carcinoma through promoter methylation. *Mol Carcinog, 43*(4), 237-245. doi: 10.1002/mc.20106

Coffman, V. C., Nile, A. H., Lee, I. J., Liu, H., & Wu, J. Q. (2009). Roles of formin nodes and myosin motor activity in Mid1p-dependent contractile-ring assembly during fission yeast cytokinesis. *Mol Biol Cell, 20*(24), 5195-5210. doi: 10.1091/mbc.E09-05-0428

Corn, P. G., Summers, M. K., Fogt, F., Virmani, A. K., Gazdar, A. F., Halazonetis, T. D., & El-Deiry, W. S. (2003). Frequent hypermethylation of the 5' CpG island of the mitotic stress checkpoint gene Chfr in colorectal and non-small cell lung cancer. *Carcinogenesis, 24*(1), 47-51.

Cortes, J. C., Konomi, M., Martins, I. M., Munoz, J., Moreno, M. B., Osumi, M., . . . Ribas, J. C. (2007). The (1,3)beta-D-glucan synthase subunit Bgs1p is responsible for the fission yeast primary septum formation. *Mol Microbiol, 65*(1), 201-217. doi: 10.1111/j.1365-2958.2007.05784.x

Cortes, J. C., Pujol, N., Sato, M., Pinar, M., Ramos, M., Moreno, B., . . . Perez, P. (2015). Cooperation between Paxillin-like Protein Pxl1 and Glucan Synthase Bgs1 Is Essential for Actomyosin Ring Stability and Septum Formation in Fission Yeast. *PLoS Genet, 11*(7), e1005358. doi: 10.1371/journal.pgen.1005358

Daga, R. R., & Chang, F. (2005). Dynamic positioning of the fission yeast cell division plane. *Proc Natl Acad Sci U S A, 102*(23), 8228-8232. doi: 10.1073/pnas.0409021102

Dekker, N., Speijer, D., Grun, C. H., van den Berg, M., de Haan, A., & Hochstenbach, F. (2004). Role of the alpha-glucanase Agn1p in fission-yeast cell separation. *Mol Biol Cell, 15*(8), 3903-3914. doi: 10.1091/mbc.E04-04-0319

Demeter, J., & Sazer, S. (1998). imp2, a new component of the actin ring in the fission yeast Schizosaccharomyces pombe. *J Cell Biol, 143*(2), 415-427.

Deshaies, R. J., & Joazeiro, C. A. (2009). RING domain E3 ubiquitin ligases. *Annu Rev Biochem, 78*, 399-434. doi: 10.1146/annurev.biochem.78.101807.093809

Dinkel, H., Van Roey, K., Michael, S., Kumar, M., Uyar, B., Altenberg, B., . . . Gibson, T. J. (2016). ELM 2016--data update and new functionality of the eukaryotic linear motif resource. *Nucleic Acids Res, 44*(D1), D294-300. doi: 10.1093/nar/gkv1291

Durocher, D., & Jackson, S. P. (2002). The FHA domain. *FEBS Lett, 513*(1), 58-66.

Durocher, D., Taylor, I. A., Sarbassova, D., Haire, L. F., Westcott, S. L., Jackson, S. P., . . . Yaffe, M. B. (2000). The molecular basis of FHA domain:phosphopeptide binding specificity and implications for phospho-dependent signaling mechanisms. *Mol Cell, 6*(5), 1169-1182.

Elmore, Z. C., Beckley, J. R., Chen, J. S., & Gould, K. L. (2014). Histone H2B ubiquitination promotes the function of the anaphase-promoting complex/cyclosome in Schizosaccharomyces pombe. *G3 (Bethesda), 4*(8), 1529-1538. doi: 10.1534/g3.114.012625

Eng, K., Naqvi, N. I., Wong, K. C., & Balasubramanian, M. K. (1998). Rng2p, a protein required for cytokinesis in fission yeast, is a component of the actomyosin ring and the spindle pole body. *Curr Biol, 8*(11), 611-621.

Erson, A. E., & Petty, E. M. (2004). CHFR-associated early G2/M checkpoint defects in breast cancer cells. *Mol Carcinog, 39*(1), 26-33. doi: 10.1002/mc.10161

Fankhauser, C., Marks, J., Reymond, A., & Simanis, V. (1993). The S. pombe cdc16 gene is required both for maintenance of p34cdc2 kinase activity and regulation of septum formation: a link between mitosis and cytokinesis? *EMBO J, 12*(7), 2697-2704.

Fankhauser, C., Reymond, A., Cerutti, L., Utzig, S., Hofmann, K., & Simanis, V. (1995). The S. pombe cdc15 gene is a key element in the reorganization of F-actin at mitosis. *Cell, 82*(3), 435-444.

Fankhauser, C., & Simanis, V. (1993). The Schizosaccharomyces pombe cdc14 gene is required for septum formation and can also inhibit nuclear division. *Mol Biol Cell, 4*(5), 531-539.

Fankhauser, C., & Simanis, V. (1994). The cdc7 protein kinase is a dosage dependent regulator of septum formation in fission yeast. *EMBO J, 13*(13), 3011-3019.

Fantes, P. A., & Hoffman, C. S. (2016). A Brief History of Schizosaccharomyces pombe Research: A Perspective Over the Past 70 Years. *Genetics, 203*(2), 621-629. doi: 10.1534/genetics.116.189407

Fededa, J. P., & Gerlich, D. W. (2012). Molecular control of animal cell cytokinesis. *Nat Cell Biol, 14*(5), 440-447. doi: 10.1038/ncb2482

Fesquet, D., Fitzpatrick, P. J., Johnson, A. L., Kramer, K. M., Toyn, J. H., & Johnston, L. H. (1999). A Bub2p-dependent spindle checkpoint pathway regulates the Dbf2p kinase in budding yeast. *EMBO J, 18*(9), 2424-2434. doi: 10.1093/emboj/18.9.2424

Fraschini, R., Bilotta, D., Lucchini, G., & Piatti, S. (2004). Functional characterization of Dma1 and Dma2, the budding yeast homologues of Schizosaccharomyces pombe Dma1 and human Chfr. *Mol Biol Cell, 15*(8), 3796-3810. doi: 10.1091/mbc.E04-02-0094

Fraschini, R., Formenti, E., Lucchini, G., & Piatti, S. (1999). Budding yeast Bub2 is localized at spindle pole bodies and activates the mitotic checkpoint via a different pathway from Mad2. *J Cell Biol, 145*(5), 979-991.

Furge, K. A., Cheng, Q. C., Jwa, M., Shin, S., Song, K., & Albright, C. F. (1999). Regions of Byr4, a regulator of septation in fission yeast, that bind Spg1 or Cdc16 and form a two-component GTPase-activating protein with Cdc16. *J Biol Chem, 274*(16), 11339-11343.

Furge, K. A., Wong, K., Armstrong, J., Balasubramanian, M., & Albright, C. F. (1998). Byr4 and Cdc16 form a two-component GTPase-activating protein for the Spg1 GTPase that controls septation in fission yeast. *Curr Biol, 8*(17), 947-954.

Garcia-Cortes, J. C., & McCollum, D. (2009). Proper timing of cytokinesis is regulated by Schizosaccharomyces pombe Etd1. *J Cell Biol, 186*(5), 739-753. doi: jcb.200902116 [pii]

10.1083/jcb.200902116

Gardner, R. D., & Burke, D. J. (2000). The spindle checkpoint: two transitions, two pathways. *Trends Cell Biol, 10*(4), 154-158.

Gilberto, S., & Peter, M. (2017). Dynamic ubiquitin signaling in cell cycle regulation. *J Cell Biol, 216*(8), 2259-2271. doi: 10.1083/jcb.201703170

Glotzer, M., Murray, A. W., & Kirschner, M. W. (1991). Cyclin is degraded by the ubiquitin pathway. *Nature, 349*(6305), 132-138. doi: 10.1038/349132a0

Gordon, C., McGurk, G., Wallace, M., & Hastie, N. D. (1996). A conditional lethal mutant in the fission yeast 26 S protease subunit mts3+ is defective in metaphase to anaphase transition. *J Biol Chem, 271*(10), 5704-5711.

Gould, K. L., Ren, L., Feoktistova, A. S., Jennings, J. L., & Link, A. J. (2004). Tandem affinity purification and identification of protein complex components. *Methods, 33*(3), 239-244. doi: 10.1016/j.ymeth.2003.11.019

Goyal, A., Takaine, M., Simanis, V., & Nakano, K. (2011). Dividing the spoils of growth and the cell cycle: The fission yeast as a model for the study of cytokinesis. *Cytoskeleton (Hoboken), 68*(2), 69-88. doi: 10.1002/cm.20500

Green, R. A., Paluch, E., & Oegema, K. (2012). Cytokinesis in animal cells. *Annu Rev Cell Dev Biol, 28*, 29-58. doi: 10.1146/annurev-cellbio-101011-155718

Gu, Y., & Oliferenko, S. (2015). Comparative biology of cell division in the fission yeast clade. *Curr Opin Microbiol, 28*, 18-25. doi: 10.1016/j.mib.2015.07.011

Guertin, D. A., Chang, L., Irshad, F., Gould, K. L., & McCollum, D. (2000). The role of the sid1p kinase and cdc14p in regulating the onset of cytokinesis in fission yeast. *EMBO J, 19*(8), 1803-1815. doi: 10.1093/emboj/19.8.1803

Guertin, D. A., & McCollum, D. (2001). Interaction between the noncatalytic region of Sid1p kinase and Cdc14p is required for full catalytic activity and localization of Sid1p. *J Biol Chem, 276*(30), 28185-28189. doi: 10.1074/jbc.M103802200

Guertin, D. A., Venkatram, S., Gould, K. L., & McCollum, D. (2002). Dma1 prevents mitotic exit and cytokinesis by inhibiting the septation initiation network (SIN). *Dev Cell, 3*(6), 779-790.

Gupta, S., Mana-Capelli, S., McLean, J. R., Chen, C. T., Ray, S., Gould, K. L., & McCollum, D. (2013). Identification of SIN pathway targets reveals mechanisms of crosstalk between NDR kinase pathways. *Curr Biol, 23*(4), 333-338. doi: 10.1016/j.cub.2013.01.014

Hagan, I., & Yanagida, M. (1995). The product of the spindle formation gene sad1+ associates with the fission yeast spindle pole body and is essential for viability. *J Cell Biol, 129*(4), 1033-1047.

Hagan, I. M., & Hyams, J. S. (1988). The use of cell division cycle mutants to investigate the control of microtubule distribution in the fission yeast Schizosaccharomyces pombe. *J Cell Sci, 89*(Pt 3)(), 343-357.

Harashima, H., Dissmeyer, N., & Schnittger, A. (2013). Cell cycle control across the eukaryotic kingdom. *Trends Cell Biol, 23*(7), 345-356. doi: 10.1016/j.tcb.2013.03.002

Hartwell, L. H., Culotti, J., Pringle, J. R., & Reid, B. J. (1974). Genetic control of the cell division cycle in yeast. *Science, 183*(4120), 46-51.

Hartwell, L. H., & Weinert, T. A. (1989). Checkpoints: controls that ensure the order of cell cycle events. *Science, 246*(4930), 629-634.

Heride, C., Urbe, S., & Clague, M. J. (2014). Ubiquitin code assembly and disassembly. *Curr Biol, 24*(6), R215-220. doi: 10.1016/j.cub.2014.02.002

Hiraoka, Y., Toda, T., & Yanagida, M. (1984). The NDA3 gene of fission yeast encodes beta-tubulin: a cold-sensitive nda3 mutation reversibly blocks spindle formation and chromosome movement in mitosis. *Cell, 39*(2 Pt 1), 349-358.

Holt, L. J. (2012). Regulatory modules: Coupling protein stability to phopshoregulation during cell division. *FEBS Lett, 586*(17), 2773-2777. doi: 10.1016/j.febslet.2012.05.045

Horowitz, N. H., & Leupold, U. (1951). Some recent studies bearing on the one geneone enzyme hypothesis. *Cold Spring Harb Symp Quant Biol, 16*, 65-74.

Hou, M. C., Guertin, D. A., & McCollum, D. (2004). Initiation of cytokinesis is controlled through multiple modes of regulation of the Sid2p-Mob1p kinase complex. *Mol Cell Biol, 24*(8), 3262-3276.

Hou, M. C., Salek, J., & McCollum, D. (2000). Mob1p interacts with the Sid2p kinase and is required for cytokinesis in fission yeast. *Curr Biol, 10*(10), 619-622.

Huang, Y. M., & Chang, C. E. (2014). Achieving peptide binding specificity and promiscuity by loops: case of the forkhead-associated domain. *PLoS One, 9*(5), e98291. doi: 10.1371/journal.pone.0098291

Huen, M. S., & Chen, J. (2010). Assembly of checkpoint and repair machineries at DNA damage sites. *Trends Biochem Sci, 35*(2), 101-108. doi: 10.1016/j.tibs.2009.09.001

Huen, M. S., Grant, R., Manke, I., Minn, K., Yu, X., Yaffe, M. B., & Chen, J. (2007). RNF8 transduces the DNA-damage signal via histone ubiquitylation and checkpoint protein assembly. *Cell, 131*(5), 901-914. doi: 10.1016/j.cell.2007.09.041

Hunter, T. (2007). The age of crosstalk: phosphorylation, ubiquitination, and beyond. *Mol Cell, 28*(5), 730-738. doi: 10.1016/j.molcel.2007.11.019

Johnson, A. E., Chen, J. S., & Gould, K. L. (2013a). CK1 is required for a mitotic checkpoint that delays cytokinesis. *Curr Biol, 23*(19), 1920-1926. doi: 10.1016/j.cub.2013.07.077

Johnson, A. E., Chen, J. S., & Gould, K. L. (2013b). CK1 is required for a mitotic checkpoint that delays cytokinesis. *Current biology : CB, 23*(19), 1920-1926. doi: 10.1016/j.cub.2013.07.077

Johnson, A. E., Collier, S. E., Ohi, M. D., & Gould, K. L. (2012a). Fission yeast Dma1 requires RING domain dimerization for its ubiquitin ligase activity and mitotic checkpoint function. *J Biol Chem, 287*(31), 25741-25748. doi: 10.1074/jbc.M112.349712

Johnson, A. E., Collier, S. E., Ohi, M. D., & Gould, K. L. (2012b). Fission yeast Dma1 requires RING domain dimerization for its ubiquitin ligase activity and mitotic checkpoint function. *The Journal of biological chemistry, 287*(31), 25741-25748. doi: 10.1074/jbc.M112.349712

Johnson, A. E., & Gould, K. L. (2011a). Dma1 ubiquitinates the SIN scaffold, Sid4, to impede the mitotic localization of Plo1 kinase. *The EMBO journal, 30*(2), 341-354. doi: 10.1038/emboj.2010.317

Johnson, A. E., & Gould, K. L. (2011b). Dma1 ubiquitinates the SIN scaffold, Sid4, to impede the mitotic localization of Plo1 kinase. *EMBO J, 30*(2), 341-354. doi: 10.1038/emboj.2010.317

Johnson, A. E., McCollum, D., & Gould, K. L. (2012a). Polar opposites: Fine-tuning cytokinesis through SIN asymmetry. *Cytoskeleton (Hoboken), 69*(10), 686-699. doi: 10.1002/cm.21044

Johnson, A. E., McCollum, D., & Gould, K. L. (2012b). Polar opposites: Fine-tuning cytokinesis through SIN asymmetry. *Cytoskeleton, 69*(10), 686-699. doi: 10.1002/cm.21044

Johnson, D. G., & Walker, C. L. (1999). Cyclins and cell cycle checkpoints. *Annu Rev Pharmacol Toxicol, 39*, 295-312. doi: 10.1146/annurev.pharmtox.39.1.295

Juanes, M. A., & Piatti, S. (2016). Control of Formin Distribution and Actin Cable Assembly by the E3 Ubiquitin Ligases Dma1 and Dma2. *Genetics, 204*(1), 205-220. doi: 10.1534/genetics.116.189258

Kang, D., Chen, J., Wong, J., & Fang, G. (2002). The checkpoint protein Chfr is a ligase that ubiquitinates Plk1 and inhibits Cdc2 at the G2 to M transition. *J Cell Biol, 156*(2), 249-259. doi: 10.1083/jcb.200108016

Kim, J. S., Park, Y. Y., Park, S. Y., Cho, H., Kang, D., & Cho, H. (2011). The auto-ubiquitylation of E3 ubiquitin-protein ligase Chfr at G2 phase is required for

accumulation of polo-like kinase 1 and mitotic entry in mammalian cells. *J Biol Chem, 286*(35), 30615-30623. doi: 10.1074/jbc.M111.231803

Kitayama, C., Sugimoto, A., & Yamamoto, M. (1997). Type II myosin heavy chain encoded by the myo2 gene composes the contractile ring during cytokinesis in Schizosaccharomyces pombe. *J Cell Biol, 137*(6), 1309-1319.

Koch, A., Krug, K., Pengelley, S., Macek, B., & Hauf, S. (2011). Mitotic substrates of the kinase aurora with roles in chromatin regulation identified through quantitative phosphoproteomics of fission yeast. *Sci Signal, 4*(179), rs6. doi: 10.1126/scisignal.2001588

Kolas, N. K., Chapman, J. R., Nakada, S., Ylanko, J., Chahwan, R., Sweeney, F. D., . . . Durocher, D. (2007). Orchestration of the DNA-damage response by the RNF8 ubiquitin ligase. *Science, 318*(5856), 1637-1640. doi: 1150034 [pii]

10.1126/science.1150034

Kouranti, I., McLean, J. R., Feoktistova, A., Liang, P., Johnson, A. E., Roberts-Galbraith, R. H., & Gould, K. L. (2010). A global census of fission yeast deubiquitinating enzyme localization and interaction networks reveals distinct compartmentalization profiles and overlapping functions in endocytosis and polarity. *PLoS Biol, 8*(9). doi: 10.1371/journal.pbio.1000471

Krapp, A., Collin, P., Cano Del Rosario, E., & Simanis, V. (2008). Homoeostasis between the GTPase Spg1p and its GAP in the regulation of cytokinesis in S. pombe. *J Cell Sci, 121*(Pt 5), 601-608. doi: 10.1242/jcs.022772

Krapp, A., Schmidt, S., Cano, E., & Simanis, V. (2001). S. pombe cdc11p, together with sid4p, provides an anchor for septation initiation network proteins on the spindle pole body. *Curr Biol, 11*(20), 1559-1568.

Krapp, A., & Simanis, V. (2008). An overview of the fission yeast septation initiation network (SIN). *Biochem Soc Trans, 36*(Pt 3), 411-415. doi: 10.1042/BST0360411

Laplante, C., Berro, J., Karatekin, E., Hernandez-Leyva, A., Lee, R., & Pollard, T. D. (2015). Three myosins contribute uniquely to the assembly and constriction of the fission yeast cytokinetic contractile ring. *Curr Biol, 25*(15), 1955-1965. doi: 10.1016/j.cub.2015.06.018

Laporte, D., Coffman, V. C., Lee, I. J., & Wu, J. Q. (2011). Assembly and architecture of precursor nodes during fission yeast cytokinesis. *J Cell Biol, 192*(6), 1005-1021. doi: 10.1083/jcb.201008171

Laporte, D., Ojkic, N., Vavylonis, D., & Wu, J. Q. (2012). alpha-Actinin and fimbrin cooperate with myosin II to organize actomyosin bundles during contractile-ring assembly. *Mol Biol Cell, 23*(16), 3094-3110. doi: 10.1091/mbc.E12-02-0123

Lee, H. J., Li, C. F., Ruan, D., Powers, S., Thompson, P. A., Frohman, M. A., & Chan, C. H. (2016). The DNA Damage Transducer RNF8 Facilitates Cancer Chemoresistance and Progression through Twist Activation. *Mol Cell, 63*(6), 1021-1033. doi: 10.1016/j.molcel.2016.08.009

Lee, I. J., Coffman, V. C., & Wu, J. Q. (2012). Contractile-ring assembly in fission yeast cytokinesis: Recent advances and new perspectives. *Cytoskeleton (Hoboken), 69*(10), 751-763. doi: 10.1002/cm.21052

Li, L., Halaby, M. J., Hakem, A., Cardoso, R., El Ghamrasni, S., Harding, S., . . . Hakem, R. (2010). Rnf8 deficiency impairs class switch recombination, spermatogenesis, and genomic integrity and predisposes for cancer. *J Exp Med, 207*(5), 983-997. doi: 10.1084/jem.20092437

Li, R. (1999). Bifurcation of the mitotic checkpoint pathway in budding yeast. *Proc Natl Acad Sci U S A, 96*(9), 4989-4994.

Liang, X., & Van Doren, S. R. (2008). Mechanistic insights into phosphoprotein-binding FHA domains. *Acc Chem Res, 41*(8), 991-999. doi: 10.1021/ar700148u

Luijsterburg, M. S., & van Attikum, H. (2012). Close encounters of the RNF8th kind: when chromatin meets DNA repair. *Curr Opin Cell Biol, 24*(3), 439-447. doi: 10.1016/j.ceb.2012.03.008

Ma, Z. Q., Dasari, S., Chambers, M. C., Litton, M. D., Sobecki, S. M., Zimmerman, L. J., . . . Tabb, D. L. (2009). IDPicker 2.0: Improved protein assembly with high discrimination peptide identification filtering. *J Proteome Res, 8*(8), 3872-3881. doi: 10.1021/pr900360j

Mah, A. S., Elia, A. E., Devgan, G., Ptacek, J., Schutkowski, M., Snyder, M., . . . Deshaies, R. J. (2005). Substrate specificity analysis of protein kinase complex Dbf2-Mob1 by peptide library and proteome array screening. *BMC Biochem, 6*, 22. doi: 10.1186/1471-2091-6-22

Mahajan, A., Yuan, C., Lee, H., Chen, E. S., Wu, P. Y., & Tsai, M. D. (2008). Structure and function of the phosphothreonine-specific FHA domain. *Sci Signal, 1*(51), re12. doi: 10.1126/scisignal.151re12

Malumbres, M. (2011). Physiological relevance of cell cycle kinases. *Physiol Rev, 91*(3), 973-1007. doi: 10.1152/physrev.00025.2010

Mariatos, G., Bothos, J., Zacharatos, P., Summers, M. K., Scolnick, D. M., Kittas, C., . . . Gorgoulis, V. G. (2003). Inactivating mutations targeting the chfr mitotic checkpoint gene in human lung cancer. *Cancer Res, 63*(21), 7185-7189.

Marks, J., Fankhauser, C., & Simanis, V. (1992). Genetic interactions in the control of septation in *Schizosaccharomyces pombe*. *J Cell Sci, 101*(Pt 4), 801-808.

Martin-Cuadrado, A. B., Duenas, E., Sipiczki, M., Vazquez de Aldana, C. R., & del Rey, F. (2003). The endo-beta-1,3-glucanase eng1p is required for dissolution of the primary septum during cell separation in Schizosaccharomyces pombe. *J Cell Sci, 116*(Pt 9), 1689-1698.

Martin-Garcia, R., Coll, P. M., & Perez, P. (2014). F-BAR domain protein Rga7 collaborates with Cdc15 and Imp2 to ensure proper cytokinesis in fission yeast. *J Cell Sci, 127*(Pt 19), 4146-4158. doi: 10.1242/jcs.146233

Matsusaka, T., & Pines, J. (2004). Chfr acts with the p38 stress kinases to block entry to mitosis in mammalian cells. *J Cell Biol, 166*(4), 507-516. doi: 10.1083/jcb.200401139

Mattiroli, F., Vissers, J. H., van Dijk, W. J., Ikpa, P., Citterio, E., Vermeulen, W., . . . Sixma, T. K. (2012). RNF168 ubiquitinates K13-15 on H2A/H2AX to drive DNA damage signaling. *Cell, 150*(6), 1182-1195. doi: 10.1016/j.cell.2012.08.005

McDonald WH, O. R., Miyamoto DT, Mitchison TJ, Yates JR III. (2002). Comparison of three directly coupled HPLC MS/MS strategies for identification of proteins from

complex mixtures: single-dimension LC-MS/MS, 2-phase MudPIT, and 3-phase MudPIT. *International Journal of Mass Spectrometry, 219*(1), 245–251.

McLean, J. R., Kouranti, I., & Gould, K. L. (2011). Survey of the phosphorylation status of the Schizosaccharomyces pombe deubiquitinating enzyme (DUB) family. *J Proteome Res, 10*(3), 1208-1215. doi: 10.1021/pr100985s

Meggio, F., Marin, O., & Pinna, L. A. (1994). Substrate specificity of protein kinase CK2. *Cell Mol Biol Res, 40*(5-6), 401-409.

Merlini, L., Fraschini, R., Boettcher, B., Barral, Y., Lucchini, G., & Piatti, S. (2012). Budding yeast dma proteins control septin dynamics and the spindle position checkpoint by promoting the recruitment of the Elm1 kinase to the bud neck. *PLoS Genet, 8*(4), e1002670. doi: 10.1371/journal.pgen.1002670

Mikhailov, A., & Rieder, C. L. (2002). Cell cycle: stressed out of mitosis. *Curr Biol, 12*(9), R331-333.

Mikhailov, A., Shinohara, M., & Rieder, C. L. (2005). The p38-mediated stress-activated checkpoint. A rapid response system for delaying progression through antephase and entry into mitosis. *Cell Cycle, 4*(1), 57-62. doi: 10.4161/cc.4.1.1357

Mitchison, J. M. (1957). The growth of single cells. I. Schizosaccharomyces pombe. *Exp Cell Res, 13*(2), 244-262.

Moreno, S., Klar, A., & Nurse, P. (1991). Molecular genetic analysis of fission yeast Schizosaccharomyces pombe. *Methods Enzymol, 194*, 795-823.

Moreno, S., & Nurse, P. (1990). Substrates for p34cdc2: in vivo veritas? *Cell, 61*(4), 549-551.

Morgan, D. O. (1997). Cyclin-dependent kinases: engines, clocks, and microprocessors. *Annu Rev Cell Dev Biol, 13*, 261-291. doi: 10.1146/annurev.cellbio.13.1.261

Morrell, J. L., Tomlin, G. C., Rajagopalan, S., Venkatram, S., Feoktistova, A. S., Tasto, J. J., . . . Gould, K. L. (2004). Sid4p-Cdc11p assembles the septation initiation network and its regulators at the S. pombe SPB. *Curr Biol, 14*(7), 579-584. doi: 10.1016/j.cub.2004.03.036

Mulvihill, D. P., Petersen, J., Ohkura, H., Glover, D. M., & Hagan, I. M. (1999). Plo1 kinase recruitment to the spindle pole body and its role in cell division in Schizosaccharomyces pombe. *Mol Biol Cell, 10*(8), 2771-2785.

Murone, M., & Simanis, V. (1996). The fission yeast dma1 gene is a component of the spindle assembly checkpoint, required to prevent septum formation and premature exit from mitosis if spindle function is compromised. *EMBO J, 15*(23), 6605-6616.

Musacchio, A. (2011). Spindle assembly checkpoint: the third decade. *Philos Trans R Soc Lond B Biol Sci, 366*(1584), 3595-3604. doi: 10.1098/rstb.2011.0072

Musacchio, A. (2015). The Molecular Biology of Spindle Assembly Checkpoint Signaling Dynamics. *Curr Biol, 25*(20), R1002-1018. doi: 10.1016/j.cub.2015.08.051

Nakada, S., Yonamine, R. M., & Matsuo, K. (2012). RNF8 regulates assembly of RAD51 at DNA double-strand breaks in the absence of BRCA1 and 53BP1. *Cancer Res, 72*(19), 4974-4983. doi: 10.1158/0008-5472.CAN-12-1057

Nakajima, H., Toyoshima-Morimoto, F., Taniguchi, E., & Nishida, E. (2003). Identification of a consensus motif for Plk (Polo-like kinase) phosphorylation

reveals Myt1 as a Plk1 substrate. *J Biol Chem, 278*(28), 25277-25280. doi: 10.1074/jbc.C300126200

Nott, T. J., Kelly, G., Stach, L., Li, J., Westcott, S., Patel, D., . . . Smerdon, S. J. (2009). An intramolecular switch regulates phosphoindependent FHA domain interactions in Mycobacterium tuberculosis. *Sci Signal, 2*(63), ra12. doi: 10.1126/scisignal.2000212

Nurse, P. (2000). A long twentieth century of the cell cycle and beyond. *Cell, 100*(1), 71-78.

Nurse, P., Thuriaux, P., & Nasmyth, K. (1976). Genetic control of the cell division cycle in the fission yeast Schizosaccharomyces pombe. *Mol Gen Genet, 146*(2), 167-178.

Ohkura, H., Hagan, I. M., & Glover, D. M. (1995). The conserved Schizosaccharomyces pombe kinase plo1, required to form a bipolar spindle, the actin ring, and septum, can drive septum formation in G1 and G2 cells. *Genes Dev, 9*(9), 1059-1073.

Orthwein, A., Fradet-Turcotte, A., Noordermeer, S. M., Canny, M. D., Brun, C. M., Strecker, J., . . . Durocher, D. (2014). Mitosis inhibits DNA double-strand break repair to guard against telomere fusions. *Science, 344*(6180), 189-193. doi: 10.1126/science.1248024

Padte, N. N., Martin, S. G., Howard, M., & Chang, F. (2006). The cell-end factor pom1p inhibits mid1p in specification of the cell division plane in fission yeast. *Curr Biol, 16*(24), 2480-2487. doi: 10.1016/j.cub.2006.11.024

Paoletti, A., & Chang, F. (2000). Analysis of mid1p, a protein required for placement of the cell division site, reveals a link between the nucleus and the cell surface in fission yeast. *Mol Biol Cell, 11*(8), 2757-2773.

Peuscher, M. H., & Jacobs, J. J. (2011). DNA-damage response and repair activities at uncapped telomeres depend on RNF8. *Nat Cell Biol, 13*(9), 1139-1145. doi: 10.1038/ncb2326

Pollard, T. D. (2010). Mechanics of cytokinesis in eukaryotes. *Curr Opin Cell Biol, 22*(1), 50-56. doi: 10.1016/j.ceb.2009.11.010

Pollard, T. D., & Wu, J. Q. (2010). Understanding cytokinesis: lessons from fission yeast. *Nat Rev Mol Cell Biol, 11*(2), 149-155. doi: 10.1038/nrm2834

Privette, L. M., & Petty, E. M. (2008). CHFR: A Novel Mitotic Checkpoint Protein and Regulator of Tumorigenesis. *Transl Oncol, 1*(2), 57-64.

Pruneda, J. N., Littlefield, P. J., Soss, S. E., Nordquist, K. A., Chazin, W. J., Brzovic, P. S., & Klevit, R. E. (2012). Structure of an E3:E2~Ub complex reveals an allosteric mechanism shared among RING/U-box ligases. *Mol Cell, 47*(6), 933-942. doi: 10.1016/j.molcel.2012.07.001

Rachfall, N., Johnson, A. E., Mehta, S., Chen, J. S., & Gould, K. L. (2014). Cdk1 promotes cytokinesis in fission yeast through activation of the septation initiation network. *Mol Biol Cell, 25*(15), 2250-2259. doi: 10.1091/mbc.E14-04-0936

Rai, R., Li, J. M., Zheng, H., Lok, G. T., Deng, Y., Huen, M. S., . . . Chang, S. (2011). The E3 ubiquitin ligase Rnf8 stabilizes Tpp1 to promote telomere end protection. *Nat Struct Mol Biol, 18*(12), 1400-1407. doi: 10.1038/nsmb.2172

Reinhardt, H. C., & Yaffe, M. B. (2013). Phospho-Ser/Thr-binding domains: navigating the cell cycle and DNA damage response. *Nat Rev Mol Cell Biol, 14*(9), 563-580. doi: 10.1038/nrm3640

Rieder, C. L., & Cole, R. (2000). Microtubule disassembly delays the G2-M transition in vertebrates. *Curr Biol, 10*(17), 1067-1070.

Rieder, C. L., & Cole, R. W. (1998). Entry into mitosis in vertebrate somatic cells is guarded by a chromosome damage checkpoint that reverses the cell cycle when triggered during early but not late prophase. *J Cell Biol, 142*(4), 1013-1022.

Rincon, S. A., & Paoletti, A. (2012). Mid1/anillin and the spatial regulation of cytokinesis in fission yeast. *Cytoskeleton (Hoboken), 69*(10), 764-777. doi: 10.1002/cm.21056

Rincon, S. A., & Paoletti, A. (2016). Molecular control of fission yeast cytokinesis. *Semin Cell Dev Biol, 53*, 28-38. doi: 10.1016/j.semcdb.2016.01.007

Roberts-Galbraith, R. H., Chen, J. S., Wang, J., & Gould, K. L. (2009). The SH3 domains of two PCH family members cooperate in assembly of the Schizosaccharomyces pombe contractile ring. *J Cell Biol, 184*(1), 113-127. doi: 10.1083/jcb.200806044

Roncero, C., & Sanchez, Y. (2010). Cell separation and the maintenance of cell integrity during cytokinesis in yeast: the assembly of a septum. *Yeast, 27*(8), 521-530. doi: 10.1002/yea.1779

Rosenberg, J. A., Tomlin, G. C., McDonald, W. H., Snydsman, B. E., Muller, E. G., Yates, J. R., 3rd, & Gould, K. L. (2006). Ppc89 links multiple proteins, including the septation initiation network, to the core of the fission yeast spindle-pole body. *Mol Biol Cell, 17*(9), 3793-3805. doi: 10.1091/mbc.E06-01-0039

Rothbauer, U., Zolghadr, K., Muyldermans, S., Schepers, A., Cardoso, M. C., & Leonhardt, H. (2008). A versatile nanotrap for biochemical and functional studies with fluorescent fusion proteins. *Mol Cell Proteomics, 7*(2), 282-289. doi: 10.1074/mcp.M700342-MCP200

Rothbauer, U., Zolghadr, K., Tillib, S., Nowak, D., Schermelleh, L., Gahl, A., . . . Leonhardt, H. (2006). Targeting and tracing antigens in live cells with fluorescent nanobodies. *Nat Methods, 3*(11), 887-889. doi: 10.1038/nmeth953

Salsman, J., & Dellaire, G. (2017). Precision genome editing in the CRISPR era. *Biochem Cell Biol, 95*(2), 187-201. doi: 10.1139/bcb-2016-0137

Samejima, I., Miller, V. J., Rincon, S. A., & Sawin, K. E. (2010). Fission yeast Mto1 regulates diversity of cytoplasmic microtubule organizing centers. *Curr Biol, 20*(21), 1959-1965. doi: 10.1016/j.cub.2010.10.006

Sanbhnani, S., & Yeong, F. M. (2012). CHFR: a key checkpoint component implicated in a wide range of cancers. *Cell Mol Life Sci, 69*(10), 1669-1687. doi: 10.1007/s00018-011-0892-2

Scolnick, D. M., & Halazonetis, T. D. (2000). Chfr defines a mitotic stress checkpoint that delays entry into metaphase. *Nature, 406*(6794), 430-435. doi: 10.1038/35019108

Seet, B. T., Dikic, I., Zhou, M. M., & Pawson, T. (2006). Reading protein modifications with interaction domains. *Nat Rev Mol Cell Biol, 7*(7), 473-483. doi: 10.1038/nrm1960

Shaner, N. C., Lambert, G. G., Chammas, A., Ni, Y., Cranfill, P. J., Baird, M. A., . . . Wang, J. (2013). A bright monomeric green fluorescent protein derived from

Branchiostoma lanceolatum. *Nat Methods, 10*(5), 407-409. doi: 10.1038/nmeth.2413

Simanis, V. (2015a). Pombe's thirteen - control of fission yeast cell division by the septation initiation network. *Journal of cell science, 128*(8), 1465-1474. doi: 10.1242/jcs.094821

Simanis, V. (2015b). Pombe's thirteen - control of fission yeast cell division by the septation initiation network. *J Cell Sci, 128*(8), 1465-1474. doi: 10.1242/jcs.094821

Skoneczna, A., Kaniak, A., & Skoneczny, M. (2015). Genetic instability in budding and fission yeast-sources and mechanisms. *FEMS Microbiol Rev, 39*(6), 917-967. doi: 10.1093/femsre/fuv028

Sohrmann, M., Fankhauser, C., Brodbeck, C., & Simanis, V. (1996). The dmf1/mid1 gene is essential for correct positioning of the division septum in fission yeast. *Genes Dev, 10*(21), 2707-2719.

Sohrmann, M., Schmidt, S., Hagan, I., & Simanis, V. (1998). Asymmetric segregation on spindle poles of the Schizosaccharomyces pombe septum-inducing protein kinase Cdc7p. *Genes Dev, 12*(1), 84-94.

Song, K., Mach, K. E., Chen, C. Y., Reynolds, T., & Albright, C. F. (1996). A novel suppressor of ras1 in fission yeast, byr4, is a dosage-dependent inhibitor of cytokinesis. *J Cell Biol, 133*(6), 1307-1319.

Songyang, Z., Blechner, S., Hoagland, N., Hoekstra, M. F., Piwnica-Worms, H., & Cantley, L. C. (1994). Use of an oriented peptide library to determine the optimal substrates of protein kinases. *Curr Biol, 4*(11), 973-982.

Songyang, Z., Lu, K. P., Kwon, Y. T., Tsai, L. H., Filhol, O., Cochet, C., . . . Cantley, L. C. (1996). A structural basis for substrate specificities of protein Ser/Thr kinases: primary sequence preference of casein kinases I and II, NIMA, phosphorylase kinase, calmodulin-dependent kinase II, CDK5, and Erk1. *Mol Cell Biol, 16*(11), 6486-6493.

Sparks, C. A., Morphew, M., & McCollum, D. (1999). Sid2p, a spindle pole body kinase that regulates the onset of cytokinesis. *J Cell Biol, 146*(4), 777-790.

Stachowiak, M. R., Laplante, C., Chin, H. F., Guirao, B., Karatekin, E., Pollard, T. D., & O'Shaughnessy, B. (2014). Mechanism of cytokinetic contractile ring constriction in fission yeast. *Dev Cell, 29*(5), 547-561. doi: 10.1016/j.devcel.2014.04.021

Stone, M., Hartmann-Petersen, R., Seeger, M., Bech-Otschir, D., Wallace, M., & Gordon, C. (2004). Uch2/Uch37 is the major deubiquitinating enzyme associated with the 26S proteasome in fission yeast. *J Mol Biol, 344*(3), 697-706. doi: 10.1016/j.jmb.2004.09.057

Stringer, D. K., & Piper, R. C. (2011). Terminating protein ubiquitination: Hasta la vista, ubiquitin. *Cell Cycle, 10*(18), 3067-3071. doi: 10.4161/cc.10.18.17191

Summers, M. K., Bothos, J., & Halazonetis, T. D. (2005). The CHFR mitotic checkpoint protein delays cell cycle progression by excluding Cyclin B1 from the nucleus. *Oncogene, 24*(16), 2589-2598. doi: 10.1038/sj.onc.1208428

Tabb, D. L., Fernando, C. G., & Chambers, M. C. (2007). MyriMatch: highly accurate tandem mass spectral peptide identification by multivariate hypergeometric analysis. *J Proteome Res, 6*(2), 654-661. doi: 10.1021/pr0604054

Tagwerker, C., Flick, K., Cui, M., Guerrero, C., Dou, Y., Auer, B., . . . Kaiser, P. (2006). A tandem affinity tag for two-step purification under fully denaturing conditions: application in ubiquitin profiling and protein complex identification combined with in vivocross-linking. *Mol Cell Proteomics, 5*(4), 737-748. doi: 10.1074/mcp.M500368-MCP200

Tanaka, K., Petersen, J., MacIver, F., Mulvihill, D. P., Glover, D. M., & Hagan, I. M. (2001). The role of Plo1 kinase in mitotic commitment and septation in Schizosaccharomyces pombe. *EMBO J, 20*(6), 1259-1270. doi: 10.1093/emboj/20.6.1259

Tolic-Norrelykke, I. M., Sacconi, L., Stringari, C., Raabe, I., & Pavone, F. S. (2005). Nuclear and division-plane positioning revealed by optical micromanipulation. *Curr Biol, 15*(13), 1212-1216. doi: 10.1016/j.cub.2005.05.052

Tomlin, G. C., Morrell, J. L., & Gould, K. L. (2002). The spindle pole body protein Cdc11p links Sid4p to the fission yeast septation initiation network. *Mol Biol Cell, 13*(4), 1203-1214. doi: 10.1091/mbc.01-09-0455

Tran, P. T., Marsh, L., Doye, V., Inoue, S., & Chang, F. (2001). A mechanism for nuclear positioning in fission yeast based on microtubule pushing. *J Cell Biol, 153*(2), 397-411.

van Vugt, M. A., Gardino, A. K., Linding, R., Ostheimer, G. J., Reinhardt, H. C., Ong, S. E., . . . Yaffe, M. B. (2010). A mitotic phosphorylation feedback network connects Cdk1, Plk1, 53BP1, and Chk2 to inactivate the G(2)/M DNA damage checkpoint. *PLoS Biol, 8*(1), e1000287. doi: 10.1371/journal.pbio.1000287

Vora, S. M., & Phillips, B. T. (2016). The benefits of local depletion: The centrosome as a scaffold for ubiquitin-proteasome-mediated degradation. *Cell Cycle, 15*(16), 2124-2134. doi: 10.1080/15384101.2016.1196306

Wach, A., Brachat, A., Pohlmann, R., & Philippsen, P. (1994). New heterologous modules for classical or PCR-based gene disruptions in Saccharomyces cerevisiae. *Yeast, 10*(13), 1793-1808.

Wang, B., & Elledge, S. J. (2007). Ubc13/Rnf8 ubiquitin ligases control foci formation of the Rap80/Abraxas/Brca1/Brcc36 complex in response to DNA damage. *Proc Natl Acad Sci U S A, 104*(52), 20759-20763. doi: 0710061104 [pii]

10.1073/pnas.0710061104

Wang, Y., Li, W. Z., Johnson, A. E., Luo, Z. Q., Sun, X. L., Feoktistova, A., . . . Jin, Q. W. (2012a). Dnt1 acts as a mitotic inhibitor of the spindle checkpoint protein dma1 in fission yeast. *Molecular biology of the cell, 23*(17), 3348-3356. doi: 10.1091/mbc.E11-12-1020

Wang, Y., Li, W. Z., Johnson, A. E., Luo, Z. Q., Sun, X. L., Feoktistova, A., . . . Jin, Q. W. (2012b). Dnt1 acts as a mitotic inhibitor of the spindle checkpoint protein dma1 in fission yeast. *Mol Biol Cell, 23*(17), 3348-3356. doi: 10.1091/mbc.E11-12-1020

Waters, J. C. (2009). Accuracy and precision in quantitative fluorescence microscopy. *J Cell Biol, 185*(7), 1135-1148. doi: 10.1083/jcb.200903097

Wickliffe, K., Williamson, A., Jin, L., & Rape, M. (2009). The multiple layers of ubiquitin-dependent cell cycle control. *Chem Rev, 109*(4), 1537-1548. doi: 10.1021/cr800414e

Willet, A. H., McDonald, N. A., Bohnert, K. A., Baird, M. A., Allen, J. R., Davidson, M. W., & Gould, K. L. (2015a). The F-BAR Cdc15 promotes contractile ring formation through the direct recruitment of the formin Cdc12. *The Journal of cell biology, 208*(4), 391-399. doi: 10.1083/jcb.201411097

Willet, A. H., McDonald, N. A., Bohnert, K. A., Baird, M. A., Allen, J. R., Davidson, M. W., & Gould, K. L. (2015b). The F-BAR Cdc15 promotes contractile ring formation through the direct recruitment of the formin Cdc12. *J Cell Biol, 208*(4), 391-399. doi: 10.1083/jcb.201411097

Wu, J. Q., Bahler, J., & Pringle, J. R. (2001). Roles of a fimbrin and an alpha-actinin-like protein in fission yeast cell polarization and cytokinesis. *Mol Biol Cell, 12*(4), 1061-1077.

Wu, J. Q., Kuhn, J. R., Kovar, D. R., & Pollard, T. D. (2003). Spatial and temporal pathway for assembly and constriction of the contractile ring in fission yeast cytokinesis. *Dev Cell, 5*(5), 723-734.

Yau, R. G., Peng, Y., Valiathan, R. R., Birkeland, S. R., Wilson, T. E., & Weisman, L. S. (2014). Release from myosin V via regulated recruitment of an E3 ubiquitin ligase controls organelle localization. *Dev Cell, 28*(5), 520-533. doi: 10.1016/j.devcel.2014.02.001

Yu, X., Minter-Dykhouse, K., Malureanu, L., Zhao, W. M., Zhang, D., Merkle, C. J., . . . Chen, J. (2005). Chfr is required for tumor suppression and Aurora A regulation. *Nat Genet, 37*(4), 401-406. doi: 10.1038/ng1538

Zhao, Y., Brickner, J. R., Majid, M. C., & Mosammaparast, N. (2014). Crosstalk between ubiquitin and other post-translational modifications on chromatin during double-

strand break repair. *Trends Cell Biol, 24*(7), 426-434. doi:

10.1016/j.tcb.2014.01.005